

**ASSOCIATION OF MASSETER MUSCLE *PITX2*, *ENPP1* and *ESR1*  
EXPRESSION, MUSCLE FIBER TYPE, TEMPOROMANDIBULAR  
JOINT DISORDERS AND SUBCLASSIFICATIONS  
OF CRANIOFACIAL ASYMMETRY**

---

A Thesis  
Submitted to  
The Temple University Graduate Board

---

In Partial Fulfillment  
of the Requirements for the Degree  
MASTER OF SCIENCE in ORAL BIOLOGY

---

By  
Tabitha Richards Barnabei, D.M.D.  
August 2017

Thesis Approval(s):

Michael J. Horton, Ph.D.  
Thesis Advisor, Temple U. Kornberg School of Dentistry, Dept. of Orthodontics

James J. Sciote, D.D.S., M.S., Ph.D.  
Committee Member, Temple U. Kornberg School of Dentistry, Dept. of Orthodontics

Jeffrey H. Godel, D.D.S., M.S.  
Committee Member, Temple U. Kornberg School of Dentistry, Dept. of Orthodontics

## ABSTRACT

Craniofacial asymmetry is a dentofacial deformity with genetic influences. The genes *PITX2*, *ENPP1* and *ESR1* have multiple genetic associations with functional properties in muscle and bone. The objectives of this study are to investigate how *PITX2*, *ENPP1* and *ESR1* gene expression associates with four subclassifications of craniofacial asymmetry, temporomandibular disorders and fiber type differences compared between right and left masseter muscles.

We developed an asymmetry classification that diagnosed four types of asymmetry with distinctive growth patterns: Group 1 – menton deviation without ramal difference (“mandibular body asymmetry”); Group 2 – menton deviation with shorter ramal height on the deviated side (“typical asymmetry”); Group 3 – shorter ramal height on the opposite side of menton deviation (“atypical asymmetry”); Group 4 – menton deviation with shorter ramal height and maxillary canting on the deviated side (“C-shaped asymmetry”). Some of these patients are at high risk for TMD; therefore, temporomandibular joint functioning is assessed as a routine part of the pre-surgical evaluation. TMD was diagnosed using the Diagnostic Criteria for TMD (DC/TMD). The clinical examination includes mandibular range of motion, palpation for pain, joint noise and bruxism. In addition, the Jaw Pain and Function (JPF) questionnaire was used to assess patient reported symptoms as an indication of perceived severity before and one year after orthognathic surgery.

Masseter muscle samples were collected from 174 subjects undergoing surgical treatment for correction of malocclusion. Muscle serial cross-sections were mounted for immunostaining with five antibodies specific for myosin heavy chain (MyHC) isoform.

We classified masseter fibers into 4 fiber type groups: type I, type I/II hybrid, type IIA and/or IIX, neonatal and atrial. With the remaining muscle samples, total RNA was isolated and *PITX2*, *ENPP1*, and *ESR1* expression was quantified using TaqMan qRT-PCR. Average relative quantity gene expression values and percent differences between left and right masseter samples were calculated.

In this population, there is a high prevalence of facial asymmetry (48%). Pre-surgical mean JPF scores are significantly different between symmetric (JPF=1.97) and asymmetric (JPF=6.9;  $p < 0.001$ ) patients; with scores  $\geq 6$  diagnostic for presence of TMD. *ENPP1* and *ESR1* expression is differentially expressed between right and left masseter muscle in patients with asymmetry. *ENPP1* is differentially expressed in asymmetry group 4 ( $p=0.01$ ) and *ESR1* is differentially expressed in asymmetry group 1 ( $p=0.048$ ), group 2 ( $p=0.004$ ) and group 4 ( $p=0.02$ ).

Masseter fiber type properties of type I, type I/II hybrid and type II fibers associate with facial asymmetry and specific subclassifications, suggesting functional differences between type I, type I/II and type II fibers may be important factors in the development of symmetry between facial sides. There are significant differences in the left-right percent differences of fiber area of type I fibers in asymmetry group 3 ( $p=0.05$ ), type I/II hybrid fibers in group 3 ( $p=0.02$ ), and type II fibers in asymmetric patients ( $p=0.03$ ), asymmetry group 2 ( $p=0.05$ ) and group 4 ( $p=0.005$ ). Additionally, there are significant differences in the left-right percent differences of percent occupancy of type I fibers in asymmetric patients ( $p=0.04$ ), asymmetry group 2 ( $p=0.01$ ) and group 3 ( $p=0.05$ ) and type II fibers in asymmetry group 2 ( $p=0.04$ ).

By comparing gene expression with masseter muscle fiber type properties, we found significant results for *PITX2* and *ENPP1* suggesting their roles as genetic factors influencing jaw bone length and masticatory muscle strength in malocclusion. There are significant positive correlations between left-right percent differences of *PITX2* and type I fiber area ( $r=0.86$ ;  $p=0.03$ ), type I/II hybrid fiber area ( $r=0.94$ ;  $p=0.006$ ), and type I/II hybrid fiber percent occupancy ( $r=0.90$ ;  $p=0.01$ ). Also, there are positive correlations approaching significance between left-right percent differences of *ENPP1* and type I fiber area ( $r=0.80$ ;  $p=0.06$ ) and type I/II hybrid fiber area ( $r=0.75$ ;  $p=0.09$ ).

Given the high prevalence of TMD in a population of patients with facial asymmetry, we compared differences in gene expression in masseter muscle of patients with specific TMD diagnostic conditions. Average *PITX2* expression is significantly increased ( $p=0.0375$ ) and average *ENPP1* is increased, but not significantly, in all TMD patients diagnosed by the clinician. Average *ESR1* is slightly increased compared to JPF scores and may be an essential factor for patient reported TMD symptoms.

With these results, *PITX2*, *ENPP1*, and *ESR1* should be considered biomarkers for asymmetry and TMD; however, further studies are needed to provide a more thorough understanding of the genetic influences on the craniofacial complex.

## **ACKNOWLEDGEMENTS**

I would like to extend my sincerest gratitude to those that supported me through the completion of this study and the course of my education. Thank you Dr. Michael Horton, Dr. James Sciote and Dr. Jeffrey Godel for your guidance and support with my research project and orthodontic education. I am honored to be given the opportunity to pursue the field of orthodontics and to be part of such a wonderful community. Thank you to my family and husband for your continued encouragement and love during my educational journey.

# TABLE OF CONTENTS

	Page
ABSTRACT .....	ii
ACKNOWLEDGEMENTS .....	v
LIST OF FIGURES .....	ix
LIST OF TABLES .....	x
CHAPTER	
1. INTRODUCTION .....	1
2. REVIEW OF THE LITERATURE .....	5
2.1 Craniofacial Asymmetry .....	5
2.1.1 Facial Esthetics .....	5
2.1.2 Asymmetry in Human Development.....	6
2.1.3 Complex Etiology of Facial Asymmetry .....	6
2.1.4 Diagnosis and Current Classifications.....	7
2.1.5 Management of Facial Asymmetry .....	9
2.2 Genetic Role in Asymmetry .....	10
2.2.1 Breaking of Symmetry .....	11
2.2.2 The Nodal Pathway .....	13
2.3 Muscle Fiber Type Influence on Malocclusion .....	15
2.4 Effects of <i>ENPP1</i> on Bone and Muscle .....	17
2.5 Asymmetry and Temporomandibular Disorders .....	18

2.5.1 Diagnostic Criteria of TMD.....	19
2.5.2 Jaw Pain and Function Analysis .....	22
2.5.3 <i>ESRI</i> and TMD .....	23
3. AIMS OF THE INVESTIGATION .....	25
4. MATERIALS AND METHODS .....	26
4.1 Patient Population .....	26
4.2 Assessment of Asymmetry .....	27
4.3 Assessment of TMD.....	31
4.4 Muscle Samples .....	32
4.5 Masseter Muscle Fiber Type Analysis .....	33
4.6 RT-PCR.....	36
4.5.1 Total RNA Isolation for RT-PCR .....	36
4.5.2 RNA Quantification .....	37
4.7 Statistical Analysis .....	42
5. RESULTS .....	43
5.1 Results Overview .....	43
5.2 Asymmetric Subclassifications.....	43
5.3 <i>PITX2</i> , <i>ENPP1</i> and <i>ESRI</i> Expression and Asymmetry Groups .....	45
5.3.1 <i>PITX2</i> .....	45
5.3.2 <i>ENPP1</i> .....	46
5.3.3 <i>ESRI</i> .....	47
5.4. Fiber Type Data and Asymmetry Groups .....	48

5.4.1 Fiber Area .....	48
5.4.2 Percent Occupancy .....	50
5.5 DC-TMD Diagnosis and Asymmetry Groups .....	51
5.6 JPF and Asymmetry Groups.....	52
5.7 <i>PITX2</i> , <i>ENPP1</i> and <i>ESR1</i> and Muscle Fiber Types.....	52
5.8 <i>PITX2</i> , <i>ENPP1</i> and <i>ESR1</i> Expression and DC-TMD Diagnosis.....	56
5.9 <i>PITX2</i> , <i>ENPP1</i> and <i>ESR1</i> Expression and JPF Scores .....	59
6. DISCUSSION .....	60
7. CONCLUSIONS .....	69
REFERENCES.....	70
APPENDICES.....	81
APPENDIX A .....	80
JAW PAIN AND FUNCTION QUESTIONNAIRE	
APPENDIX B .....	81
SUMMARY OF SUBJECTS	
APPENDIX C .....	85
<i>PITX2</i> SUMMARY OF RAW DATA	
APPENDIX D.....	87
<i>ENPP1</i> SUMMARY OF RAW DATA	
APPENDIX E.....	89
<i>ESR1</i> SUMMARY OF RAW DATA	
APPENDIX F.....	91
FIBER TYPE AREA SUMMARY OF RAW DATA	
APPENDIX G .....	92
FIBER TYPE OCCUPANCY SUMMARY OF RAW DATA	
APPENDIX H.....	93
DC-TMD SUMMARY OF RAW DATA	

## LIST OF FIGURES

Figure	Page
1. Diagnostic Criteria for Temporomandibular Disorders: Diagnostic Decision Tree 1.....	21
2. Diagnostic Criteria for Temporomandibular Disorders: Diagnostic Decision Tree 2.....	22
3. Prototypes of Four Asymmetric Subtypes and Illustration of PA Cephalometric Tracing.....	28
4. Masseter Muscle Sample Collection.....	33
5. Mean Fiber Area, Proportion and Percent Occupancy of the Fiber Types in Vastus Lateralis and Masseter Muscle.....	35
6. Immunostaining of Serial Sections of Masseter Muscle Biopsy.....	36
7. Amplification Plots and Standard Curves for the <i>PITX2</i> and <i>ENPP1</i> Genes.....	39
8. Amplification Plots and Standard Curves for the <i>ESR1</i> Gene .....	40
9. Histogram of Cephalometric Measurement Comparisons by Different Asymmetry Groups.....	44
10. Left-Right Percent Difference of Fiber Type Area and <i>PITX2</i> Correlation.....	53
11. Left-Right Percent Difference of Fiber Type Area and <i>ENPP1</i> Correlation.....	54
12. Left-Right Percent Difference of Fiber Type Area and <i>ESR1</i> Correlation .....	54
13. Left-Right Percent Difference of Fiber Type Occupancy and <i>PITX2</i> Correlation.....	55
14. Left-Right Percent Difference of Fiber Type Occupancy and <i>ENPP1</i> Correlation.....	55
15. Left-Right Percent Difference of Fiber Type Occupancy and <i>ESR1</i> Correlation.....	56

## LIST OF TABLES

Table	Page
1. Landmarks used for PA cephalometric analysis .....	29
2. Measurements used for evaluation of asymmetry in the maxilla and mandible .....	30
3. Amplification Properties for <i>HPRT1</i> , <i>PITX2</i> , and <i>ENPPI</i> .....	39
4. Amplification Properties for <i>HPRT1</i> and <i>ESR1</i> .....	40
5. Cephalometric measurement comparison between symmetric and asymmetric subjects and statistical results .....	44
6. Average <i>PITX2</i> Expression .....	45
7. Percent Difference <i>PITX2</i> Expression .....	46
8. Average <i>ENPPI</i> Expression.....	46
9. Percent Difference <i>ENPPI</i> Expression.....	47
10. Average <i>ESR1</i> Expression.....	47
11. Percent Difference <i>ESR1</i> Expression.....	48
12. Left-Right Percent Difference of Type I Mean Fiber Area.....	49
13. Left-Right Percent Difference of Type I/II Hybrid Mean Fiber Area .....	49
14. Left-Right Percent Difference of Type II Mean Fiber Area .....	49
15. Left-Right Percent Difference of Type I Percent Occupancy .....	50
16. Left-Right Percent Difference of Type I/II Hybrid Percent Occupancy.....	50
17. Left-Right Percent Difference of Type II Percent Occupancy .....	51
18. Percentage of DC-TMD Diagnosis Among Asymmetry Classification Groups.....	51
19. Pre-Surgical JPF Scores in Asymmetry Classification Groups.....	52

20. Percent Difference in Fiber Area vs. Percent Difference in RQ Gene Expression Between Left and Right Sides .....	53
21. Percent Difference in Fiber Type Occupancy vs. Percent Difference in RQ Gene Expression Between Left and Right Sides.....	55
22. Average <i>PITX2</i> Expression in DC-TMD Subgroups.....	57
23. Percent Difference <i>PITX2</i> Expression in DC-TMD Subgroups.....	57
24. Average <i>ENPP1</i> Expression in DC-TMD Subgroups .....	57
25. Percent Difference <i>ENPP1</i> Expression in DC-TMD Subgroups .....	58
26. Average <i>ESR1</i> Expression in DC-TMD Subgroups .....	58
27. Percent Difference <i>ESR1</i> Expression in DC-TMD Subgroups .....	58
28. JPF Scores and Average RQ Expression in Asymmetry Classifications .....	59
29. JPF Scores and Percent Difference RQ Expression in Asymmetry Classifications.....	59

# CHAPTER 1

## INTRODUCTION

Craniofacial asymmetry is a complex trait condition, developing from interplay of genetic and environmental influences (Miller, 2014). Most asymmetries commonly found in patients with skeletal malocclusions are rarely considered unaesthetic. However, some patients with facial asymmetry as a result of severe dentofacial disorders may elect to undergo orthodontic treatment and orthognathic surgery to correct their malocclusion. Causes of serious facial asymmetry that require corrective surgery include pathologies, such as craniofacial anomalies, trauma, arthritis, condylar aplasia, and ocular hypertelorism (Proffit et al., 1980). The incidence of facial asymmetry in certain groups of individuals suggests evidence of a genetic influence; yet investigations into specific genetic causes of craniofacial asymmetry have been limited (Severt & Proffit, 1997).

Masticatory muscles are frequently involved in development of sagittal malocclusion. The paired masseter muscles, like other skeletal muscles, are composed of fibers that are classified into functionally and biochemically distinct phenotypes, whose properties are influenced by genetic variations (Sciote et al., 1994). A significant difference has been identified in type II (fast) fiber occupancy between left and right masseter muscle samples from patients with mandibular asymmetry in an orthognathic surgery population (Raoul et al., 2011). Specifically, type II occupancy was increased on the same facial side where the asymmetry deviation occurred.

Genotyping, the determination of genetic constitution in individuals, has been applied to particular genes of interest in malocclusion subjects. The single nucleotide

polymorphism (SNP) 577XX is a nonsense mutation producing a stop codon in the cytoskeletal protein gene for Actinin Alpha-3 (*ACTN3*), causing diminution of translated product. Instead of promoting a debilitating disorder in skeletal muscle, however, loss of the Actinin Alpha-3 protein results in lower muscle strength and power in 577XX individuals (Lek et al., 2009). In a genotyping study of an orthognathic surgery population, Zebrick et al., (2014) demonstrated that *ACTN3* 577XX was preferentially found in subjects with skeletal Class II malocclusion, indicating an association between differential masticatory muscle function and vertical skeletal dimensions.

Evidence also suggests that genotype and gene expression levels of particular genes of interest, along masticatory muscle fiber-type properties, are all interrelated in patients with craniofacial asymmetry. Patterns of normal symmetry involve many genes that when altered in form and/or expression, may cause breaking of developmental patterns to promote resultant asymmetry. For example, the Nodal signal transduction pathway provides significant information for positional development and patterning during embryogenesis. In a study of Nodal signaling pathway genes, Nicot et al. (2014) reported that Paired-like Homeodomain Transcription Factor 2 (*PITX2*) may be down regulated during development of facial asymmetry. *PITX2* is an upstream effector of Nodal Growth Differentiation Factor (NODAL) and Left-Right Determination Factor (LEFTY) genes in the signaling pathway. In this same study, *PITX2* was found to be differentially expressed between left and right side masseter muscles in adult humans with facial asymmetry.

The same combination of genetic input along with muscle fiber composition may also interact to associate craniofacial asymmetry with temporomandibular joint disorders (TMD). Pain in the temporomandibular joint or masticatory muscles is a common and often

debilitating comorbid condition, estimated to occur in over 50% of patients with facial asymmetry (Dhalberg et al., 1995). Data from Nicot et al. (2016) indicates that the AA genotype of SNP rs1643821 in the Estrogen Receptor- $\alpha$  (*ESR1*) gene associates as a risk factor for dysfunctional worsening of TMD after orthognathic surgery. In contrast, the TT genotype of SNP rs858339 in the Ectonucleotide Pyrophosphatase Phosphodiesterase-1 (*ENPP1*) gene may provide protection against TMD in patients with dentofacial deformities.

To identify overall genetic contributions to skeletal asymmetry, we developed etiologic-based classifications of craniofacial phenotypes that recognizes four groups with distinctive patterns of asymmetric growth. Gene expression data for masseter muscle *PITX2*, *ENPP1* and *ESR1* are assigned to these four distinct classes of this phenomics database. RNA from masseter muscle samples, obtained at the time of the corrective orthognathic surgery, is used for the analysis. Thus, data collected in the same patient population is used to characterize genetic associations between malocclusion, facial asymmetry and TMD.

To more fully understand how *PITX2*, *ENPP1* and *ESR1* expression and muscle fiber type contribute to craniofacial asymmetry and temporomandibular joint disorders, additional genetic studies are needed. In the present study, we explore associations between these genes, fiber type properties, subclassifications of asymmetry, patient reported symptoms of TMD, and clinician diagnosed TMD. Quantitative data will be generated and used to determine possible associations between genetic and fiber-type characteristics and craniofacial discrepancies among different phenotypic classes of surgical subjects with severe malocclusions. Any associations that are identified will be tested for statistical

significance and discussed within the context of diagnostic information about the occurrence and manifestation of symptoms of malocclusion in orthodontic patients.

## **CHAPTER 2**

### **REVIEW OF LITERATURE**

#### **2.1 Craniofacial Asymmetry**

In the human body, symmetry is the balanced distribution of homologous structures and asymmetry is the lack of proportionality between duplicate body parts. When applied to the human face, asymmetry refers to an imbalance and dissimilarity between the left and right sides. Facial asymmetry is a common characteristic of the human face, with reported prevalence of 21-85% (Severt & Proffit, 1997). It is a naturally occurring phenomenon and to a degree is considered normal and acceptable. Slight asymmetry of the face, also known as relative symmetry, subclinical asymmetry, or normal asymmetry, remains unperceived by most people (Thiesen & Kim, 2016).

##### **2.1.1 Facial Esthetics**

The study of facial esthetics is paramount to the specialty of orthodontics, as the goals of orthodontic treatment often include esthetic improvement. Facial esthetics are frequently associated with facial symmetry (Baudouin & Tiberghien, 2004). Literature shows facial symmetry is an essential factor in attractiveness (Thornhill & Gangestad, 1999). Facial esthetics in terms of symmetry and balance refers to the state of facial equilibrium, the correspondence in size, form and arrangement of facial features (Shah & Joshi, 1978). A perfectly bilateral and symmetric face rarely exists in the human population (Lindauer, 1998). A slight skeletal and facial asymmetry can be found in normal individuals, including those with esthetically pleasing faces. Some literature suggests that

an extent of asymmetry actually serves to characterize and individualize the esthetically pleasing face rather than to disfigure it (Peck & Peck, 1991).

### **2.1.2 Asymmetry in Human Development**

During human development, the body develops with bilateral symmetry across the sagittal plane, implying right and left sides are identical mirror images. However, both biological and environmental factors result in the formation of asymmetries. Structural asymmetry and right-left differences occur as part of normal development.

This laterality is well illustrated by right vs. left facedness. Facedness, or facial asymmetry, refers to the differences in the left and right side of the face. The term indicates greater muscular control and intensity of expression on one side of the face relative to the other (Borod et al., 1981). While, the cause of such laterality remains unknown, studies suggest the differences in size of the hemiface as a possible cause. Haraguchi et al. (2008) examined facial laterality in 1800 Japanese subjects. The study focused on two perspectives: which side of the hemiface is most likely to be wider and which side does the chin tend to deviate. Results indicated 79.7% of the subjects had a wider right hemiface and 79.3% of the subjects had a chin-deviation to the left. These results are consistent with multiple previous studies reporting a wider hemiface on the right compared to the left (Burke et al., 1979; Koff et al., 1981; Farkas et al., 1981; Koff et al., 1985).

### **2.1.3 Complex Etiology of Facial Asymmetry**

In the literature, a number of causal factors are discussed in the development of facial asymmetries. According to Severt and Proffit (1997), asymmetry affects the upper third facial region in five percent of cases, the middle third region in 36% of cases, and the

lower third region in 74% of cases. Deviation of the lower face, particularly the chin, is the most frequent facial asymmetry, which may be attributed to the longer span of postnatal growth. Chia et al. (2008) suggested mandibular asymmetries have pathological, traumatic, functional or development causal factors. Developmental factors included hemimandibular elongation, hemimandibular hyperplasia, hemifacial microsomia, hemifacial hypertrophy, hemifacial atrophy, torticollis, and achondroplasia. Pathological factors include tumors and cysts, infection and condylar resorption. Traumatic factors consisted of condylar fractures and functional factors consisted of mandibular displacement.

Lundstrom et al. (1961) reported facial asymmetries could be of genetic etiology, non-genetic etiology, or a combination of the two. Similarly, Haraguchi et al. (2008) grouped facial asymmetries into hereditary factors of prenatal origin and acquired factors of postnatal origin. Despite multiple known causes, the etiology remains unknown in many cases of asymmetry. In these idiopathic cases, it is termed asymmetry of development, and typically does not appear at an early age. These asymmetries appear gradually throughout craniofacial development, usually becoming apparent in the teenage years (Cheong & Lo, 2011).

#### **2.1.4 Diagnosis and Current Classifications**

Based on the craniofacial structures involved, facial asymmetry can be classified as dental, skeletal, muscular or functional (Bishara et al., 1994). In order to properly diagnose the asymmetry, a comprehensive evaluation consisting of patient history, clinical examination, photography, radiographs, and sometimes 3-dimensional computed tomography is necessary (Cheong & Lo, 2011). Skeletal asymmetry can be masked by the

overlying soft tissues making the assessment of soft-tissue morphology an essential part of the assessment of facial asymmetry. The clinical examination allows the clinician to evaluate the asymmetry in the sagittal, coronal and vertical planes. The dental midline should be evaluated with an open mouth, in centric relation, at initial contact and in centric occlusion to detect true dental and skeletal asymmetry or a mandibular functional shift (Cheong & Lo, 2011).

The clinical examination should be supplemented by photographs and conventional diagnostic radiographs. Posterioranterior cephalograms and submentovertex projections are important diagnostic tools for the assessment of facial asymmetry. Cephalometric radiographs are useful for an objective diagnosis of oral and maxillofacial deformities and treatment planning orthognathic surgery. In orthodontics, there have been many approaches for classification of skeletal asymmetry utilizing either posterior anterior cephalograms or submentovortex radiographs; however, there is not a universally accepted method or classification system.

Focusing on mandibular changes, Bruce and Hayward classified mandibular asymmetry into three distinct groups: deviation prognathism, unilateral condylar hyperplasia and unilateral macrognathism (1968). Obwegeser and Makek also emphasized mandibular changes and classified asymmetries into two categories: hemimandibular elongation or hemimandibular hyperplasia. Hemimandibular elongation occurs as a result of an increase of the condyle or the ramus in the vertical plane, or the mandibular body in the horizontal plane; while, hemimandibular hyperplasia occurs as a result of an increase on one side of the mandible as a whole (1986).

Hwang developed a classification system based on skeletal analysis of deviation of the chin and bilateral difference between mandibular rami length. He established four types of asymmetry: patients with bilateral difference between mandibular rami length, patients with deviation of the chin, patients with both bilateral difference between mandibular rami length and deviation of the chin, and patient with changes in volume on one side of the mandible without deviation of the chin or discrepancy between mandibular rami length (2007).

Most recently, Baek et al. analyzed skeletal structures with computed tomography and considered the entire facial asymmetry, including maxillary and mandibular asymmetries (2012). They divided patients into four distinct groups based on their anatomic features, which arise from different growth imbalances of the jaws, teeth, nasal septum and cranial base. Group 1 included subjects with a shift or lateralization of the mandible, Group 2 included subjects with a difference in left and right ramus height, Group 3 included subjects with atypical asymmetry, and Group 4 included subjects with a C-shaped asymmetry. The Baek classification could help remove much of the previous diagnostic uncertainty, since asymmetry can be masked by variations in head posture, canting of the occlusal plane or other dental and soft tissue compensations.

### **2.1.5 Management of Facial Asymmetry**

In the overall population, facial asymmetry presents subclinically and rarely requires treatment; however, in a small subset of the population, significant facial asymmetry causes both functional and esthetic problems. There is no definable point when normal asymmetry becomes abnormal asymmetry. The limit between what is acceptable

and unacceptable is not clear. Several studies suggest a skeletal deviation equal to or greater than 4 mm renders an asymmetry visible in an individual's face (Masuoka et al., 2007; Silva et al., 2011; Lee et al., 2014). Depending on the age of the patient and severity of deformity, therapeutic approaches include asymmetric mechanics, asymmetric extractions, or orthognathic surgery (Burstone, 1998). In cases with mild dentofacial deformities, the mild asymmetry rarely requires surgical treatment, as it is masked by the soft-tissue envelope, dental compensation and change in head posture (Burstone, 1998). In cases with severe dentofacial deformities, patients may elect to undergo treatment and orthognathic surgery to correct the malocclusion.

## **2.2 Genetic Role in Asymmetry**

Human embryos begin development with bilateral symmetry across the sagittal plane. Externally, the vertebrate body appears bilaterally symmetric; however, internal organs are arranged significantly asymmetric across the midline. During embryogenesis, the generation of left-right sidedness occurs in reference to the embryonic midline and translates into the asymmetric development and placement of visceral organs. The development of consistent asymmetry along the left-right axis is a widespread and highly conserved feature of almost all vertebrate (Palmer, 2004). Understanding the genetic role in breaking of symmetry and formation of chirality provides valuable information for the biomedicine of a wide range of birth defects and human genetic syndromes (Levin, 2004).

### **2.2.1 Breaking of Symmetry**

Embryogenesis, a complex process involving the formation and development of the embryo, occurs during the first eight weeks following fertilization. As cells divide and differentiate, a single celled zygote evolves into a fetus. During the germinal stage, a zygote rapidly divides to form a blastocyst that is implanted in the uterus. Following implantation and during the third week of embryogenesis, the formation of the primitive streak occurs from the caudal end towards the rostral end. The primitive streak establishes bilateral symmetry by defining the midline of the body and creating left and right mirror images. In addition, the streak initiates germ layer formation and determines the site of gastrulation. The embryo is reorganized into three layers: the ectoderm, the endoderm, and the mesoderm. Each germ layer continues to differentiate in specific organs and structures. Beneath the primitive streak at the cephalic end, the mesoderm forms the notochord, a defining structure of chordates that forms the midline axis and serves as a source of midline signals to pattern surrounding tissues in development (Stemple, 2005). The primitive node induces ectoderm to differentiate into the neural plate, which extends the length of the rostral-caudal axis. As the neural plate develops, it forms the neural tube and neural crest. The neural tube differentiates into the brain and spinal cord, while the neural crest differentiates into many different cell types.

In the later stages of gastrulation and early stages of neurulation, there is a breaking of symmetry to establish a consistent asymmetry, as shown in the shape and placement of organs. Embryonic morphogenesis occurs along three axes: anterior-posterior, dorsal-ventral and left-right. The pattern formation of the left-right axis is fundamentally different from anterior-posterior and dorsal-ventral, as there are no known macroscopic force of nature that differentiates left and right (Levin, 2004).

Although no mechanism is conclusively shown to initiate left-right patterning, it is thought that establishing consistent asymmetry occurs in three major phases. First, the left-right axis is oriented with respect to the anterior-posterior and dorsal-ventral axes. Errors in this process can result in a loss of asymmetry, such as midline heart, polysplenia, or asplenia (Vandenberg and Levin 2009). Following the initial symmetry breaking event, a differential expression of genes occurs on each side of the midline, specifically involving genes from the Nodal pathway. The gene expression is amplified and transmitted prior to organogenesis, suggesting the Nodal cascade plays a role in left-right signals to developing organs (Levin and Mercola, 1998). During this stage, the midline acts as a barrier to keep left and right signals separate. In the third and final phase, the differential gene expression transfers positional information to developing organs. Errors during these signals lead to a loss of organs' interpretation of left-right information, leading to heterotaxia (Vandenberg and Levin 2009). Heterotaxia, also known as situs ambiguous, is a rare congenital defect resulting in abnormal distribution of major visceral organs. Situs inversus, a form of herteotaxy, results in the mirror image of the normal arrangement internal organs. Situs inversus occurs in 0.01% of the population and rarely results in medical complications (Splitt et al., 1996). The normal placement of visceral organs is known as situs solitus.

### **2.2.2 The Nodal Pathway**

During embryogenesis of chordate development, the activation of the Nodal pathway plays an important role in early pattern formation and differentiation. The Nodal

pathway, a complex series of signaling genes, functions to establish laterality in vertebrates through the induction of mesoderm and endoderm. Four highly conserved genes of the Nodal pathway, *NODAL*, *LEFTY1*, *LEFTY2* and *PITX2*, are asymmetrically expressed to the left of the midline of in the lateral plate mesoderm during embryogenesis in all vertebrates (Palmer, 2004).

*Nodal*, a transforming growth factor beta superfamily factor, determines left-right asymmetry through unilateral activation of downstream genes. Members of the *NODAL* gene family signal mesoderm and endoderm induction and neural patterning. The pathway is activated as the ligands bind to type I and type II serine-threonine kinase receptors and activate Smad2/Smad3 via phosphorylation. The Smad 4 complex forms transcriptional complexes in the nucleus, leading to the induction of *NODAL* and *LEFTY*. During left-right patterning, *NODAL* transcripts are expressed along the left lateral plate mesoderm. This is a highly conserved phase amongst all vertebrate embryos that have been studied, including the chick, mouse, zebrafish, quail and rabbit (Raya and Belmonte 2006). It is proposed the presence of *NODAL* signals determines 'left-sidedness', while the absence of *NODAL* signals determines 'right-sidedness' (Schier and Shen, 2000).

*NODAL* expression is regulated by left-right determination factors, *LEFTY1* and *LEFTY2*, which antagonize *NODAL* unction. Studies show *LEFTY* genes, which are also members of the transforming growth factor beta superfamily, provide an inhibitory effect on *Nodal* (Bisgrove et al. 1999, Cheng et al. 2000). *LEFTY* serves as a negative feedback inhibitor by binding to both the *Nodal* protein and receptors, while *NODAL* serves as a positive feedback to maintain its' own expression (Burdine and Schier 2000). *LEFTY2* inhibition functions to isolate *NODAL* to the left side of the midline only (Nakamura et al.,

2006). Both the positive and negative regulatory loops of *NODAL* expression play a role in the complex pathway involved in asymmetric organogenesis.

The highly conserved transcription factor *PITX2*, a downstream target of *NODAL* signaling, establishes the third stage of left-right patterning. *PITX2* expression is first observed at the onset of organogenesis and maintained throughout embryogenesis (Ryan et al., 1998). Similar to *NODAL*, *PITX2* plays a fundamental role in providing left-right cues in organogenesis through gradient density signaling and differential gene expression in the left lateral plate mesoderm. Asymmetric *NODAL* signals induce the activation of the paired-like homeodomain transcription factor 2, which is then regulated through the expression of *NODAL* and *LEFTY* genes. Overexpression of *NODAL* induces *PITX2* expression, while overexpression of *LEFTY* will inhibit *PITX2* expression (Logan et al., 1998 and Ryan et al., 1998).

*PITX2* is responsible for proper positioning of organs that are asymmetric across the left-right axis of the embryo. During the development and looping of both the heart and gastrointestinal tract, *PITX2* is detected only on the left side (Ryan et al., 1998). *PITX2* plays a central role in the development of mesoderm-derived first brachial arch structures, making it essential for the development of the human jaw complex. Also, it is necessary for cellular differentiation of pre-myoblast cells and the development of masticatory muscles. *PITX2* is up-regulated in adult muscle satellite cells to increase myogenic differentiation and allow for maintenance and repair of skeletal muscle (Knopp et al., 2013). In more recent studies, differential expression of *PITX2* has been identified between left and right side masticatory muscles in patients with facial asymmetry (Nicot et al., 2014).

### **2.3 Muscle Fiber Type Influence on Malocclusion**

Malocclusion often develops as a complex trait condition, which is influenced by combinations of transcription and growth factors acting on bone, teeth, and skeletal muscle (Sciote et al., 2013). General heritability estimates for muscle strength and bone length are relatively high (more than 80%); therefore, genetic contributions to growth of jaw bones and muscles are important determining factors in the etiology of malocclusion (Beunen et al., 2003; Tassopoulou-Fishell et al., 2012). Gene expression influences muscular growth and development, which in turn influences development and morphology of bone.

The composition of the muscles of mastication differs greatly from the composition of other skeletal muscles throughout the body (Laakso, 2008). The majority of skeletal muscle throughout the body are composed of three main fiber types: type I, type IIA, and IIX myosin heavy chain isoforms. In contrast, skeletal muscle of the masseter is composed of eight different fiber types: type I, IM, IIA, IIC and IIX fibers, neonatal, and atrial myosin fibers (Sciote, 1994). In addition to the complexity of the fiber type composition, the masseter muscle displays a wide variability of expression of these fiber types between individuals.

In healthy adult skeletal muscle, fibers can be classified based on their myofibrillar ATPase activity into three major groups: type I (slow-twitch), type IIA and type IIB (fast-twitch) (Brooke and Kaiser 1970). Different isoforms of myosin result in different contractile activity to fibers, therefore creating different shortening speeds and energy tension costs (Bottinelli & Reggiani, 2000). Type I fibers are slow contracting and fatigue resistant; and therefore, contribute to a large proportion of postural muscles. Type II fibers

are fast moving and highly fatigueable; and therefore, contribute to muscles requiring explosive, powerful movements. Sciote et al. subdivided type II fibers into type IIA fibers (fast and intermediate in tension cost) and type IIX fibers (fastest and least economic) (1994). The hybrid fibers, which are commonly found in masticatory muscle and rarely found in skeletal muscle, combine both slow and fast contractile properties (Sciote et al., 1994).

Muscle size is influenced by activity: increased activity leads to compensatory growth and decreased activity induces tissue atrophy. A change in the fibertype composition of muscles can be due to occurrences in development, alternate functional demand, age or pathology (Goldspink, 1980). During endurance training, there is an adaptive transition from type II to type I/II hybrid to type I fibers allowing for greater resistance to fatigue. Similarly, during resistance training, there is an adaptive transition from type I to type I/II hybrid to type II fibers (Schiaffino et al., 1994; Holloszy et al., 1976). In limb muscles, an increase in the proportion of hybrid fibers containing both fast and slow myosins is a response to changes in activity. Masticatory muscle is unusual in that a high proportion of hybrid fibers are commonly found, ranging from two isoforms to many possible combinations of isoforms (Rowlerson et al., 2005). The type I/II hybrids possess an intermediate physiologic capacity with characteristics of both type I and type II fibers and (Morris et al., 2001). Masticatory muscles are also unique due to a tendency for many of the type-II muscle fibers to be very small in diameter, whereas in most limb muscle they are similar in size or even larger than the type-I fibers (Sciote et al., 2013).

Previous masseter muscle biopsy studies show an increased size or proportion of type II fibers are associated with skeletal deep bite malocclusion, and a decreased size or

proportion of type II fibers are associated with skeletal open bite (Sciote et al., 2012; 2013). In addition to affecting the vertical dimension, fiber area and occupancy have also been shown to affect facial symmetry. Patients with mandibular asymmetry show an increase in type II fibers on the shorter side of the mandible, while individuals that were relatively symmetric did not have significant fiber type size or occupancy differences between their right and left masseter muscles (Sciote et al., 2013).

#### **2.4 Effects of *ENPPI* on Bone and Muscle**

There are recent findings for heritable influences on bone length and muscle strength phenotypes. Ectonucleotide pyrophosphatase/phosphodiesterase-1 (*ENPPI*), coded by the gene *ENPPI*, is a membrane-bound, nucleoside triphosphate pyrophosphohydrolase responsible for generating pyrophosphate by hydrolyzing nucleotides and nucleotide sugars (Evans et al., 1973; Terkeltaub et al., 1994). Mature osteoblasts and chondrocytes both express *ENPPI* and are responsible for bone growth and remodeling (Johnson et al., 1999; 2000). *ENPPI* is an important negative regulator of bone mineralization, and cultured osteoblasts with elevated *ENPPI* expression have reduced mineral formation (Mackenzie et al., 2012). Pyrophosphate exhibits an inhibition effect on hydroxyapatite crystallization and growth; and, through the expression of pyrophosphate, *ENPPI* plays an inhibitory role on hard and soft tissue mineralization (Fleisch et al., 1966; Register and Wutheier, 1985). Using microarray analysis, Yang et al. (2011) showed an increase in *ENPPI* expression has an inhibitory effect that reduces bone mineralization and growth.

In addition to the effects on bone, *ENPP1* down-regulates insulin signaling in cells by inhibiting the tyrosine kinase activity of the insulin receptor, leading to decreased signal transduction (Maddux and Goldfine, 2000). *ENPP1* is expressed in multiple tissues including three targets of insulin action: adipose tissue, skeletal muscle, and liver (Stefan et al., 2005). Pizzuti *et al.* (1999) first identified a single nucleotide polymorphism in *ENPP1* (rs1044498), in which lysine 121 is replaced by glutamine (K121Q) in a healthy, nonobese, nondiabetic Sicilian subjects. They identified a higher risk of being hyperinsulinemic and insulin resistant in the minor Q allele carriers. Further, a meta-analysis reported an association of the K121Q polymorphism and type 2 diabetes (Meyre et al., 2007). Using data from the Framingham Heart Study, Stolerman et al. (2008) studied associations between *ENPP1* variants and quantitative glycemic traits and confirmed the association of *ENPP1* K121Q with hyperglycemia. Additionally, they found a stronger association of K121Q with diabetes-related quantitative traits in people with a higher BMI.

## **2.5 Asymmetry and Temporomandibular Disorders**

According to the American Academy of Orofacial Pain (AAOP), temporomandibular disorders are a group of musculoskeletal and neuromuscular disorders, which involve the masticatory musculature, the temporomandibular joints and associated structures (de Leeuw and Klasser, 2013). They create a significant health problem affecting approximately 7-15% of the population (LeResche et al., 1997). The relationship between occlusion and TMD has been debated for a long time (Pullinger et al., 1993).

Patients with dentofacial deformities are reported to have a higher prevalence of temporomandibular disorders. Dhalberg et al. (1995) found an increased frequency of disc

displacement in patient with dentofacial anomalies. Kobayashi et al. (1999) identified a higher incidence of disc displacement in patients with mild protrusion and severe asymmetry of the mandible. Inui et al. (1999) evaluated frontal cephalograms in patients with internal derangement of the TMJ and concluded that facial asymmetry due to mandibular lateral displacement is a common problem in these individuals. Dujoncquoy et al. (2010) observed a higher prevalence of TMD in patients with maxilla-mandibular deformities. Finally, Takeshita, et al. (2013) noted increased TMD symptoms, including joint sounds (clicking or crepitus), pain, limited opening, and anterior disc displacement in patients with mandibular asymmetry.

### **2.5.1 Diagnostic Criteria for TMD**

The Research Diagnostic Criteria for Temporomandibular Disorders (RDC-TMD) was published in 1992 and was the most widely employed diagnostic protocol for TMD research. This dual-axis system included an Axis I physical assessment, using reliable and well-operationalized diagnostic criteria, and an Axis II assessment of psychosocial status and pain-related disability. In 2014, Schiffman updated the classification system with a new dual-axis Diagnostic Criteria for TMD (DC/TMD) to provide evidence-based criteria for the clinician to use when assessing patients, and to facilitate communication regarding consultations, referrals, and prognosis (Schiffman et al., 2014). The updated version utilizes short and simple screening instruments for Axis I and Axis II and these validated instruments allow for identification of patients with a range of simple to complex TMD presentations. The 12 common TMD include arthralgia, myalgia, local myalgia, myofascial pain, myofascial pain with referral, four disc displacement disorders, degenerative joint disease, subluxation, and headache attributed to TMD.

Axis I utilizes decision trees as diagnostic algorithms for the most common pain-related TMD as part of a comprehensive TMD taxonomic classification structure. (Figure 1 and 2). Axis II assesses pain intensity, pain disability, jaw functioning, psychosocial distress, parafunctional behaviors and widespread pain.

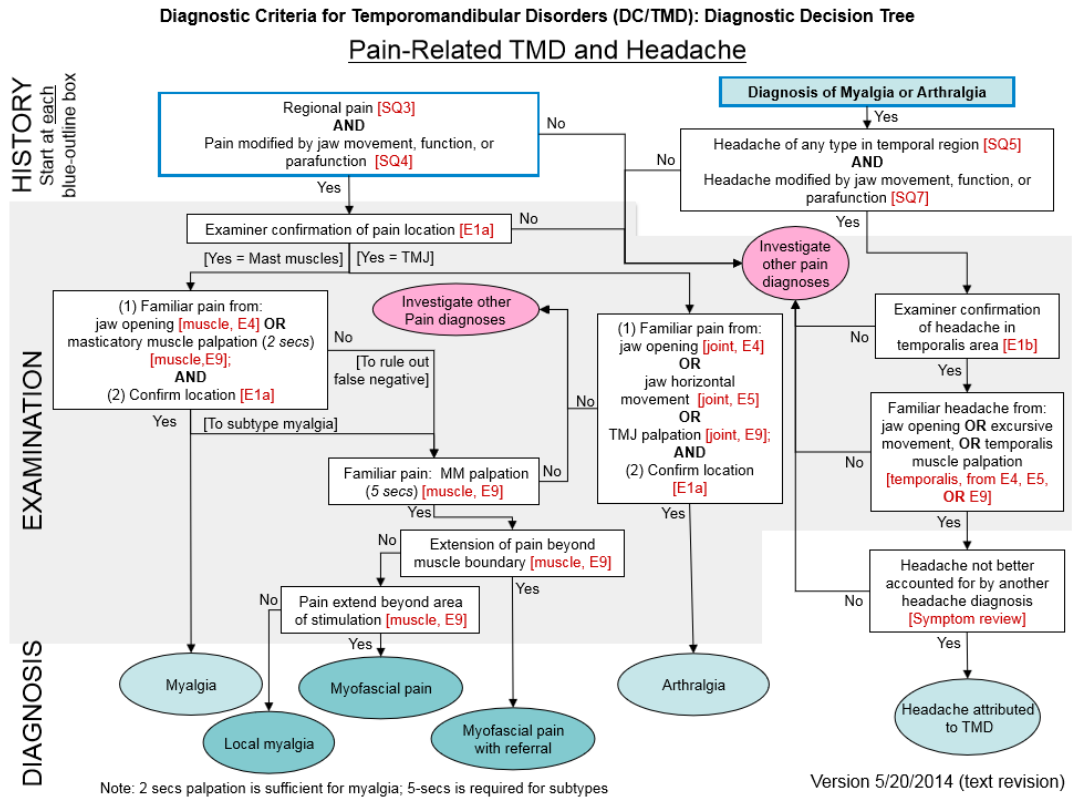


**Figure 1: Diagnostic Criteria for Temporomandibular Disorders: Diagnostic Decision Tree 1.** This diagram includes selection processes for identification of pain-related-TMD and headache. From: <http://www.rdc-tmdinternational.org/TMDAssessmentDiagnosis/DCTMD.aspx>

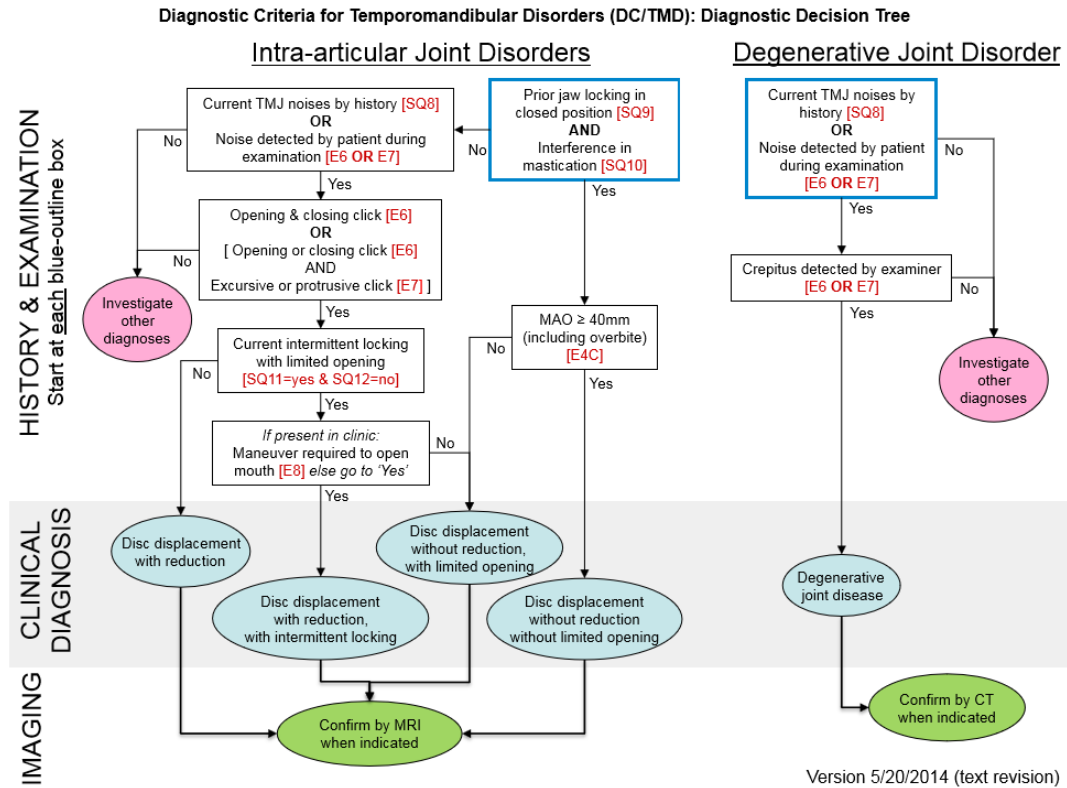


**Figure 2: Diagnostic Criteria for Temporomandibular Disorders: Diagnostic Decision Tree 2.** This diagram includes selection processes for identification of intra-articular and degenerative joint disorders. From: <http://www.rdctmdinternational.org/TMDAssessmentDiagnosis/DCTMD.aspx>

### 2.5.2 Jaw Pain and Function Analysis

The Jaw Pain and Function (JPF) Questionnaire was developed as a screening tool to determine presence or absence of TMD conditions with a self-rating scale for evidence of TMD. (Clark et al, 1989). It consists of 8 questions relating to jaw pain and 5 questions related to jaw function, with each question rated from 0 to 4 depending on the intensity of symptoms. (Gerstner et al., 1994; Undt et al., 2006). An example of the JPF questionnaire can be reviewed in Appendix A. The questionnaire has been validated to reliably

distinguish the detection of TMD when a cut off score of 6 is used for responses with 98% sensitivity and 100% specificity (Gerstner et al, 1994).

### **2.5.3. *ESRI* and TMD**

Temporomandibular joints disorders are multifactorial in etiology and the result of a complex and multifactorial pathogenesis. Increasing scientific evidence suggests that genetic factors play a significant role in the pathology of TMD. Temporomandibular joint disorders affect women with greater frequency than men; and, although the reasons for this female predominance have not been determined, sex hormones may contribute to this female predominance (Lee et al., 2006).

The role of estrogen in the occurrence of TMD has been investigated for many years. The estrogen receptor is a protein of the steroid receptors family, which acts through two receptors, estrogen receptor- $\alpha$  and estrogen receptor- $\beta$ , producing effects on the inflammatory process (McEwen & Alves, 1999). The role of estrogen via the  $\alpha$  receptor in the pathophysiology of TMD functions through the inflammatory response, bone mineralization and nervous system (Craft, 2007). Estrogen negatively regulates the production of interleukin-1 (Polan et al., 1988), interleukin-6 (Pottratz et al., 1994) and tumor necrosis factor  $\alpha$  (Ralston et al., 1990). The cytokines IL-1 and IL-6 are present in the TMJ synovium during inflammation (Kubota et al., 1998). The cytokines IL-1 and TNF- $\alpha$  promote cartilage reabsorption, inhibit synthesis of proteoglycans, and promote inflammation in the majority of TMD structures (Pettipher et al., 1986; Saklatvala, 1986).

Through the inflammatory component, estrogen can play an important role in pain severity and TMD predisposition. As a result, a genetic variation in *ESRI* could lead to

significant modifications in the physiological role of estrogen and consequently in TMJ derangements. Yamada et al. identified estrogen receptor- $\alpha$  in synovial cells, articular disc stromal cells and chondrocytes of the TMD in rats (2003). Abubaker et al. identified the presence of estrogen receptors at the TMJ disc in adult males and females by immunohistochemistry (1993). Ushiyama et al. confirmed the estrogen receptor- $\alpha$  as a fundamental biological mediator in the temporomandibular pathophysiology by transcriptomics (1999). More recently, Kim et al. identified significant associations between SNPs of ESR1 and symptoms of TMD (2010). The SNP rs1643821 of *ESR1* was also identified to be as risk factor for symptomatic worsening in a population of patients after orthognathic surgery (Nicot, 2016).

## CHAPTER 3

### AIMS OF THE INVESTIGATION

This project, conducted to fulfill the requirements for a MS in Oral Biology from Temple University Graduate School, investigates subclassifications of facial asymmetry, *PITX2*, *ENPP1*, and *ESR1* gene expression, fiber type properties and prevalence of TMD in a population of surgical patients. The purpose of this study is to utilize a newly developed asymmetry classification according to PA cephalograms and evaluate potential associations with differences in gene expression and fiber type properties in right and left masseter muscle samples; and, to evaluate gene expression with both patient reported symptoms and clinician diagnosed temporomandibular joint disorders in each of the asymmetric subtypes.

## **CHAPTER 4**

### **MATERIAL AND METHODS**

#### **4.1 Patient Population**

174 subjects undergoing orthodontic and maxillofacial surgery treatment for correction of malocclusion were recruited from the Universite de Lille Department of Oral and Maxillofacial Surgery. The subjects were identified from the dentofacial deformities population and were treatment planned to undergo mandibular or mandibular and maxillary osteotomies for correction of malocclusion with concurrent marked jaw discrepancies. Consent for subject participation was obtained according to human subject research protocols approved by the French Independent Ethical Committee and the Institutional Review Board Committees at the University of Pittsburgh and Temple University.

The patient population has a mean age of 25.7 years, majority female (76%), and a normal mixture of sagittal (66% Class II, 33% Class III) and vertical jaw deformations (75% open bite, 25% deep bite). Sagittal and vertical malocclusion classifications were based on the Delaire Cephalometric Analysis of lateral cephalograms, which is useful in planning the type of surgical repositioning needed to correct the malocclusion (Brevi et al., 2015). Patients with a history of facial trauma, arthritis, cancer, or any systemic or developmental conditions that might affect craniofacial growth are excluded. All subjects had a non-contributory medical history.

Pre-surgical patient records include de-identified demographics and posterior-anterior cephalograms, submentovertex and panoramic radiographs. Saliva samples were

collected prior to surgery and masseter muscle samples were obtained during the surgical procedure. TMD was assessed both clinically by examination and subjectively with a questionnaire.

#### **4.2 Assessment of Asymmetry**

A modification of the classification system of Baek et al. 2012 was used to classify our patients' skeletal asymmetry into one of four groups: Group 1 – lateralization of mandibular body only (“mandibular body asymmetry”); Group 2 – difference in ramus heights with menton deviation to the shorter ramus side (“ramus asymmetry”); Group 3 – difference in ramus heights with menton deviation to the longer ramus side, gonion contour more prominent on larger mandibular side and reverse maxillary canting (“atypical asymmetry”); Group 4 – difference in ramus heights with menton deviation to short ramus side and severe maxillary canting (“C-shaped asymmetry”) (Figure 3).

Since Baek's classification system was derived from CBCT images, we developed a posterior anterior cephalometric analysis, which allowed us to perform comparable measurements using digital two-dimensional images with Dolphin morphometric software. The cephalometric landmarks used are shown in Table 1. As described by Chung et al. (2017), six cephalometric measurements were used: occlusal plane tilt, maxillary canting (JR or JL to ZR or ZL), menton deviation (A to Me to MSR), mandibular width to midsagittal plane (AG or GA to MSR), mandibular width to menton (AG or GA to Me), and ramal height (Table 2).

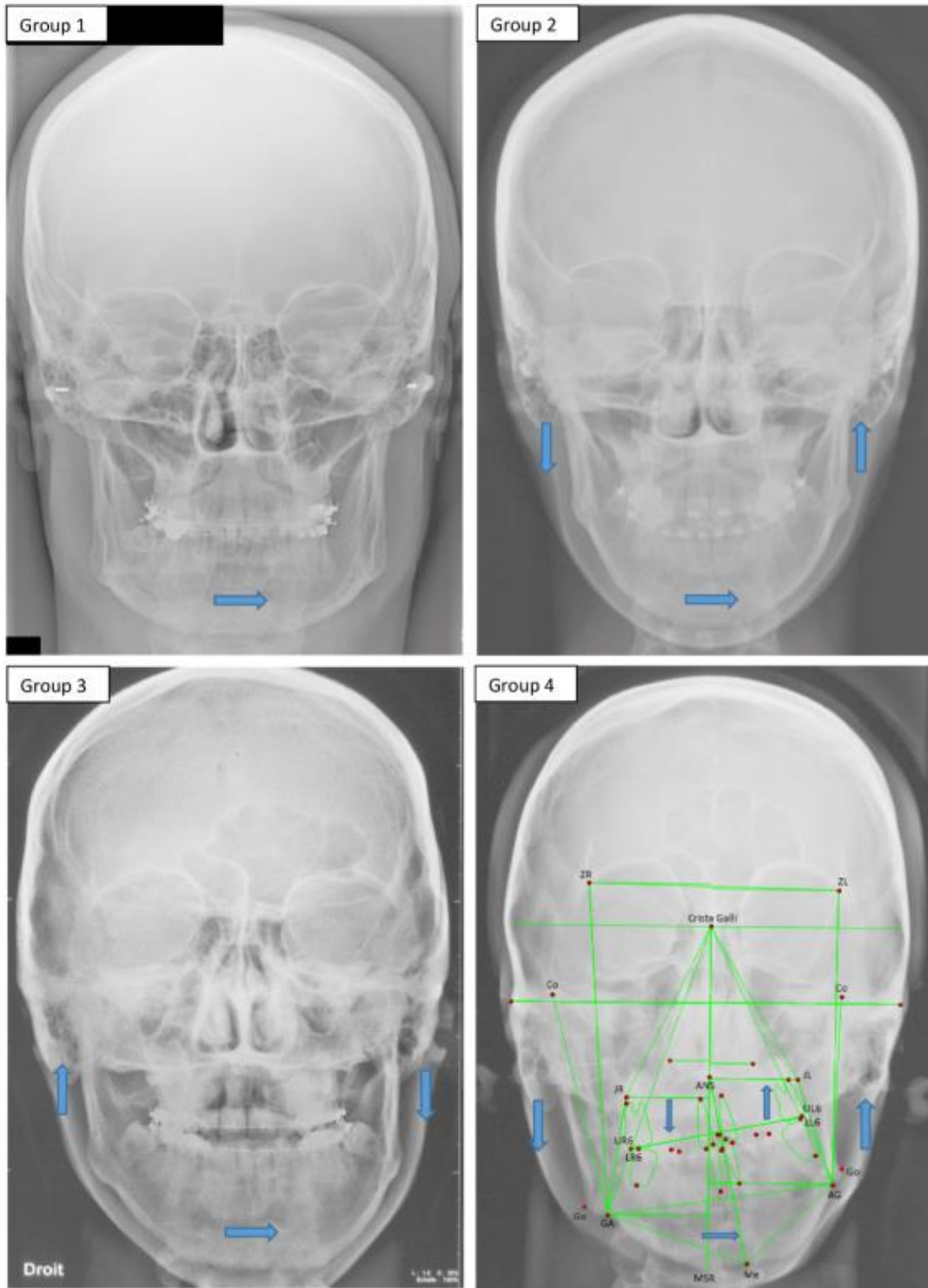


**Figure 3: Prototypes of Four Asymmetric Subtypes and Illustration of PA Cephalometric Tracing.** Group 1 – mandibular body asymmetry, Group 2 – ramus asymmetry, Group 3 – atypical asymmetry, and Group 4 – C-shaped asymmetry. Landmarks used for cephalometric analysis labeled in Group 4.

**Table 1: Landmarks used for PA cephalometric analysis**

Landmarks	Definitions
ANS	Anterior nasal spine
AG/GA	The highest point in the <u>antegonial</u> notch (left and right)
Co	<u>Condylion</u> ; Most superior point on condylar head
Crista <u>Galli</u>	Most superior point at its intersection with the sphenoid
<u>Gonion</u> /Most Lateral Ramus	Most inferior, posterior, and lateral point at the <u>gonial</u> angle of the mandible
JL/JR	Bilateral points on the <u>jugal</u> process at the intersection of the outline of the tuberosity of the maxilla and <u>zygomatic</u> buttress
Me	<u>Menton</u> ; most inferior point at <u>symphysis</u>
<u>Midsagittal</u> Plane	A plane bisecting the head and face through the crista <u>galli</u> , ANS, and genial tubercles in a symmetric face
Occlusal Plane	Horizontal line bisecting UR6 and LR6 as well as UL6 and LL6
UR6/UL6	Buccal cusp tip of right/left maxillary molar
LR6/LL6	Buccal cusp tip of right/left mandibular molar
ZL/ZR	Medial aspect of <u>frontozygomatic</u> suture (Bilateral)

**Table 2: Measurements used for evaluation of asymmetry in the maxilla and mandible**

Measurements	Definitions
<b>Maxilla:</b>	
Occlusal Plane Tilt (°)	Difference between Frankfort Horizontal and the horizontal line bisecting UR6 and LR6 as well as UL6 and LL6
Maxillary Canting JL or JR – ZL or ZR (mm)	Difference between vertical distance from left or right jugal process between left or right frontozygomatic suture
<b>Mandible:</b>	
Menton Deviation A-Me-MSR (°)	Angle formed between midsagittal plane and line going through ANS and menton
Mandibular Width to Midsagittal Plane GA or AG-MSR (mm)	Distance between left or right antegonial notch and midsagittal plane
Mandibular Width to Menton GA or AG-Menton (mm)	Distance between left or right antegonial notch and menton
Ramal Height (R or L) (mm)	Linear distance between condyion to most lateral ramus (gonion)

As described by previously, in the maxilla, occlusal plane tilt was determined by the difference between Frankfort Horizontal and the horizontal line bisecting the buccal cusp tips of UR6 and LR6, as well as the buccal cusp tips of UL6 and LL6, measured in degrees (°). If the occlusal plane tilt was greater than 2°, the subject was considered to have maxillary canting. To further verify the maxillary canting was skeletal in etiology, left and right vertical distances from jugal process and frontozygomatic suture were compared. If the difference between the left and the right side was greater than 3 mm, the subject was considered to have maxillary canting. In the mandible, menton deviation was determined by the angle between midsagittal plane and the line connecting ANS and menton. If the angle was greater than 2°, the subject was considered to have mandibular facial asymmetry with menton deviation. To compare the left and right mandibular width, the distance between antegonial notch and midsagittal plane was compared to the contralateral side. If

the difference was greater than 2 mm, it was considered to have mandibular deviation. We also measured the distance between antegonial notch and menton, and compared it with its' contralateral side. Again, if the difference was greater than 2mm, it was considered to have mandibular body asymmetry. Lastly, ramal height of left and right side was compared. If the difference between left and right side was greater than 3 mm, ramus asymmetry was diagnosed. Tests for measurement error included intra-rater reliability in cephalometric measurements by repeating cephalometric tracing on 10% of the radiographs by one examiner, which resulted in an  $R^2$  value of 0.98 (Chung et al., 2017).

### **4.3 Assessment of TMD**

Signs and symptoms of temporomandibular disorder were evaluated in all subjects at the time of the pre-surgical examination. TMD was assessed using the routine clinical examination done by the maxillofacial surgeons before surgical treatment and entered into the Diagnostic Criteria for Temporomandibular Disorders (DC/TMD) (Nicot et al , 2016). In addition, the Jaw Pain and Function (JPF) questionnaire was used to determine the presence and severity of TMD, as a subjective patient report. The questionnaire was first developed in English with the purpose to classify patients with tempomandibular disorder, those without tempomandibular disorder, and subjects with tension-type headaches; however, it was found the questionnaire could not distinguish TMD from those with muscular related headaches (Gerstner et al., 1994). The questionnaire was later translated into Germanic and French as a standard assessment of presence and severity of TMD (Undt et al., 2006; Nicot et al., 2006; Sciote et al., 2013). Crepitus, muscular pain from palpation, bruxism, and nail biting were signs and symptoms that were recorded as positive findings by the surgeons as part of their clinical exam. At the pre-surgery exam, TMD was

considered present if patients had a diagnosis of: myalgia, arthralgia or disc displacement with reduction; or positive subjective reporting of symptoms from a JPF score  $\geq 6$ . We narrowed our focus on myalgia, arthralgia and disc displacement with reduction, as they are the most common in our population. Subjects with positive clinical diagnosis for other, less common forms of TMD in our population were excluded from study.

#### **4.4 Muscle Samples**

During the surgeries, all subjects had at minimum a mandibular bilateral sagittal split osteotomy with Epker's technique, which separates the ascending branch of the mandible from the dental arch and mandibular body to permit repositioning of the mandible in to a better occlusal position after adaptive movement. Depending on the correction needed, it was sometimes necessary to cut the pterygo-masseteric sling to reposition and realign bones. A Tessier's distractor was used to completely separate the two bony pieces by more than one inch. During the procedure the deep portion of the masseter muscle was exposed, and muscle fibers are lacerated in the middle of the split (Figure 4). Before closing the surgical approach, these lacerated, exposed masseter muscle fibers are removed as clinical waste to avoid being interpositioned between the bony pieces or being caught in the suction drain. During this procedure, approximately  $0.5\text{cm}^3$  of masseter muscle tissue was excised on left and right sides from a consistent site in the middle of the deep layer 1.5 cm from the lowest point of the mandible's angle as described previously by Rowlerson et al. (2005).

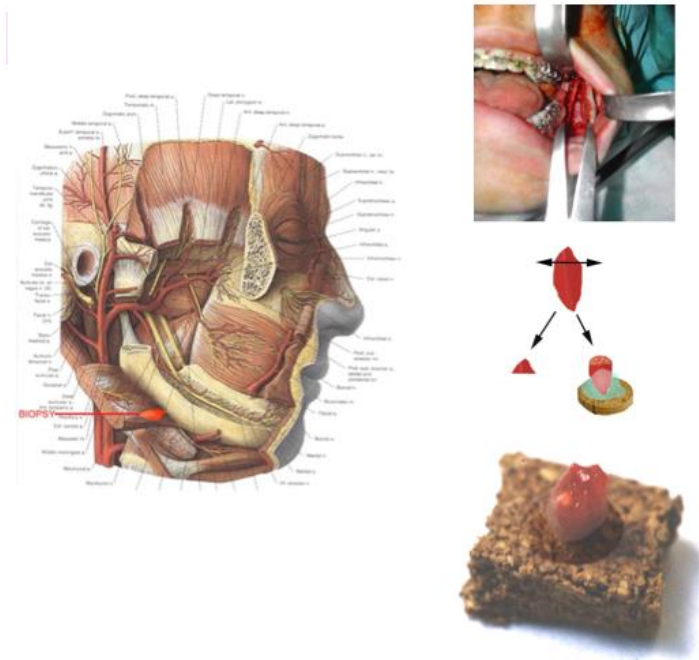


**Figure 4: Masseter Muscle Sample Collection.** Illustration of site of muscle sample taken during mandibular osteotomies performed on subjects. Lacerated muscle fibers were removed as clinical waste to avoid being interpositioned between the bony pieces or being caught in the suction drain.

The masseter muscle samples from left and right sides were mounted for sectioning, snap frozen in isopentane and stored at  $-80^{\circ}\text{C}$ . The samples were then transported on dry ice in lots of 60 specimens to Dr. Sciote's laboratory at the Kornberg School of Dentistry at Temple University. Upon arrival, muscle was stored at  $-80^{\circ}\text{C}$  prior to histologic analysis and gene expression.

#### 4.5 Masseter Muscle Fiber Type Analysis

Frozen masseter muscle samples were cryosectioned at  $10\ \mu\text{m}$  thickness to obtain serial cross sectional slices, and sections were mounted on glass microscope slides for immunostaining with five antibodies specific for myosin heavy chain (MyHC) isoforms: anti-type I, anti-type IIX, anti-type IIA, anti-type neonatal and anti- $\alpha$ -cardiac (atrial) as

described previously (Sciote et al., 1994; 1998). Masseter fibers were classified into 4 fiber type groups as type I, type I/II hybrid (containing both type I and II MyHCs), type II (containing only type IIA and/or IIX MyHCs), and type neonatal-atrial (containing the neonatal and/or  $\alpha$ -cardiac MyHCs in combination with other type I and II isoforms).

The relative number of fibers and fiber areas were measured, and mean fiber area (MFA) and percent occupancy (MPO) were calculated for fiber type I, type I/II hybrid and type II, as described previously (Rowlerson et al., 2005) (Figure 5). Although neo-atrial fibers are present, these fibers are rare and not studied in our analysis. For fiber type classification, only tissue section series with consistent antibody reactions for all stains and acceptable morphology of muscle fibers were used, while any tissue section series that did not have consistent antibody reactions for all stains or acceptable morphology of muscle fibers were discarded. Specific areas were identified on each of the serially immunostained sections, as shown in Figure 6. These areas were photographed in all relevant stained sections, and individual fibers were identified on serial images and classified by fiber type. Image J image-analysis software, available from the National Institutes of Health, was used to measure fiber type cross-sectional areas. The outer border of each fiber was traced to determine the average fiber area. Tests for measurement error included intra-rater reliability in determination of fiber area (one examiner repeated morphometric tracing of all fiber areas in one biopsy), which resulted in an  $R^2$  value of 0.94 (Rowlerson et al., 2005).

After the fiber area was measured, muscle fiber type percent occupancy was derived from the product of the average fiber number multiplied by average fiber diameter for each fiber type. The total fiber area for all the fiber types was summed, and each fiber type was

calculated to be a specific fraction of the total sum, which determined the overall percent tissue composition. This represented the fractional area of the sample occupied by that fiber type. To calculate the difference between sides as a percentage, the right and left values (either area or percent occupancy) were added together and divided by the larger value. The percent difference between the mean area and percent occupancy between right and left masseter muscle was calculated for each of the fiber types.

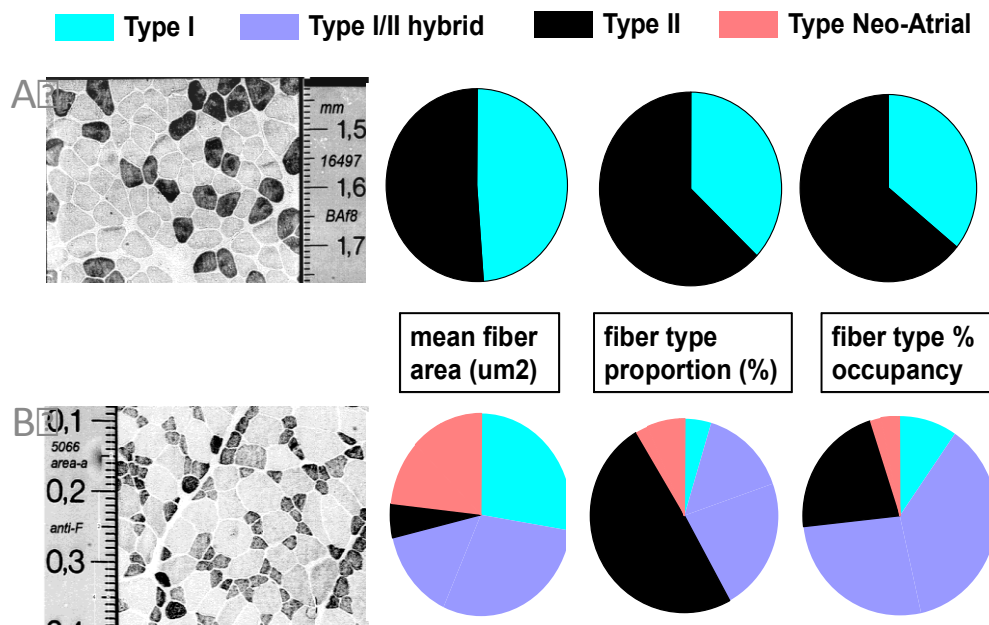


**Figure 5: Mean Fiber Area, Proportion and Percent Occupancy of the Fiber Types in Vastus Lateralis and Masseter Muscle. A.** Type I and type II fibers in vastus lateralis, **B.** Type I, type I/II hybrid, type II, and neo-atrial fibers in masseter muscle.

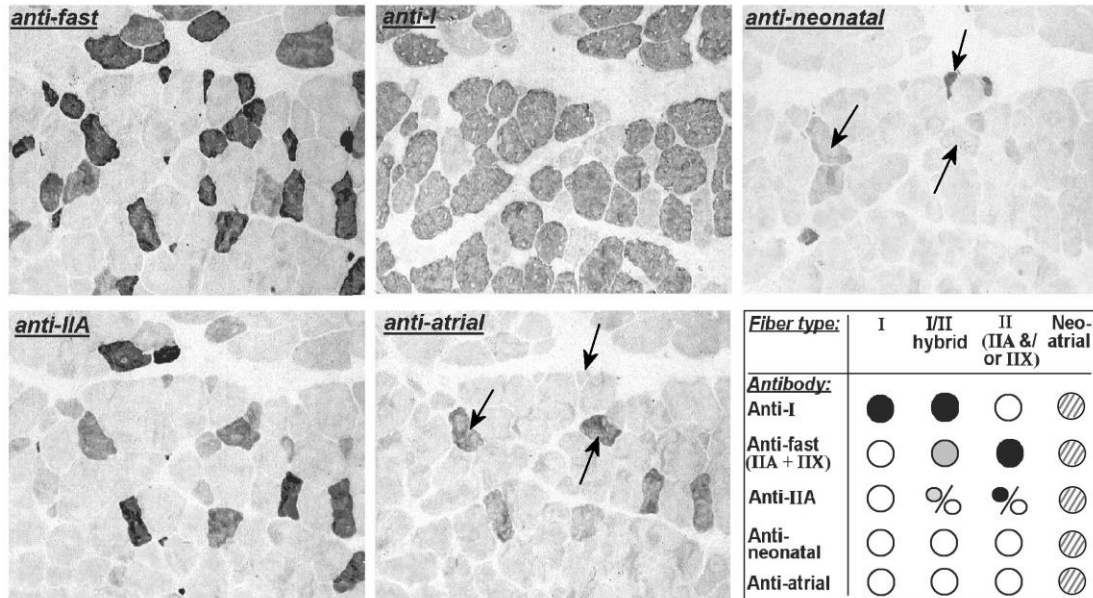


**Figure 6: Immunostaining of serial sections of masseter muscle biopsy.** Panels show staining with anti-fast, anti-IIA, anti-I, anti-atrial and anti-neonatal. Lower right panel shows staining profiles for type classification. Arrows indicate some fibers of neonatal/atrial category.

## 4.6 RT-PCR

### 4.6.1 Total RNA Isolation for RT-PCR

After cryosectioning, total RNA was isolated from the muscle biopsies with TRIzol as described previously (Horton et al., 2008). RNA was isolated from the remaining muscle by homogenizing with TRIzol™ reagent (Invitrogen, Carlsbad, CA). RNA extracts were resuspended in reaction buffer (10mM Tris-HCl, 2.5mM MgCl<sub>2</sub>, 0.5mM CaCl<sub>2</sub>, pH 7.6), digested with 10 U DNase I, and heated at 65° C to inactivate the enzyme. The digests were then re-isolated and purified with RNAqueous® (Ambion, Austin, TX). The presence and concentration of isolated RNA was verified and quantified by absorbance at A<sub>260</sub>.

### 4.6.2 RNA Quantification

RT-PCR was performed for the three genes selected for analysis. The genes of interest were an upstream regulator of *Nodal* (*PITX2*), insulin receptor inhibitor (*ENPPI*), and estrogen receptor (*ESR1*). *PITX2*, *ENPPI* and *ESR1* were quantified by TaqMan<sup>®</sup> (Applied Biosystems, Foster City, CA) quantitative real time PCR (qRT-PCR). The purified RNA was reverse transcribed to produce complimentary DNA, which was subsequently amplified by one-step PCR with primer probe sets specific for the genes of interest. Reverse transcription polymerase chain reaction (RT-PCR) assays were performed in triplicate for each of the genes. The TaqMan<sup>®</sup> RT-PCR protocol utilized commercial gene specific primer probe sets and an endogenous control gene hypoxanthine phosphoribosyltransferase 1 (*HPRT1*) in a RNA-to-C<sub>T</sub> 1-Step<sup>®</sup> reagent in an Applied Biosystems Step One Plus<sup>®</sup> instrument.

The *HPRT1* gene functions in the synthesis of purine nucleotides and is expressed in all human tissues, so it is considered a 'housekeeping' gene. RNA expressed as relative quantities were determined by the comparative threshold cycle ( $\Delta\Delta C_T$ ) method, which measures the fold difference between normalized quantities of target in the sample and in the reference standard (Livak & Schmittgen, 2001). This method allows for a comparison between the relative RNA quantities of the target sample with the RNA quantities of reference gene, which is constitutively expressed in all tissues.

For this method to be utilized accurately, standardized plots comparing the slopes of the genes of interest with *HPRT1* should be approximately parallel. Data from assays were considered reliable when standard curves were approximately parallel with slope values within 10% of one another and amplification efficiency for both the target genes and reference gene were greater than 90%. Commercial preparations of purified human

skeletal and liver muscle RNA (Ambion) were used as the standard controls or calibrators. Standard plots for amplification comparisons were made using 1, 10 and 100ng of skeletal and liver muscle RNA prepared by serial dilution.

Figure 7 shows amplification plots for the target genes, *PITX2* (Figure 7A) and *ENPPI* (Figure 7B), and the internal control gene *HPRT1* (Figure 7C), along with standard curves for each gene (Figure 7D). The standard curves in Figure 7D were approximately parallel for *HRPT1*, *PITX2*, and *ENPPI*. Arithmetic values for the amplification properties of the standard curves, summarized in Table 3, show that efficiency percent of amplification for the genes were within 10% of each other.

Figure 8 shows amplification plots for the target gene, *ENPPI* (Figure 8A), and the internal control gene *HPRT1* (Figure 8B), along with standard curves for each gene (Figure 8C). The standard curves in Figure 8C were approximately parallel for *HRPT1*, *PITX2*, and *ENPPI*. Arithmetic values for the amplification properties of the standard curves, summarized in Table 4, show that efficiency percent of amplification for the genes were within 10% of each other.

The standard curves for *PITX2*, *ENPPI*, and *ESR1* met the conditions for quantification by the  $\Delta\Delta\text{CT}$  method. These slopes had minor differences, but were considered to be parallel. Accordingly, all of the genes were amplified greater than 90%. The comparative CT (concentration threshold) method could be applied to quantify the gene expression in the masseter muscle samples, based on the results of this experiment.

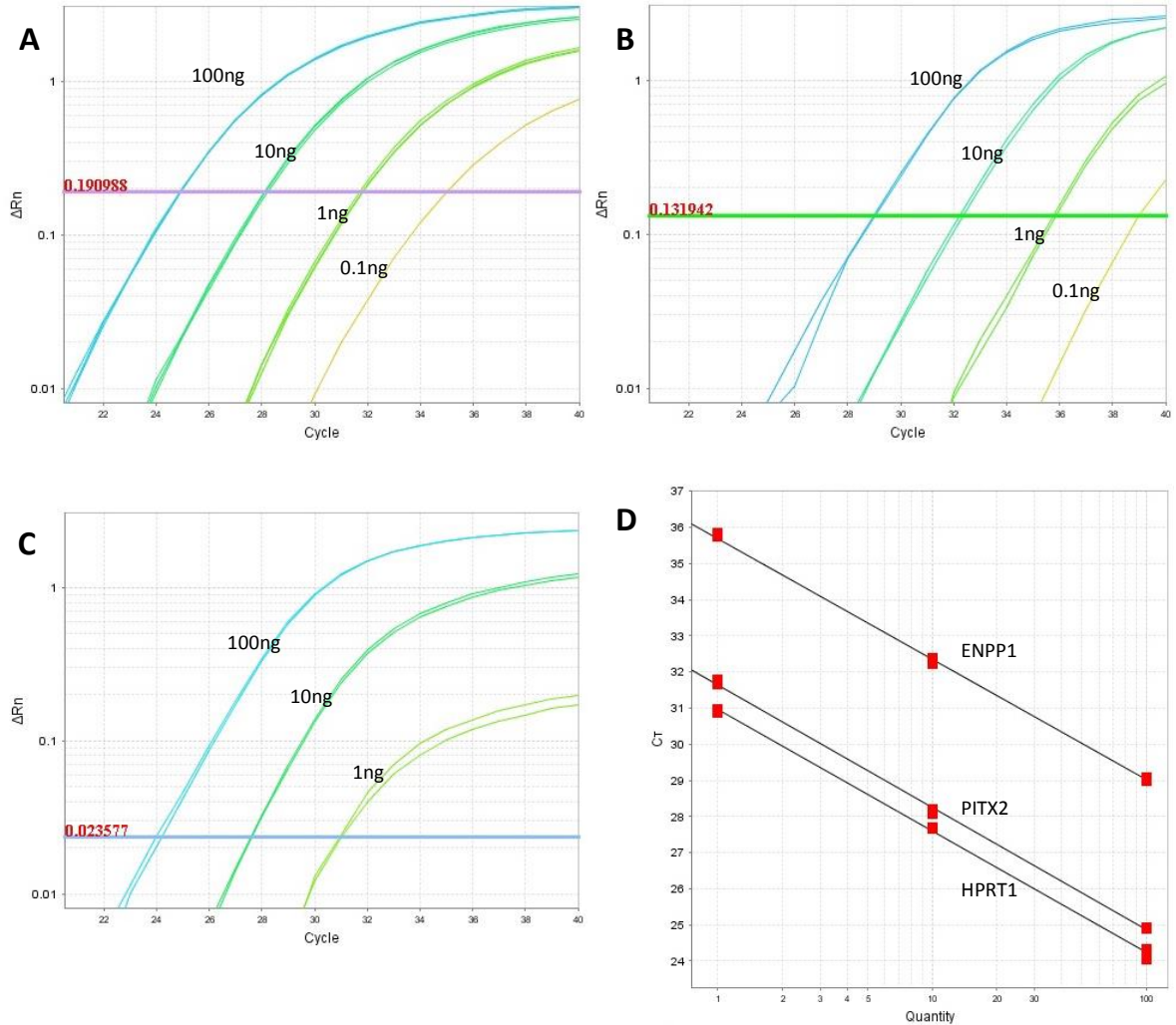


**Figure 7: Amplification Plots and Standard Curves for the *PITX2* and *ENPPI* Genes.** Plots were generated using 1ng, 10ng and 100ng of standard skeletal muscle RNA, **A.** *PITX2* (target gene), **B.** *ENPPI* (target gene), **C.** *HPRT1* (internal control) and **D.** standard curves for the three genes. Horizontal lines indicate the amplification threshold cycle for each plot.

**Table 3: Amplification Properties for *HPRT1*, *PITX2*, and *ENPPI***

Gene	Slope	Y-Intercept	R <sup>2</sup>	Efficiency %
<i>HPRT1</i>	-3.37	30.96	0.99	98.18
<i>PITX2</i>	-3.39	31.65	0.99	97.18
<i>ENPPI</i>	-3.33	35.70	0.99	99.53

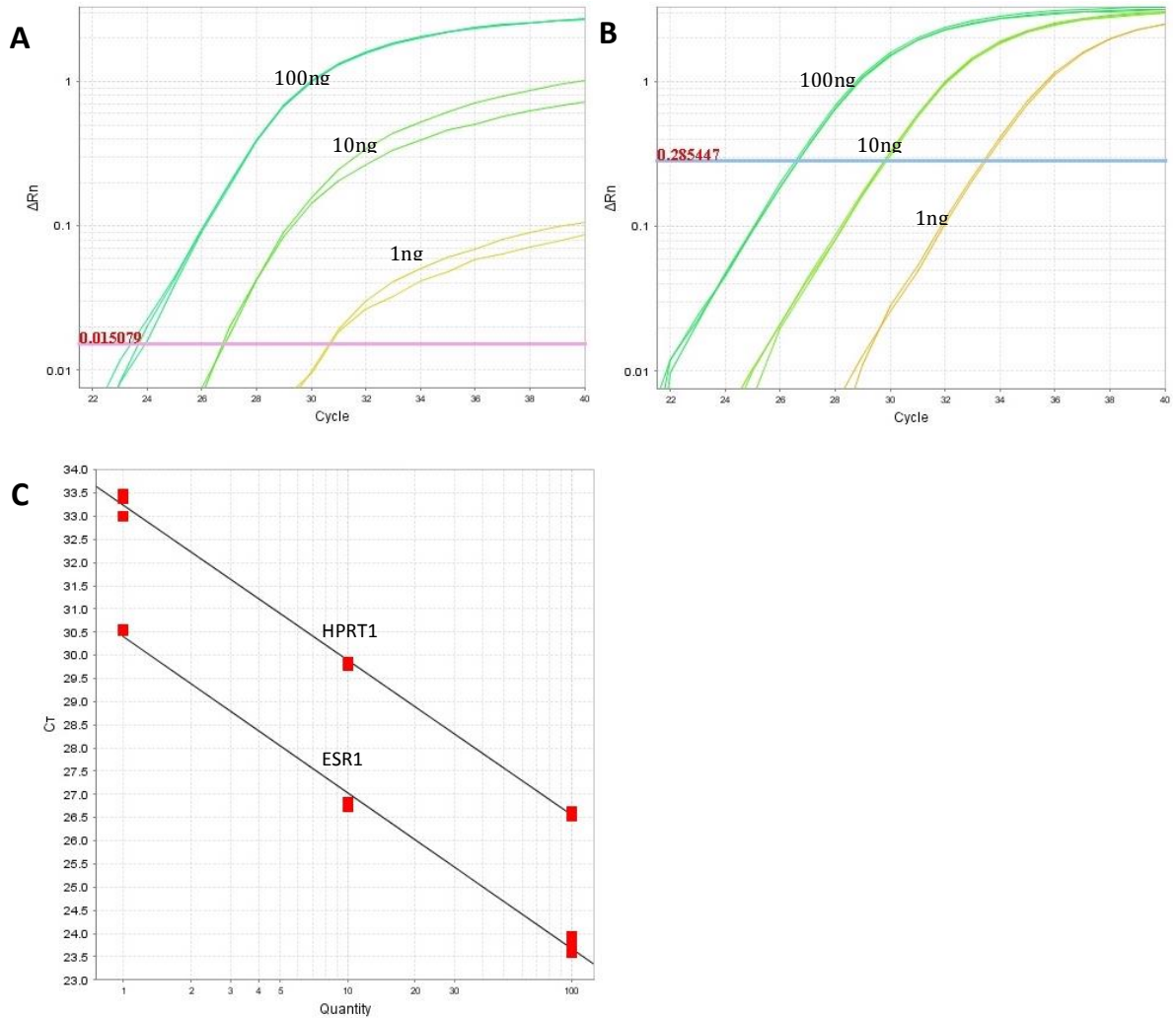


**Figure 8: Amplification Plots and Standard Curves for the *ESR1* Gene.** Plots were generated using 1ng, 10ng and 100ng of standard liver muscle RNA, **A.** *ESR1* (target gene), **B.** *HPRT1* (internal control), and **C.** standard curves for the two genes. Horizontal lines indicate the amplification threshold cycle for each plot.

**Table 4: Amplification Properties for *HPRT1* and *ESR1***

Gene	Slope	Y-Intercept	R <sup>2</sup>	Efficiency %
<i>HPRT1</i>	-3.34	33.24	0.99	99.223
<i>ESR1</i>	-3.37	30.42	0.99	98.052

After conditions were established with the initial tests, a reference calibrator (15ng of commercial skeletal muscle or 15ng of commercial liver muscle) was utilized for each assay and relative expression quantities of *PITX2*, *ENPP1*, and *ESR1* were determined using the  $\Delta\Delta CT$  method (Livak & Schmittgen, 2001). Using the following equation, the fold change in RNA expression was calculated:

1. Fold Change =  $2^{-\Delta\Delta CT}$  in which:
2.  $\Delta CT$  (Masseter Muscle Sample) = CT (PITX2, Masseter RNA) – CT (HPRT1, Masseter RNA)
3.  $\Delta CT$  (Masseter Muscle Sample) = CT (ENPP1, Masseter RNA) – CT (HPRT1, Masseter RNA)
4.  $\Delta CT$  (Masseter Muscle Sample) = CT (ESR1, Masseter RNA) – CT (HPRT1, Masseter RNA)
5.  $\Delta CT$  (Calibrator Skeletal Muscle Sample) = CT (PITX2, Skeletal Muscle RNA) – CT (HPRT1, Skeletal Muscle RNA)
6.  $\Delta CT$  (Calibrator Skeletal Muscle Sample) = CT (ENPP1, Skeletal Muscle RNA) – CT (HPRT1, Skeletal Muscle RNA)
7.  $\Delta CT$  (Calibrator Skeletal Muscle Sample) = CT (ESR1, Skeletal Muscle RNA) – CT (HPRT1, Liver Muscle RNA)
8.  $\Delta\Delta CT$  =  $\Delta CT$  (Masseter Muscle Sample) –  $\Delta CT$  (Commercial Skeletal Muscle Sample)
9.  $2^{-\Delta\Delta CT} = 2^{-[\Delta CT$  (Masseter Muscle Sample)– $\Delta CT$  (Commercial Skeletal Muscle Sample)]}

In these completed experiments, fold change data (i.e. fold change of expression in masseter muscle samples in comparison to the skeletal or liver muscle calibrator) are presented as relative quantities for comparison of *PITX2*, *ENPP1*, and *ESR1* expression between subjects. Relative quantity (RQ) values for expressivity of *PITX2*, *ENPP1*, and *ESR1* are the averages of triplicate assays of each masseter muscle sample. Relative quantity values were averaged between left and right masseter samples to determine the average gene expression values. To calculate the difference between sides as a percentage, the right and left values were added together and divided by the larger value. The percent difference (%  $\Delta n$ ) between left and right masseter samples were calculated to determine the differences in the relative quantity between sides.

#### **4.7 Statistical Analysis**

For comparisons between subclassifications of asymmetry, gene expression, fiber type, and TMD status, unpaired t-tests were used to determine if differences between two groups were significant. Analyses between averages of three or more groups were done by a one-way analysis of variance (ANOVA) to determine whether there were any significant differences. Pearson correlation coefficients were calculated to measure linear associations between variables. A  $p$ -value  $\leq 0.05$  was considered to be significant.

## CHAPTER 5

### RESULTS

#### 5.1 Results Overview

The patient population represented a normal demographic distribution of subjects seeking orthodontic and orthognathic surgery treatment of dentofacial deformity malocclusion from France. After identifying four anatomically different forms of asymmetry, we compared differences in *PITX*, *ENPP1* and *ESR1* gene expression, masseter muscle fiber type, clinician diagnosed TMD, and patient reported TMD symptoms in symmetric and asymmetric subtypes.

#### 5.2 Asymmetric Subclassifications

52% of patients were diagnosed as symmetric and 48% were diagnosed as asymmetric. As described by Chung et al. (2017), the asymmetric subjects were divided into the four subtypes utilizing 11 cephalometric anatomic landmarks and 6 cephalometric measurements (Table 1 and Table 2). The six PA cephalometric measurements were compared between symmetric and asymmetric patients using unpaired t-tests (Table 5). The six PA cephalometric measurements were compared across the four asymmetry groups using an ANOVA (Figure 9). Results of the PA cephalometric analysis demonstrated a significant difference in all six cephalometric measurements between symmetric and asymmetric patients.

**Table 5: Cephalometric measurement comparison between symmetric and asymmetric subjects and statistical results**

Measurements	Symmetric	Asymmetric	P value*
Occlusal Plane Tilt (°)	0.87 ± 0.59	1.36 ± 1.47	0.0040
Maxillary Canting JL or JR – ZL or ZR (mm)	0.68 ± 0.44	2.70 ± 5.17	0.0003
Menton Deviation A-Me-MSR (°)	0.31 ± 0.29	4.47 ± 2.10	<0.0001
Mandibular Width to Midsagittal Plane GA or AG-MSR (mm)	1.51 ± 1.31	14.2 ± 12.8	<0.0001
Mandibular Width to Menton GA or AG-Menton (mm)	1.51 ± 2.69	21.4 ± 14.9	<0.0001
Ramal Height (mm)	1.41 ± 0.79	14.5 ± 12.1	<0.0001

\*Unpaired t-test derived from mean and SD.

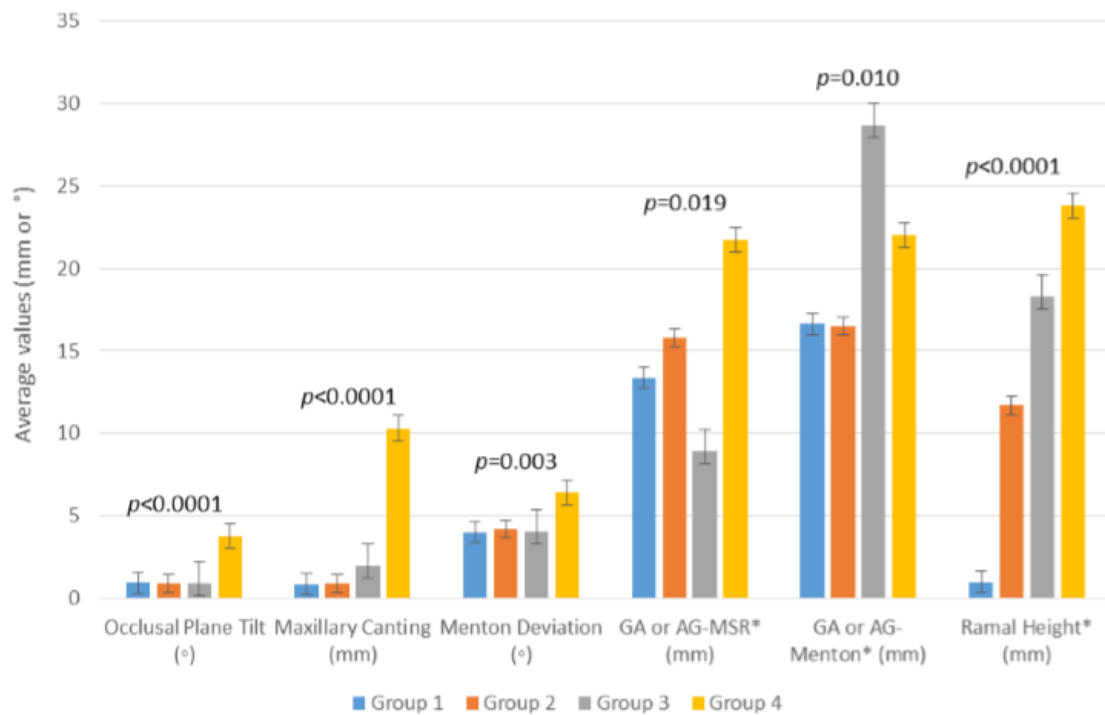


**Figure 9: Histogram of Cephalometric Measurement Comparisons by Different Asymmetry Groups.** Average values for each cephalometric measurement were compared across different asymmetry subgroups. Average values are expressed in mm for maxillary canting, GA or AG-MSR, GA or AG-Menton and ramal height, and degrees for occlusal plane tilt and menton deviation (Chung et al., 2017).

### 5.3 *PITX2*, *ENPP1* and *ESR1* Expression and Asymmetry Groups

The genes of interest were analyzed to characterize differential expression levels in masseter muscle samples. RT-PCR was performed on RNA from masseter muscle samples of the orthognathic surgery patients to quantify the three genes. The average expression and percent differences between left and right sides of the symmetric controls were compared to each of the asymmetric subclassifications with unpaired t-tests. The average expression and percent difference between left and right sides of symmetric controls and the four asymmetric subclassifications were compared by an ANOVA.

#### 5.3.1 *PITX2*

The average expression of *PITX2* (Table 6) and the percent difference between right and left sides of *PITX2* expression (Table 7) were statistically insignificant when comparing symmetric controls to all asymmetry subjects and to each of the asymmetric subclassifications with unpaired t-tests. An ANOVA analysis revealed no significant differences amongst the symmetric patients and asymmetry subclassifications for both average expression ( $p=0.65$ ) and percent difference in *PITX2* expression ( $p=0.93$ )

**Table 6: Average *PITX2* Expression**

Patient Diagnosis Groups	Average <i>PITX2</i> Expression	SD	n	<i>p</i> -value
Symmetric	1.18	0.45	28	-
Asymmetric	1.33	0.41	46	$p = 0.15$
Group 1	1.37	0.48	5	$p = 0.38$
Group 2	1.37	0.31	21	$p = 0.11$
Group 3	1.28	0.40	15	$p = 0.48$
Group 4	1.25	0.63	5	$p = 0.77$

**Table 7: Percent Difference PITX2 Expression**

Patient Diagnosis Groups	% Δn PITX2 Expression	SD	n	p-value
Symmetric	21.51	14.33	20	-
Asymmetric	21.39	22.01	39	$p = 0.98$
Group 1	12.76	8.87	3	$p = 0.32$
Group 2	19.42	21.41	19	$p = 0.72$
Group 3	26.03	25.20	12	$p = 0.52$
Group 4	22.88	18.75	5	$p = 0.86$

### 5.3.2 ENPPI

The average expression of *ENPPI* was statistically insignificant when comparing symmetric controls to all asymmetry subjects and to asymmetric subclassifications with unpaired t-tests (Table 8). The percent difference between right and left sides of *ENPPI* expression was significant for asymmetry group 4 with unpaired t-tests (Table 9). An ANOVA analysis revealed no significant differences in average *ENPPI* expression amongst the symmetric patients and asymmetry subclassifications ( $p=0.97$ ). However, an ANOVA analysis revealed significant percent differences of *ENPPI* expression between right and left sides amongst the symmetric patients and asymmetry subclassifications ( $p=0.04$ ).

**Table 8: Average ENPPI Expression**

Patient Diagnosis Groups	Average ENPPI Expression	SD	n	p-value
Symmetric	2.22	0.53	26	-
Asymmetric	2.24	0.59	46	$p = 0.91$
Group 1	2.32	0.73	5	$p = 0.72$
Group 2	2.28	0.55	21	$p = 0.71$
Group 3	2.22	0.60	15	$p = 0.98$
Group 4	2.03	0.45	5	$p = 0.47$

**Table 9: Percent Difference ENPP1 Expression**

Patient Diagnosis Groups	% $\Delta$ n ENPP1 Expression	SD	n	p-value
Symmetric	16.20	11.90	18	-
Asymmetric	18.99	16.03	36	$p = 0.52$
Group 1	12.55	3.01	3	$p = 0.61$
Group 2	12.77	7.35	17	$p = 0.32$
Group 3	25.50	20.81	11	$p = 0.14$
Group 4	34.35	16.52	5	$p = 0.01$

### 5.3.3 ESRI

The average expression of *ESRI* was statistically insignificant when comparing symmetric controls to all asymmetry subjects and to asymmetric subclassifications with unpaired t-tests (Table 10). The percent difference between right and left sides of *ESRI* expression was significant for asymmetry group 1, group 2 and group 4 with unpaired t-tests (Table 11). An ANOVA analysis revealed no significant differences in average *ESRI* expression amongst the symmetric patients and asymmetry subclassifications ( $p=0.70$ ). However, an ANOVA analysis revealed very significant percent differences of *ESRI* expression between right and left sides amongst the symmetric patients and asymmetry subclassifications ( $p=0.006$ ).

**Table 10: Average ESRI Expression**

Patient Diagnosis Groups	Average ESRI Expression	SD	n	p-value
Symmetric	4.68	1.68	28	-
Asymmetric	5.14	1.89	45	$p = 0.34$
Group 1	5.53	2.20	4	$p = 0.37$
Group 2	5.43	1.75	21	$p = 0.14$
Group 3	4.81	1.89	15	$p = 0.83$
Group 4	4.61	1.86	5	$p = 0.93$

**Table 11: Percent Difference ESR1 Expression**

Patient Diagnosis Groups	% $\Delta$ n ESR1 Expression	SD	n	<i>p</i> -value
Symmetric	18.34	11.44	22	-
Asymmetric	18.42	16.26	36	<i>p</i> = 0.98
Group 1	32.45	2.29	3	<b><i>p</i> = 0.048</b>
Group 2	9.10	5.81	17	<b><i>p</i> = 0.004</b>
Group 3	22.24	18.52	12	<i>p</i> = 0.45
Group 4	36.05	18.20	4	<b><i>p</i> = 0.02</b>

### 5.4 Fiber Type Data and Asymmetry Groups

To determine if muscle imbalance contributes to facial asymmetry, we compared fiber types between right and left masseter muscles. Staining and fiber typing was performed as described in the Materials and Methods and both mean fiber area (MFA) and percent occupancy (MPO) were calculated for each fiber type. The mean fiber area and percent occupancy of the symmetric controls were compared to all of the asymmetric subjects and to each of the asymmetric subclassifications with unpaired t-tests. The mean fiber area and muscle percent occupancy of symmetric controls and the four asymmetric subclassifications were compared by an ANOVA.

#### 5.4.1 Fiber Area

We identified significant differences in the left-right percent differences of type I fiber area in asymmetry group 3 with unpaired t-tests (Table 12). An ANOVA revealed no significance amongst the subgroups and left-right percent differences of type I fiber area (*p*=0.15). We also identified significant differences in the fiber area of type I/II hybrid fibers in asymmetry group 3 with unpaired t-tests (Table 13). An ANOVA analysis showed significant differences in mean type I/II hybrid fibers amongst all groups (*p*=0.04). Finally,

we found significant differences in the fiber area of type II fibers in asymmetric patients, asymmetry group 2 and group 4 with unpaired t-tests (Table 14). An ANOVA revealed no significance amongst the subgroups and left-right percent differences of type II fiber area ( $p=0.07$ ).

**Table 12: Left-Right Percent Difference of Type I Mean Fiber Area**

Patient Diagnosis Groups	MFA Type I % Difference	SD	n	p-value
Symmetry	17.23	18.29	13	-
Asymmetry	26.50	18.15	38	$p = 0.12$
Group 1	11.39	9.30	4	$p = 0.55$
Group 2	23.95	17.39	17	$p = 0.31$
Group 3	32.68	18.29	11	<b><math>p = 0.05</math></b>
Group 4	32.46	16.80	6	$p = 0.10$

**Table 13: Left-Right Percent Difference of Type I/II Hybrid Mean Fiber Area**

Patient Diagnosis Groups	MFA Type I/II % Difference	SD	n	p-value
Symmetry	17.37	17.98	12	-
Asymmetry	25.09	17.48	36	$p = 0.19$
Group 1	5.30	4.54	4	$p = 0.21$
Group 2	22.41	16.10	17	$p = 0.45$
Group 3	35.08	13.56	9	<b><math>p = 0.02</math></b>
Group 4	30.89	18.53	6	$p = 0.16$

**Table 14: Left-Right Percent Difference of Type II Mean Fiber Area**

Patient Diagnosis Groups	MFA Type II % Difference	SD	n	p-value
Symmetry	19.60	21.10	13	-
Asymmetry	36.70	24.60	38	<b><math>p = 0.03</math></b>
Group 1	22.20	16.88	4	$p = 0.83$
Group 2	38.50	27.65	17	<b><math>p = 0.05</math></b>
Group 3	31.00	19.70	11	$p = 0.19$
Group 4	51.90	18.36	6	<b><math>p = 0.005</math></b>

### 5.4.2 Percent Occupancy

We identified significantly greater left-right percent differences of type I fiber percent occupancy in all asymmetric subjects, and in asymmetry groups 2 and 4 with unpaired t-tests (Table 15). An ANOVA revealed no significance in left-right percent differences of type I percent occupancy amongst the subgroups ( $p=0.09$ ). There are no detectable differences in the left-right percent differences of type I/II hybrid fiber percent occupancy with unpaired t-tests (Table 16); and, an ANOVA revealed no significance amongst the subgroups ( $p=0.63$ ). We identified significantly greater left-right percent differences of type II fiber percent occupancy in asymmetry group 2 with unpaired t-tests (Table 17). An ANOVA revealed no significance amongst the subgroups and left-right percent differences of type II percent occupancy ( $p=0.16$ ).

**Table 15: Left-Right Percent Difference of Type I Percent Occupancy**

Patient Diagnosis Groups	MPO Type I % Difference	SD	n	p-value
Symmetry	14.36%	13.25	13	-
Asymmetry	28.60%	23.38	38	<b><math>p = 0.04</math></b>
Group 1	5.53%	4.13	4	$p = 0.22$
Group 2	32.23%	21.50	17	<b><math>p = 0.01</math></b>
Group 3	30.38%	24.37	11	<b><math>p = 0.05</math></b>
Group 4	30.43%	25.49	6	$p = 0.08$

**Table 16: Left-Right Percent Difference of Type I/II Hybrid Percent Occupancy**

Patient Diagnosis Groups	MPO Type I/II % Difference	SD	n	p-value
Symmetry	24.91%	21.31	12	-
Asymmetry	27.91%	21.27	36	$p = 0.67$
Group 1	11.23%	1.70	4	$p = 0.23$
Group 2	29.42%	24.07	17	$p = 0.61$
Group 3	31.08%	17.91	9	$p = 0.49$
Group 4	30.01%	19.45	6	$p = 0.63$

**Table 17. Left-Right Percent Difference of Type II Percent Occupancy**

Patient Diagnosis Groups	MPO Type II % Difference	SD	n	p-value
Symmetry	27.75%	32.41	13	-
Asymmetry	45.69%	29.17	38	$p = 0.07$
Group 1	20.30%	16.51	4	$p = 0.67$
Group 2	52.41%	28.98	17	<b><math>p = 0.04</math></b>
Group 3	46.19%	26.80	11	$p = 0.15$
Group 4	42.68%	30.67	6	$p = 0.36$

### 5.5 DC-TMD Diagnosis and Asymmetry Groups

Using the Diagnostic Criteria for TMD, temporomandibular joint functioning was assessed as a routine part of the pre-surgical evaluation. Overall, clinician diagnosed TMD was less prevalent in symmetric patients compared to asymmetric (Table 18). The three common Axis I disorders associated with asymmetry in the population were disc displacement with reduction (78%), followed by myalgia of masticatory muscles (61%), and arthralgia (33%). Patients may be diagnosed with any combination of these DC-TMD diagnoses. The population did not present with fibromyalgia or pain related disability diagnosed in Axis II of the diagnostic criteria.

**Table 18: Percentage of DC-TMD diagnosis among asymmetry classification groups**

Patient Diagnosis Groups	DC-TMD Diagnosis		
	DDR	Myalgia	Arthralgia
Symmetric	3%	4%	1%
Asymmetric	78%	61%	33%
Group 1	11%	11%	0%
Group 2	29%	33%	17%
Group 3	52%	44%	19%
Group 4	23%	23%	8%

## 5.6 JPF and Asymmetry Groups

Using the Jaw Pain and Function (JPF) Questionnaire, we evaluated the severity of patient-reported TMD symptoms. Comparing JPF scores between groups, a t-test demonstrated very significant differences between symmetric and asymmetric patients ( $p < 0.0001$ ); with scores  $\geq 6$  diagnostic for presence of TMD (Table 19). Most symmetric subjects had little to no symptoms (JPF=1.97), while asymmetric subjects had significantly higher JPF scores (JPF=6.9). Asymmetry groups 2 and 3 had the highest scores (JPF=6.94 and JPF=9.11), while asymmetry groups 1 and 4 had the lowest scores (JPF=3.75 and JPF=4.0). Within the population, an ANOVA comparison also revealed significant differences between the groups ( $p < 0.0001$ ).

**Table 19: Pre-surgical JPF scores in asymmetry classification groups**

Patient Diagnosis Groups	Mean JPF Scores	SD	n	p-value
Symmetric	1.97	2.53	90	-
Asymmetric	6.87	5.43	84	<b><math>p &lt; 0.0001</math></b>
Group 1	3.75	4.09	9	$p = 0.062$
Group 2	6.94	5.46	35	<b><math>p &lt; 0.0001</math></b>
Group 3	9.11	5.62	27	<b><math>p &lt; 0.0001</math></b>
Group 4	4.00	3.61	13	<b><math>p = 0.012</math></b>

## 5.7 PITX2, ENPP1 and ESR1 and Muscle Fiber Types

To determine the relationship between gene expression and muscle fiber type, we compared the percent differences of *PITX2*, *ENPP1* and *ESR1* expression and the percent differences of the fiber area and composition of the masseter muscle fiber types. Pearson correlation coefficients were calculated to measure the linear association between percent differences in gene expression and fiber area (Table 20). Fiber area differences between

left and right masseter samples of fiber type I and type I/II are positively correlated to right and left differences in *PITX2* RQ. When the six groups are plotted for differences between left and right samples, there is a significant association with *PITX2*. There is a 0.86 correlation between differences in type I fiber area and differences in *PITX2* expression between right and left sides and a 0.94 correlation between differences in type I/II fiber area in differences in *PITX2* expression between right and left sides (Figure 10). There is a 0.80 correlation between differences in type I fiber area and differences in *ENPP1* expression between right and right sides, which is approaching significance ( $p=0.06$ ) (Figure 11). There are no significant correlations with *ESR1* (Figure 12).

**Table 20: Percent Difference in Fiber Area vs. Percent Difference in RQ Gene Expression Between Left and Right Sides**

Patient Diagnosis Groups	Fiber Type Area % Differences			RQ % Differences		
	MFA Type I	MFA Type I/II	MFA Type II	% $\Delta n$ <i>PITX2</i>	% $\Delta n$ <i>ENPP1</i>	% $\Delta n$ <i>ESR1</i>
Symmetric	17.23	17.37	19.60	21.51	16.20	18.34
Asymmetric	26.50	25.09	36.70	21.39	18.99	18.42
Group 1	11.39	5.30	22.20	12.76	12.55	32.45
Group 2	23.95	22.41	38.50	19.42	12.77	9.10
Group 3	32.68	35.08	31.00	26.03	25.50	22.24
Group 4	32.46	30.89	51.90	22.88	34.35	36.05

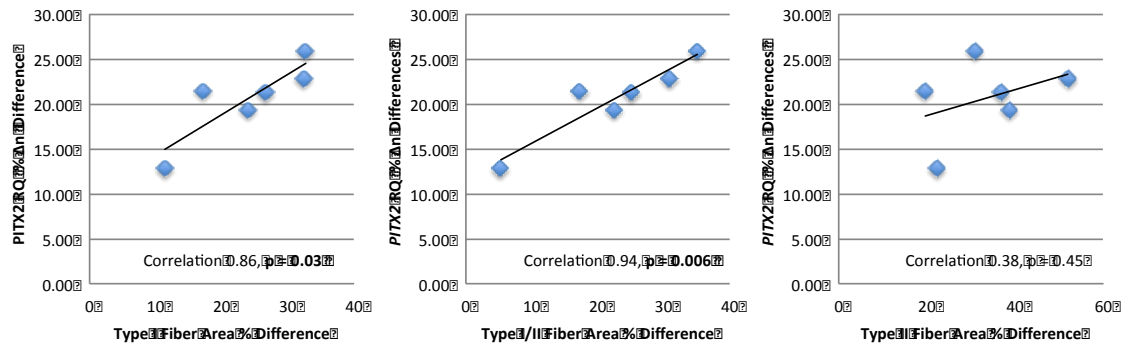


**Figure 10: Left-Right Percent Difference of Fiber Type Area and *PITX2* Correlation.** Correlation between fiber type area and *PITX2* expression with Pearson correlation coefficient and p-value

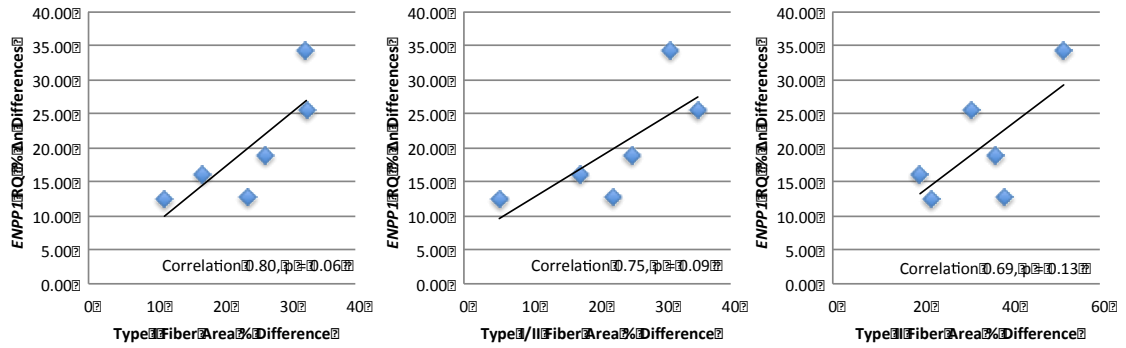


**Figure 11: Left-Right Percent Difference of Fiber Type Area and *ENPP1* Correlation.** Correlation between fiber type area and *PITX2* expression with Pearson correlation coefficient and p-value

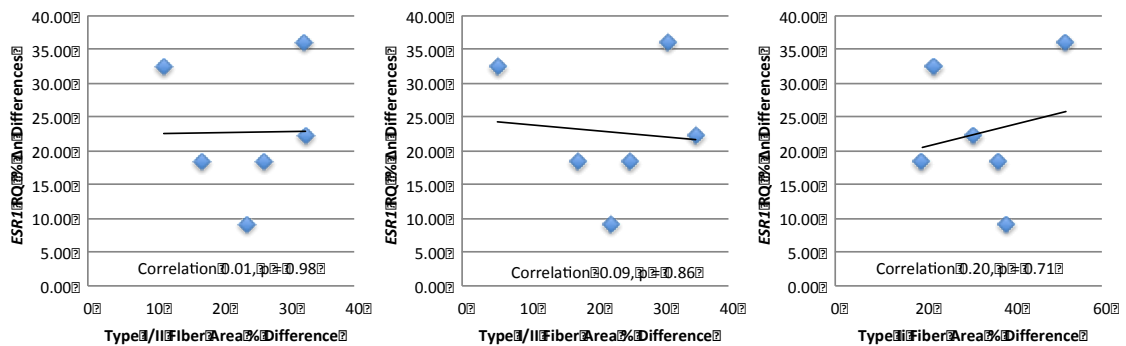


**Figure 12: Left-Right Percent Difference of Fiber Type Area and *ESRI* Correlation.** Correlation between fiber type area and *PITX2* expression with Pearson correlation coefficient and p-value

Pearson correlation coefficients were calculated to measure the linear association between percent differences in gene expression and fiber type percent occupancy (Table 21). There is a 0.90 correlation between differences in type I/II hybrid fiber occupancy and differences in *PITX2* expression between right and left sides (Figure 13). There are no significant correlations with *ENPP1* and *ESRI* (Figures 14 and 15).

**Table 21. Percent Difference in Fiber Type Occupancy vs. Percent Difference in RQ Gene Expression Between Left and Right Sides**

Patient Diagnosis Groups	Fiber Type Occupancy % Differences			RQ % Differences		
	MPO Type I	MPO Type I/II	MPO Type II	% $\Delta n$ <i>PITX2</i>	% $\Delta n$ <i>ENPP1</i>	% $\Delta n$ <i>ESR1</i>
Symmetric	14.36	24.91	27.75	21.51	16.20	18.34
Asymmetric	28.60	27.91	45.69	21.39	18.99	18.42
Group 1	5.53	11.23	20.30	12.76	12.55	32.45
Group 2	32.23	29.42	52.41	19.42	12.77	9.10
Group 3	30.38	31.08	46.19	26.03	25.50	22.24
Group 4	30.43	30.01	42.68	22.88	34.35	36.05

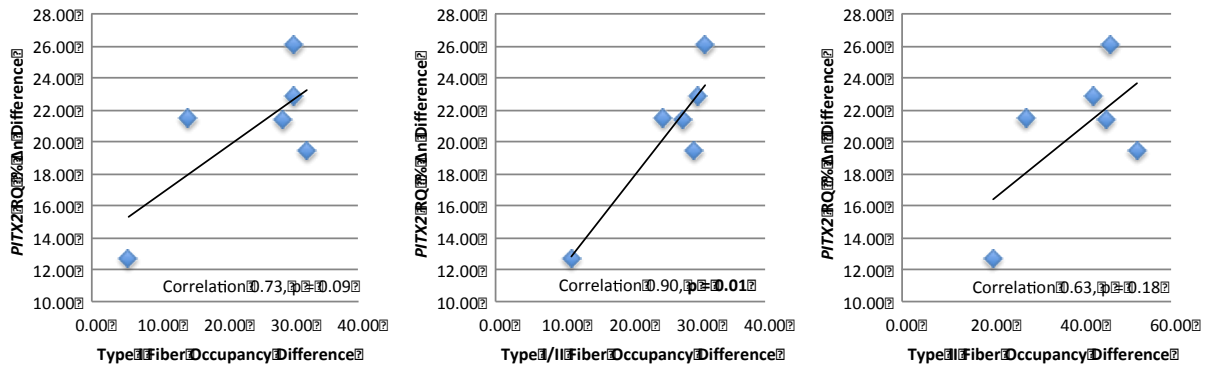


**Figure 13: Left-Right Percent Difference of Fiber Type Occupancy and *PITX2* Correlation.** Correlation between fiber type occupancy and *PITX2* expression with Pearson correlation coefficient and p-value

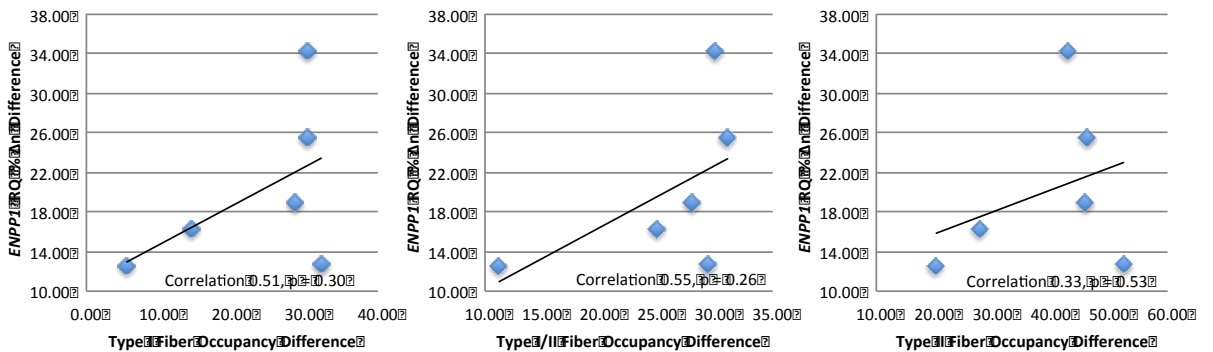


**Figure 14: Left-Right Percent Difference of Fiber Type Occupancy and *ENPP1* Correlation.** Correlation between fiber type occupancy and *ENPP1* expression with Pearson correlation coefficient and p-value

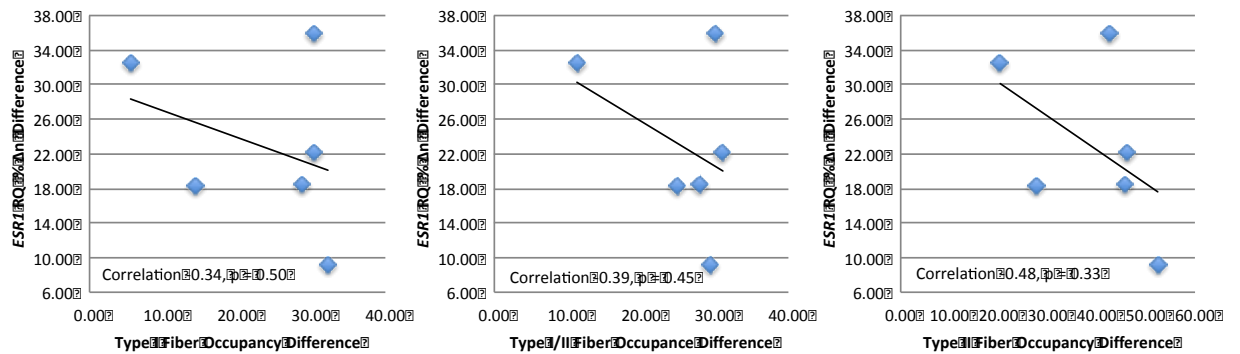


**Figure 15: Left-Right Percent Difference of Fiber Type Occupancy and *ESRI* Correlation.** Correlation between fiber type occupancy and *ESRI* expression with Pearson correlation coefficient and p-value

### 5.8 *PITX2*, *ENPP1* and *ESRI* Expression and DC-TMD Diagnosis

To determine if our three genes of interest for asymmetry and TMD had different gene expression in masseter muscle of patients with specific TMD diagnostic conditions, we compared average RQ and RQ percent differences between left and right sides of *PITX2*, *ENPP1* and *ESRI* masseter expression to the major TMD diagnoses. The three major subgroups of TMD include disc displacement with reduction (DDR), myalgia, and arthralgia. The average *PITX2* expression is significantly increased in all patients with a clinician diagnosis of TMD, but not specific for subgroups (Table 22). There is no significant association between the percent difference of *PITX2* and TMD subgroups (Table 23). The average *ENPP1* expression is increased in all patients with a clinician diagnosis of TMD, but not significantly (Table 24). There is no significant association between the percent difference of *ENPP1* and TMD subgroups (Table 25). There is no significant association between average *ESRI* expression and TMD subgroups (Table 26).

The percent difference between left and right masseter of *ESR1* is significantly decreased in all patients with a clinician diagnosis of TMD, specifically for patients with disc displacement with reduction (Table 27).

**Table 22: Average *PITX2* Expression in DC-TMD Subgroups**

DC-TMD	Average <i>PITX2</i> Expression	SD	n	p-value
No TMD	1.18	0.45	32	-
All TMD	1.45	0.41	19	<b><math>p = 0.0375</math></b>
DDR	1.44	0.42	14	$p = 0.0739$
Myalgia	1.38	0.46	14	$p = 0.1745$
Arthralgia	1.00	0.46	5	$p = 0.4230$

**Table 23: Percent Difference *PITX2* Expression in DC-TMD Subgroups**

DC-TMD	% $\Delta$ n <i>PITX2</i> Expression	SD	n	p-value
No TMD	21.08	16.66	28	-
All TMD	17.32	19.99	16	$p = 0.5071$
DDR	15.40	11.34	11	$p = 0.3067$
Myalgia	20.04	22.22	12	$p = 0.8717$
Arthralgia	31.92	27.49	5	$p = 0.2344$

**Table 24: Average *ENPP1* Expression in DC-TMD Subgroups**

DC-TMD	Average <i>ENPP1</i> Expression	SD	n	p-value
No TMD	2.12	0.54	36	-
All TMD	2.37	0.62	23	$p = 0.1176$
DDR	2.36	0.68	18	$p = 0.1734$
Myalgia	2.41	0.67	15	$p = 0.1170$
Arthralgia	2.32	0.81	7	$p = 0.4231$

**Table 25: Percent Difference ENPP1 Expression in DC-TMD Subgroups**

DC-TMD	% $\Delta$ n ENPP1 Expression	SD	n	p-value
No TMD	17.88	15.29	28	-
All TMD	18.35	16.02	18	$p = 0.9204$
DDR	20.12	17.54	13	$p = 0.6787$
Myalgia	19.81	18.10	12	$p = 0.7312$
Arthralgia	24.39	21.80	7	$p = 0.3619$

**Table 26: Average ESRI Expression in DC-TMD Subgroups**

DC-TMD	Average ESRI Expression	SD	n	p-value
No TMD	4.97	1.94	43	-
All TMD	4.94	1.57	24	$p = 0.9590$
DDR	4.90	1.58	18	$p = 0.899$
Myalgia	4.80	1.76	15	$p = 0.7686$
Arthralgia	4.14	0.95	6	$p = 0.3152$

**Table 27: Percent Difference ESRI Expression in DC-TMD Subgroups**

DC-TMD	% $\Delta$ n ESRI Expression	SD	n	p-value
No TMD	23.06	15.98	33	-
All TMD	11.24	10.13	18	$p = 0.0066$
DDR	12.50	11.22	13	$p = 0.0351$
Myalgia	13.46	11.49	12	$p = 0.0635$
Arthralgia	13.62	15.38	6	$p = 0.1887$

### 5.9 PITX2, ENPP1 and ESRI Expression and JPF Scores

To determine if the expression of our three genes of interest for asymmetry relate to patient reporting of TMD symptoms in asymmetry classifications, we compared both the average expression and the percent differences between left and right sides of *PITX2*, *ENPP1* and *ESRI* masseter expression to patient reported JPF scores with Pearson

correlation statistics (Table 28 and 29). While there are no significant differences in gene expression and patient-reported TMD symptoms, we can see a slight increase in *ESR1* expression for asymmetry subjects. No correlation plots were constructed due to lack of statistical significance.

**Table 28: JPF Scores and Average Gene Expression in Asymmetry Classifications**

Patient Diagnosis Groups	JPF Scores	<i>PITX2</i>	<i>ENPP1</i>	<i>ESR1</i>
Symmetric	1.97	1.18	2.22	4.68
Asymmetric	6.87	1.33	2.24	5.14
Group 1	3.75	1.37	2.32	5.53
Group 2	6.94	1.37	2.28	5.43
Group 3	9.11	1.28	2.22	4.81
Group 4	4.00	1.25	2.03	4.61
<b>Correlation Coefficient: p-value:</b>		r = 0.45, p = 0.37	r = 0.16, p = 0.76	r = 0.18, p = 0.73

**Table 29: JPF Scores and Percent Difference Gene Expression in Asymmetry Classifications**

Patient Diagnosis Groups	JPF Scores	<i>PITX2</i>	<i>ENPP1</i>	<i>ESR1</i>
Symmetric	1.97	21.51	16.2	18.34
Asymmetric	6.87	21.39	18.99	18.42
Group 1	3.75	12.76	12.55	32.45
Group 2	6.94	19.42	12.77	9.1
Group 3	9.11	26.03	25.5	22.24
Group 4	4.00	22.88	34.35	36.05
<b>Correlation Coefficient: p-value:</b>		r = 0.45, p = 0.37	r = 0.12, p = 0.82	r = -0.37, p = 0.47

## CHAPTER 6

### DISCUSSION

Craniofacial asymmetry is a complex trait condition, developing from genetic and environmental influences. Facial asymmetry can range from mild cases that go undetected to severe cases that require surgical correction. Variations in craniofacial asymmetry variation can have a distinct etiology, resulting in distinct characteristics. We developed a posterior anterior cephalometric diagnostic classification system recognizing this phenotypic variation by adapting the 3-dimensional classification system of Baek et al. (2012). The asymmetry classification demonstrated significant cephalometric differences between symmetric and asymmetric groups, and across the four asymmetric subtypes: Group 1 - mandibular body asymmetry, Group 2 – ramus asymmetry, Group 3 - atypical asymmetry and Group 4 - "C-shaped" asymmetry. These differences in PA cephalometric measurements indicate the four subtypes may be considered as anatomically different forms of asymmetry. Utilizing an etiologic-based phenotypic classification system can be useful in identifying associations between gene expression and facial asymmetry, as each of the subgroups are developmentally different forms of asymmetry.

#### ***ENPP1 and ESRI associate with facial asymmetry***

With knowledge that *PITX2*, *ENPP1* and *ESRI* contribute to sagittal and vertical malocclusion, we wanted to determine if these genes also contribute to facial asymmetry. By comparing average gene expression and percent differences between right and left sides between symmetric and asymmetric patients and between the asymmetric groups, we identified associations with *ENPP1* and *ESRI*. Although previous studies reported an

association with differential *PITX2* expression and facial asymmetry, we did not find any significant results. It is still possible the variation in *PITX2* gene expression has an association with facial asymmetry, and warrants further research. One possibility to be investigated is that *PITX2* may interact with *ENPP1* to produce differences in mineral density and bone growth between facial sides.

Percent differences in *ENPP1* expression between left and right sides are very significantly increased in asymmetry group 4 compared to symmetric subjects and an ANOVA revealed significant differences between the asymmetry subgroups. The *ENPP1* gene is essential for bone morphology and plays an important role as a negative regulator of bone mineralization. Cultured osteoblasts with elevated *ENPP1* expression have reduced mineral formation (Mackenzie et al., 2012). *ENPP1* polymorphisms are associated with differences in height, hip geometric indices and facial morphology (Ermakov et al., 2010; Cheung et al., 2010). Group 4 displays “C-shaped asymmetry” with difference in ramus heights with menton deviation to short ramus side and severe maxillary canting. It is possible the differential expression of *ENPP1* between right and left sides contributes to the differences in mandibular ramal height found in asymmetry group 4. These results further support the appropriateness of the asymmetry subclassifications, as this phenotypic organization can be utilized to recognize meaningful gene expression.

Percent differences in *ESR1* expression between left and right sides are significantly different in asymmetry groups 1, 2, and 4 compared to symmetric subjects and an ANOVA revealed significant differences between the asymmetry subgroups. Estrogen plays a fundamental role in growth, development, maturation, and maintenance of the skeleton (Lindsay, 1992). Estrogen is essential for the development and maintenance

of optimal bone mass acting through activation of estrogen receptor  $\alpha$ . Estrogen has been proven clinically useful as a treatment for growth disorders. Estrogen can induce height gain in those with short statures and can arrest growth by promoting epiphyseal fusion in tall individuals (Rallison, 1986). Lee et al. suggests that an *ESR1* polymorphism could differentially contribute to the mandibular body length in female symptomatic TMJ patients (2006). In light of previous findings and the significance of our results, it is likely differential expression of *ESR1* contributes to the development of facial asymmetry through its critical role in bone development and mineralization.

### **Fiber type properties associate with asymmetry**

Skeletal muscle is composed of a variety of fiber types with different functional and histologic characteristics. Since we know from previous studies that the size and occupancy of fiber type influence skeletal malocclusion, we wanted to evaluate the potential influence of fiber type properties on facial asymmetry. By comparing differences in fiber type area and percent occupancy between symmetry patients and asymmetric subclassifications, we identified highly significant differences suggesting a strong influence of fiber type properties on facial asymmetry.

Asymmetry group 3 has a greater difference in fiber area of both type I fibers and type I/II hybrid fibers between left and right sides. Also, all asymmetric patients and asymmetry groups 2 and 3, have a greater differences in percent occupancy of type I fiber area between right and left masseter muscle compared to symmetric controls. These results suggest an influence of type I and I/II fibers on the development of asymmetry, specifically in asymmetry groups 2 and 3. Patients diagnosed with asymmetry group 2 display a “ramus

asymmetry” with a shorter ramal height on the same side of the menton deviation, while patients diagnosed with asymmetry group 3 display an “atypical asymmetry” with a shorter ramal height on the opposite side of the menton deviation. Both subgroups present with significant differences in ramal heights between sides. Variations in both type I muscle fiber area and percent occupancy between left and right sides of asymmetry patients may contribute to this left-right differences in ramal height. Type I fibers are slow contracting and fatigue resistant, used most commonly to maintain postural freeway space. They tend to predominate in masseter muscles, and have the largest mean area and often are the most numerous type. They have been found to be substantially decreased in occupancy in deep bite subjects (Rowlerson et al., 2005).

All asymmetric patients and asymmetry groups 2 and 4, have greater differences in type II fiber area between right and left masseter muscle compared to symmetric controls. Additionally, asymmetry group 2 has greater differences in percent occupancy of type II fibers between right and left sides. Type II fibers are fast contracting and are either fatigue resistant (type IIA) or fatigueable (type IIX). In our population, differences of type II mean fiber areas and percent occupancies are related to increases in facial asymmetry with type II fibers being substantially increased in size and abundance in either the left or right masseter muscle. Type II fibers in masseter muscle have a substantially smaller mean area than type I fibers and therefore produce substantially less force. In deep bite patients, type II fibers are substantially increased in occupancy (Rowlerson et al., 2005). Also, previous studies recognized type II fast-contracting fibers are increased in masseter muscle on the same side as the deviation and the vertical facial dimension is decreased (Raoul et al. 2011; Sciote et al. 2012). The significant variations in both type II muscle fiber area and percent

occupancy between left and right sides of asymmetry patients appears contribute to the development of asymmetries.

These results suggest a very close association exists between muscle fiber type area and percent occupancy and asymmetric development of the face. Differential skeletal muscle morphology potentially results in one side being stronger than the other. This could create an asymmetry as the forces on the bone would not be the same on either side, thereby resulting in a skeletal disharmony. The present findings give us some clues as to which influences are most important in the interaction between muscle and bone during craniofacial growth. Functional differences between type I, type I/II and type II fibers are important factors in the development of symmetry between facial sides. With this knowledge, an important question to consider is whether the muscle phenotype differences between facial sides are associated with *PITX2*, *ENPP1* or *ESR1* expression.

### ***PITX2* and *ENPP1* expression and masseter fiber type properties**

To further explore how genetic variation might influence masticatory muscle function and skeletal shape, we studied gene expression in association with masseter muscle fiber type properties. *ENPP1* and *PITX2* are key genetic factors that influence jaw bone length and masticatory muscle strength in malocclusion.

*PITX2* expression demonstrates a consistent relationship to masseter muscles fiber type properties when compared between groups. As skeletal asymmetry becomes more pronounced, *PITX2* expression and fiber type differences increase proportionally. Fiber area differences between left and right masseter samples of type I fibers are positively correlated to differences in *PITX2* expression. This relationship agrees with previous

findings that *PITX2* is essential for non-limb myogenesis and muscle maintenance (Hebert et al., 2013). Decreased expression of this gene results in a decreased ability of the organ to build and maintain muscle, particularly Type I fibers.

Also, there is a very strong correlation between differences in fiber area and percent occupancy of type I/II fibers and differences in *PITX2* expression between sides. A unique feature of masseter muscle is the high proportion of hybrid fibers, in comparison to limb muscles. The presence of hybrid fibers in the masseter is so common it is regarded as normal. Interestingly, we see the strongest correlation exists between *PITX2* expression and fiber type I/II hybrids. *PITX2* expression and fiber type area and occupancy have a direct, positive correlation, which may increase the risk for TMD due to unbalanced musculoskeletal forces.

*ENPP1* may be a key genetic influence and needs further careful consideration. The correlation between differences in type I fiber area and *ENPP1* expression between left and right sides were approaching significance ( $p=0.06$ ). *ENPP1* binds directly to skeletal muscle insulin receptors, and a polymorphism is known to produce insulin resistance (Kato et al., 2012; Maddux et al., 2006). Over time, insulin resistance alters the proportion of type I versus type II skeletal muscle fibers, which could also influence development of asymmetry (Oberbach et al., 2006; Sciote et al., 2012; Ringqvist, 1974; Gregor et al., 2013).

### **Increased TMD prevalence in facial asymmetry**

Since TMD is often present in this population of surgical patients before initiation of treatment, we wanted to know if there was a higher prevalence within and between

asymmetry subclassifications. While TMD diagnosis was positive in only 3% of symmetric patients, diagnoses of disc displacement with reduction, masticatory muscle myalgia and arthralgia were highly prevalent in the asymmetry groups. In addition to a higher prevalence of clinician diagnosed TMD, we found an increase in patient reported perception of presence and severity of TMD through Jaw Pain and Function Questionnaires. Most symmetric subjects had little to no symptoms for TMD, while asymmetric subjects had significantly higher JPF scores, especially in groups 2 and 3. Given the significant difference between groups, the cephalometric analysis may be used to subclassify types of asymmetry, therefore, predicting which patients are likely to have symptomatic reporting of TMD related to their malocclusion.

In the field of orthodontics, it is commonly thought that little to no relationship exists between specific types of malocclusions and development of TMD (Mohlin et al., 2007); however, our findings show TMD prevalence is much higher in our patients with asymmetry compared to patients without asymmetry. These results indicate there is an increased chance for signs or symptoms of TMD when asymmetry is part of a patient's dentofacial deformity and than asymmetry may be considered a risk factor of TMD.

### ***PITX2, ENPP1, and ESRI* expression and TMD diagnosis**

Facial skeletal imbalances appear to play a role in the development of TMJ dysfunction. To understand more about this potential link, we compared differences in gene expression of our three genes of interest in masseter muscle of patients with specific TMD diagnostic conditions. Average *PITX2* expression was significantly increased for patients with TMD and approaching significance for DDR. Average *ENPP1* expression was

increased in all patients with a clinician diagnosis of TMD, but not significantly. The percent difference between left and right masseter of *ESRI* is significantly decreased in all patients with a clinician diagnosis of TMD, specifically for patients with disc displacement with reduction.

While the mechanisms of *PITX2* and *ENPP1* are unknown in their effect on TMD, it is known that these genes have multiple genetic associations with functional properties in muscle and bone. It is possible *ENPP1* has an effect through variations in bone mineralization may predispose individuals to musculoskeletal susceptibility for TMD. Sciote et al. also found *ENPP1* polymorphisms contribute to development of TMD-related muscle pain (2015). Additional studies are needed to explore the biologic effects of *ENPP1*, but it is possible arthralgia and disc displacement may be related to *ENPP1* biomineralization functions and myalgia may be related to insulin signaling in skeletal muscle. Understanding how these differences in gene expression relate to TMD should provide new insights, especially for masticatory muscle myalgia, the most common temporomandibular disorder.

### ***ESRI* expression influence patient-reported TMD symptoms**

In addition to differential expression of *ESRI* between right and left masseter muscle in patients with clinican diagnosed TMD, we see slight increases in average values of *ESRI* RQ compared to JPF scores of asymmetric patients. Although not significant, attention is warranted to the role *ESRI* in patient reported symptoms of TMD. A previously identified SNP rs1643821 associates *ESRI* with symptomatic worsening of TMD (Nicot et al., 2016). Via the  $\alpha$  receptor, estrogen plays an important role in the pathophysiology of

TMD through the inflammatory response, the bone mineralization and the nervous system (Craft, 2007). Low et al. demonstrated genetic variation of the estrogen metabolism pathway, particularly genes involved in the production of estrogen through androgen conversion, influences the risk for the development of estrogen-sensitive breast cancer (2010). It is possible similar variations in hormonal levels, such as estrogen, could influence the development craniofacial asymmetry and temporomandibular joints. Although, more subjects are necessary to determine relationships between masseter muscle *ESR1* expression and TMD, other studies emphasize the need for further investigations of *ESR1* genotype and gene expression and relation to chronic orofacial pain (Smith et al., 2014).

Our study is one of the first to consider heritable influences on both muscle and bone in producing variations in craniofacial growth and temporomandibular disorders. Although we have preliminary findings for our genes of interest, they must be investigated more comprehensively before translation into biological function or clinical testing. With increased knowledge, heritability can be more fully examined to ensure that findings are effectively translated into clinical diagnosis and the type or timing of most effective treatments. Further studies on the role of the genetic markers relevant to the craniofacial growth and adaptation could improve our understanding regarding the development of asymmetry and temporomandibular disorders.

## CHAPTER 7

### CONCLUSIONS

1. The asymmetry classification system can be useful in diagnosing four subtypes of asymmetry with distinctive growth patterns. Utilizing an etiologic-based phenotypic classification system is useful in identifying associations with facial asymmetry.
2. Differential expression of *ENPP1*, a negative regulator of mineralization, associates with asymmetry group 4 and differential expression of *ESR1* associates with asymmetry group 1, group 2 and group 4.
3. Masseter fiber type properties of type I, type I/II hybrid and type II fibers associate with facial asymmetry and specific subclassifications
4. *PITX2* gene expression correlates with differences in type I fiber area and type I/II fiber area and percent occupancy
5. TMD prevalence is much higher in patients with asymmetry compared to patients without. The most common TMD presentations were disc displacement with reduction, masticatory muscle myalgia and arthralgia. JPF scores are increased in all asymmetric subjects, specifically asymmetry groups 2, 3 and 4.
6. *PITX2* and *ENPP1*, and *ESR1* expression associate with clinician diagnosed TMD
7. Future studies should evaluate potential influence of increased *ESR1* gene expression on patient-reported TMD symptoms evaluated by JPF questionnaires in patients with asymmetry.

## REFERENCES

- Abubaker Ao, Raslan WF, Sotereanos GC. (1993). Estrogen and progesterone receptors in temporomandibular joint discs of symptomatic and asymptomatic persons: a preliminary study. *Journal of Oral and Maxillofacial Surgery*, 51(10):1096-1100.
- Baek C, Paeng JY, Lee JS, Hong J. (2012). Morphologic evaluation and classification of facial asymmetry using 3-dimensional computed tomography. *Journal of Oral and Maxillofacial Surgery*, 70(5):1161-9.
- Baudouin JY, Tiberghien G. (2004). Symmetry, averageness, and feature size in the facial attractiveness of women. *Acta Psychologica*, 117(3):313-32.
- Beunen GM, Thomis M, Peeters M, Maes HH, Claessens AL, Vlietinck R. (2003). Genetics of strength and power characteristics in children and adolescents. *Pediatric Exercise Science*, 15:128-138.
- Bishara SE, Burkey PS, Kharouf JG. (1994). Dental and facial asymmetries: a review. *The Angle Orthodontics*, 64(2):89-98.
- Bisgrove BW, Essner JJ, Yost HJ. (1999). Regulation of midline development by antagonism of lefty and nodal signaling. *Development*, 126(14):3253-62.
- Borod JC, Caron HS, Koff E. (1981). Asymmetry of facial expression related to handedness, footedness, and eyedness: a quantitative study. *Cortex*, 18:381-390.
- Bottinelli R, Reggiani C. (2000). Human skeletal muscle fibres: molecular and functional diversity. *Progress in Biophysics and Molecular Biology*, 73:195-262.
- Brevi B, DiBlasio A, DiBlasio C, Piazza F, D'Ascanio I, Sesenna E. (2015). Which cephalometric analysis for maxillo-mandibular surgery in patients with obstructive sleep apnea syndrome? Quale analisi cefalometrica per la chirurgia maxillo-mandibolare in pazienti con sindrome delle apnee ostruttive notturne. *Acta Otorhinolaryngologica Italica*, 35:332-337.
- Brooke M, Kaiser K. (1970). Muscle fiber types: how many and what kind. *Archives of Neurology*, 23:369-379.
- Bruce RA, Hayward JR. (1968). Condylar hyperplasia and mandibular asymmetry: A review. *Journal of Oral Surgery*, 26:281.
- Burdine RD, Schier AF. (2000). Conserved and divergent mechanisms in left-right axis formation. *Genes & Development*, 14:763-776.
- Burke PH. (1979). Growth of the soft tissues of middle third of the face between 9 and 16 years. *European Journal of Orthodontics*, 1:1-13.
- Burstone CJ. (1998). Diagnosis and Treatment Planning of Patients with Asymmetries. *Seminars in Orthodontics*. 4(3):153-64.

- Cheng AM, Thisse B, Thisse C, Wright CV. (2000). The lefty-related factor Xatv acts as a feedback inhibitor of nodal signaling in mesoderm induction and L-R axis development in xenopus. *Development*, 27(5):1049-61.
- Cheong YW, Lo LJ. (2011). Facial asymmetry: etiology, evaluation and management. *Chang Gung Medical Journal*, 34(4):341-51.
- Cheung CL, et al. (2010). Hip geometry variation is associated with bone mineralization pathway gene variants: The Framingham Study. *Journal of Bone and Mineral Research*, 25(7):1564-71.
- Chia MS, Naini FB, Gill DS. (2008). The aetiology, diagnosis and management of mandibular asymmetry. *Ortho Update*, 1(1):44-52.
- Chung K, Richards T, Nicot R, Vieira AR, Cruz CV, Raoul G, Ferri J, Sciote J. (2017). ENPP1 and ESR1 genotypes associate with subclassifications of craniofacial asymmetry and severity of TMD. *American Journal of Orthodontics and Dentofacial Orthopedics*, third revision.
- Clark GT, Seligman D, Solberg WK, Pullinger AG. (1989). Guidelines for the examination and diagnosis of temporomandibular disorders. *Journal of Craniomandibular Disorders*, 3:7-14.
- Craft RM. (2007). Modulation of pain by estrogens. *Pain*, 132(1):S3-12.
- de Leeuw, R., Klasser, G. (2013). Orofacial pain: guidelines for assessment, diagnosis, and management. *Quintessence*: Chicago, 127-186.
- Dhalberg G., et al. (1995). Disk displacement and temporomandibular joint symptoms in orthognathic surgery patients. *Oral Surgery, Oral Medicine, Oral Pathology*, 79:273-277.
- Dujoncquoy J-P., et al. (2010). Temporomandibular joint dysfunction and orthognathic surgery: a retrospective study. *Head and Face Medicine*. 6:2-7.
- Ermakov S, Rosenbaum MG, Malkin I, Livshits G. (2010). Family-based study of association between ENPP1 genetic variants and craniofacial morphology. *Annals of Human Biology*, 37(3):754-766.
- Evans, W, Hood, D, Gurd, J. (1973). Purification and properties of a mouse liver plasma membrane glycoprotein hydrolysing nucleotide pyrophosphate and phosphodiester bonds. *Biochemical Journal*, 135(4):819–826.
- Farkas LG, Cheung G. (1981). Facial asymmetry in healthy North American Caucasians. An anthropometrical study. *Angle Orthodontist*, 51:70–77.
- Fleisch, H, Straumann, F, Schenk, R, Bisaz, S, Allgöwer, M. (1966). Effect of condensed phosphates on calcification of chick embryo femurs in tissue culture. *American Journal of Physiology*, 211(3):821-825.

- Froese EA, Houston ME. (1985). Torque-velocity characteristics and muscle fiber type in human vastus lateralis. *Journal of Applied Physiology*, 59:309.
- GeneCards: The Human Gene Compendium. Weizmann Institute of Science, Life Map Sciences. PITX2. www.genecards.org
- Gerstner GE, Clark GT, Goulet JP. (1994). Validity of a brief questionnaire in screening asymptomatic subjects from subjects with tension-type headaches or temporomandibular disorders. *Community Dentistry and Oral Epidemiology*, 22:235-242.
- Gerdle B, Wretling ML, Henriksson-Larsen K. (1988). Do the fibre-type proportion and the angular velocity influence the mean power frequency of the electromyogram? *Acta Physiol Scand*, 134:341.
- Goldspink, DF. (1980). The influence of contractile activity and nerve supply on muscle size and protein turnover. In: Pette D, editor. *Plasticity of muscle*. de Gruyter; Berlin
- Gregor C, Hietschold V, Harzer W. (2013). A <sup>31</sup>P-magnet resonance spectroscopy study on the metabolism of human masseter in individuals with different vertical facial pattern. *Oral Surgery, Oral Medicine, Oral Pathology, Oral Radiology*, 115:406-414.
- Grummons DC, Kappeyne Van De Coppelo MA. (1987). A Frontal Asymmetry Analysis. *Journal of Clinical Orthodontics*, 21(7):448-465.
- Haraguchi S, Iguchi Y, Takada K. (2008). Asymmetry of the face in orthodontic patients. *The Angle Orthodontist*, 78(3):421-6.
- Herbert SL, Daniel ML, McKloon LK. (2013). The Role of Pitx2 in Maintaining the Phenotype of Myogenic Precursor Cells in the Extraocular Muscles. *PLoS ONE*. 8(3):e58405.
- Holloszy, JO and Booth, FW. (1976) Biochemical adaptations to endurance exercise in muscle. *Annual Review of Physiology*, 38:273–291.
- Horton MJ, Rosen C, Close JM, Sciote JJ. (2008). Quantification of myosin heavy chain RNA in human laryngeal muscles: differential expression in the vertical and horizontal posterior cricoarytenoid and thyroarytenoid. *The Laryngoscope*, 118(3):472-477.
- Hu SK, Mitcho YL, Rath NC. (1988). Effect of estradiol on interleukin 1 synthesis by macrophages. *International Journal of Immunopharmacology*, 10:247–252.
- Hwang HS, Youn IS, Lee KH, Lim HJ. (2007). Classification of facial asymmetry by cluster analysis. *American Journal of Orthodontics and Dentofacial Orthopedics*, 132(3):279.
- Inui M, Fushima K, Sato S. (1999). Facial asymmetry in temporomandibular joint disorders. *Journal of Oral Rehabilitation*, 26:402-406.
- Johnson, K, Moffa, A, Chen, Y, Pritzker, K, Goding, J, Terkeltaub, R. (1999). Matrix vesicle plasma cell membrane glycoprotein-1 regulates mineralization by murine osteoblastic MC3T3 cells. *Journal of Bone and Mineral Research*, 14:883–892.

- Johnson, K, Vaingankar, S, Chen, Y, Moffa, A, Goldring, MB, Sano, K, Jin-Hua, P, Sali, A, Goding, J, Terkeltaub, R. (1999). Differential mechanisms of inorganic pyrophosphate production by plasma cell membrane glycoprotein-1 and B10 in chondrocytes. *Arthritis & Rheumatism*, 42:1986–1997.
- Johnson, KA, Hessle, L, Vaingankar, S, Wennerg, C, Mauro, S, Narisawa, S, Goding, JW, Sano, K, Millan, JL, Terkeltaub, R. (2000). Osteoblast tissue-nonspecific alkaline phosphatase antagonizes and regulates PC-1. *American Journal of Physiology - Regulatory, Integrative, and Comparative Physiology*, 279.
- Kato, K., Nishimasu, H., Okudaira, S., Mihara, E., Ishitani, R., Takagi, J. (2012). Crystal structure of Enpp1, an extracellular glycoprotein involved in bone mineralization and insulin signaling. *Proceedings of the National Academy of Sciences*, 109(42):16876-16881.
- Kim BS, Kim YK, Yun PY, Lee I, Bae J. (2010). The effects of estrogen receptor  $\alpha$  polymorphism on the prevalence of symptomatic temporomandibular disorders. *Journal of Oral and Maxillofacial Surgery*, 68:2975-2979.
- Knopp P, Figeac N, Fortier M, Moyle L, Zammit PS. (2013). *Pitx* genes are redeployed in adult myogenesis where they can act to promote myogenic differentiation in muscle satellite cells. *Developmental Biology*, 377:293.
- Kobayashi T., et al. (1999). Temporomandibular joint symptoms and disc displacement in patients with mandibular prognathism. *British Journal of Oral and Maxillofacial Surgery*, 37:455-458.
- Koff E, Borod J, Strauss E. (1985). Development of hemiface size asymmetry. *Cortex*, 21:153-156.
- Koff E, Borod JC, White B. (1981). Asymmetries for hemiface size and mobility. *Neuropsychologia*, 19:825–83.
- Kubota E, Kubota T, Matsumoto J, Shibata T, Murakami K. (1998). Synovial fluid cytokines and proteinases as markers of temporomandibular joint disease. *Journal of Maxillofacial Surgery*, 56(2):192-8.
- Laakso, JM, Lewis, JH, Shuman, H, Ostap, EM. (2008) Myosin I can act as a molecular force sensor. *Science*, 321:133–136.
- Lee JK, Jung PK, Moon CH. (2014). Three-dimensional cone beam computed tomographic image reorientation using soft tissues as reference for facial asymmetry diagnosis. *Angle Orthodontist*, 84(1):38-47.
- Lee DG, Kim TW, Kang SC, Kim ST. (2006). Estrogen receptor gene polymorphism and craniofacial morphology in female TMJ osteoarthritis patients. *International Journal of Oral and Maxillofacial Surgery*, 35:165–169.

- Lek M, Quinlan K, North KN. (2009). The evolution of skeletal muscle performance: gene duplication and divergence of human sarcomeric  $\alpha$ -actinins. *Bioessays*, 32:17-25.
- LeResche L. (1997). Epidemiology of Temporomandibular Disorders: Implications for the investigation of etiologic factors. *Critical Reviews in Oral Biology and Medicine*, 8(3):291-305.
- LeResche L Saunders K, Von Korff MR, Barlow W, Dworkin SF. (1997) Use of exogenous hormones and risk of temporomandibular disorder pain. *Pain*, 69:153-160.
- Levin M. (2004). Left-right asymmetry in embryonic development: a comprehensive review. *Mechanisms of Development*, 122(1):3-25.
- Levin M, Mercola M. (1998). Gap junctions are involved in the early generation of left-right asymmetry. *Developmental Biology*, 203(1):90-105.
- Lindauer SJ. (1998). Asymmetries: diagnosis and treatment (editorial). *Seminars in Orthodontics*, 4(3):133.
- Lindsay R, Cosman F. (1992) Primary osteoporosis. In: Coe FL, Favus MJ, eds. Disorders of bone and mineral metabolism. New York: Raven Press; 841.
- Livak, KJ, Schmittgen, TD (2001). Analysis of relative gene expression data using real-time quantitative PCR and the  $2^{-\Delta\Delta C_T}$  method. *Elsevier Science*, 25:402-408.
- Logan M, Pagan-Westphal SM, Smith DM, Paganess L, Tabin CJ. (1998). The transcription factor Pitx2 mediates situs-specific morphogenesis in response to left-right asymmetric signals. *Cell*, 94:307-317.
- Low YL, Li Y, Humphreys K, Thalamuthu A, Darabi H, Wedren S, Bonnard C, Czene K, Iles MM, Heikkinen T, Aittomäki K, Blomqvist C, Nevanlinna H, Hall P, Liu ET, Liu J. (2010). Multi-variant pathway association analysis reveals the importance of genetic determinants of estrogen metabolism in breast and endometrial cancer susceptibility. *PLoS Genetics*, 6:e1001012.
- Lundstrom A. (1961). Some asymmetries of the dental arches, jaws, and skull, and their etiological significance. *American Journal of Orthodontics and Dentofacial Orthopedics*, 47:81-106.
- Mackenzie, N., Huesa, C., Rutsch, F., MacRae, V. (2012). New insights into *ENPP1* function: lessons from clinical and animal studies. *Bones*, 51:961-968.
- Maddux B, Chang YN, Accili D, McGuinness OP, Youngren JF, Goldfine ID. (2006). Overexpression of the insulin receptor inhibitor PC-1/ENPP1 induces insulin resistance and hyperglycemia. *American Journal of Physiology, Endocrinology and Metabolism*, 290(4):746-9.
- Maddux BA, Goldfine ID. (2000). Membrane glycoprotein PC-1 inhibition of insulin receptor function occurs via direct interaction with the receptor  $\alpha$ -subunit. *Diabetes*, 49:13-19.

- Masuoka N, Muramatsu A, Ariji Y, Nawa H, Goto S, Ariji E. (2007). Discriminative thresholds of cephalometric indexes in the subjective evaluation of facial asymmetry. *American Journal of Orthodontics and Dentofacial Orthopedics*, 131(5):609-13.
- McEwen BS, Alves SE. (1999). Estrogen actions in the central nervous system. *Endocrine Reviews*, 20:279-307.
- Meyre D, Bouatia-Naji N, Vatin V, Veslot J, Samson C, Tichet J, Marre M, Balkau B, Froguel P. (2007). *ENPP1* K121Q polymorphism and obesity, hyperglycaemia and type 2 diabetes in the prospective DESIR Study. *Diabetologia*, 50:2090-2096.
- Miller SF, Weinberg SM, Nidey NL, Defay DK, Marazita ML, Wehby GL, Moreno-Uribe LM. (2014). Exploratory genotype phenotype correlations of facial form and asymmetry in unaffected relatives of children with non-syndromic cleft lip and/or palate. *Journal of Anatomy*, 224:688-709.
- Mohlin B, Axelsson S, Paulin G, Pietila T, Bondemark L, Brattstrom V, Hansen K, Holm AK. (2007). TMD in relation to malocclusion and orthodontic treatment. A systematic review. *Angle Orthodontist*, 77(3):542-548.
- Morris, TJ, Brandon, CA, Horton, MJ, Sciote, JJ. (2001). Maximum shortening velocity and myosin heavy-chain isoform expression in human masseter fibers. *Journal of Dental Research*, 80:1845-1848.
- Nakamura T, Mine N, Nakaguchi E, Mochizuki A, Yamamoto M, Yashiro K, Meno C, Hamada H. (2006). Generation of robust left-right asymmetry in the mouse embryo requires a self-enhancement and lateral-inhibition system. *Developmental Cell*, 11(4):495-504.
- Nicot R, Hottenstein M, Raoul G, Ferri J, Horton M, Tobias JW, Barton E, Gele P, Sciote JJ. (2014). Nodal pathway genes are down-regulated in facial asymmetry. *Journal of Craniofacial Surgery*, 25(6):e458-e555.
- Nicot R, Vieira AR, Raoul G, Delmotte C, Ferri J, Sciote JJ. (2016). Role of *ENPP1* and *ESR1* genotypes in the TMD of patients with dento-facial deformities. *Journal of Craniomaxillofacial Surgery*, 44:1226-1237.
- Oberbach, A., Bossen, Y., Lehmann, S., Niebauer, J., Adams, V., Paschke, R. (2006). Altered fiber distribution and fiber specific glycolytic and oxidative enzyme activity in skeletal muscle of patients with type 2 diabetes. *Diabetes Care*, 29(4):895-900.
- Obwegeser HL, Makek MS. (1986). Hemimandibular hyperplasia: hemimandibular elongation. *Journal of Maxillofacial Surgery*, 14(4):183-208.
- Palmer AR. (2004). Symmetry breaking and evolution of development. *Science*, 306(5697):828-33.
- Peck H, Peck S. (1970). A concept of facial esthetics. *Angle Orthodontist*, 4(40):284-318.
- Peck H, Peck S, Kataja M. (1991). Skeletal asymmetry in esthetically pleasing faces. *Angle Orthodontist*, 61(1):43-48.

- Pettipher ER, Higgs GA, Henderson B. (1986). Interleukin 1 induces leukocyte infiltration and cartilage proteoglycan degradation in the synovial joint. *Proceedings of the National Academy of Sciences*, 83:8749-8753.
- Pizzuti A, Frittitta L, Argiolas A, Baratta R, Goldfine ID, Bozzali M, Ercolino T, Scarlato G, Iacoviello L, Vigneri R, Tassi V, Trischitta V (1999) A polymorphism (K121Q) of the human glycoprotein PC-1 gene coding region is strongly associated with insulin resistance. *Diabetes*, 48:1881-1884.
- Polan, M.L., Daniele, A., Kuo, A. (1988). Gonadal steroids modulate human monocyte interleukin-1 (IL-1) activity. *Fertility and Sterility*, 49:964-968.
- Pottratz, S.T., Bellido, T., Mocharla, H., Crabb, D., Manolagas, S.C. (1994). 17 beta-Estradiol inhibits expression of human interleukin-6 promoter-reporter constructs by a receptor-dependent mechanism. *Journal of Clinical Investigation*, 93:944.
- Proffit, W. R., White, Jr, R. P., & Sarver, D. M. (2002). *Contemporary Treatment of Dentofacial Deformity*. Mosby.
- Pullinger, A.G., Seligman, D.A., Gornbein, J.A. (1993). A multiple logistic regression analysis of the risk and relative odds of temporomandibular disorders as a function of common occlusal features. *Journal of Dental Research*, 72:968-979.
- Rallison ML. (1986). Growth disorders in infants, children and adolescents. New York: *Wiley and Sons*, 367.
- Ralston SH, Russell RG, Gowen M. (1990). Estrogen inhibits release of tumor necrosis factor from peripheral blood mono-nuclear cells in postmenopausal women. *Journal of Bone and Mineral Research*, 5:983-988.
- Raoul G., et al. (2011). Masseter myosin heavy chain composition varies with mandibular asymmetry. *Journal of Craniofacial Surgery*, 22:1093-1098.
- Register, T, Wuthier, R. (1985). Effect of pyrophosphate and two diphosphonates on <sup>45</sup>Ca and <sup>32</sup>Pi uptake and mineralization by matrix vesicle-enriched fractions and by hydroxyapatite. *Bone*, 6(5):307-312.
- Ringqvist, M. (1974). Fiber types in human masticatory muscles relation to function. *European Journal of Oral Sciences*, 82:333-335.
- Rowlerson, A, Raoul, G, Daniel, Y, Close, J, Maurage, C, Ferri J, Sciote, J. (2005). Fiber-type differences in masseter muscle associated with different facial morphologies. *American Journal of Orthodontics and Dentofacial Orthopedics*, 127(1):37-46.
- Ryan AK, Blumberg B, Rodriguez-Esteban C, Yonei-Tamura S. (1998). Pitx2 determines left-right asymmetry of internal organs in vertebrates. *Nature*, 394(6):545.
- Saklatvala J. (1986). Tumour necrosis factor alpha stimulates resorption and inhibits synthesis of proteoglycan in cartilage. *Nature*, 322:547-549.

- Schiaffino, S, Reggiani, C. (1994). Myosin isoforms in mammalian skeletal muscle. *Journal of Applied Physiology*, 77:493-501.
- Schiffman E., et al. (2014). Diagnostic criteria for temporomandibular disorders (DC/TMD) for clinical and Research Applications. *Journal of Oral Facial Pain and Headache*, 28(1):6-27.
- Schier AF, Shen MM. (2000). Nodal signaling in vertebrate development. *Nature*, 403:385-389.
- Sciote, JJ, Kentish, JC. (1994). Unloading shortening velocities of rabbit masseter muscle fibres expressing skeletal or  $\alpha$ -cardiac myosin heavy chains. *The Journal of Physiology*, 492:659-667.
- Sciote, JJ, Rowlerson, AM, Hopper, C, Hunt, NP. (1994). A fiber type classification scheme for the human masseter muscle. *Journal of the Neurological Sciences*, 126:15-24.
- Sciote, JJ, Rowlerson, A. (1998). Skeletal fiber types and spindle distribution in limb and jaw muscles of the adult and neonatal opossum, *Monodelphis domestica*. *The Anatomical Record*, 251:548-562.
- Sciote JJ, Horton MJ, Rowlerson AM, Ferri J, Close J, Raoul G. (2012). Human Masseter, Malocclusions and muscle growth factor expression. *Journal of Oral and Maxillofacial Surgery*, 70:440.
- Sciote JJ, Raoul G, Ferri J, Close J, Horton MJ, Rowlerson A. (2013). Masseter Function and Skeletal Malocclusion. *Revue de Stomatologie et de Chirurgie Maxillo-faciale*, 114:79-85.
- Sciote, J.J., Vieira, A.R., Nicot, R., Ferri, J., Raoul, G., Horton, M.J. (2015). ENPP1 and CACNA2D1 associate with TMD-related Masticatory Muscle Pain. *Journal of Dental Research*, 94(A): 2115516.
- Severt TR, Proffit WR. (1997). The prevalence of facial asymmetry in the dentofacial deformities population at the University of North Carolina. *International Journal of Adult Orthodontics Orthognathic Surgery*, 12(3):171.
- Shah SM, Joshi MR. (1978). An Assessment of Asymmetry in the Normal Craniofacial Complex. *The Angle Orthodontist*, 48:141-148.
- Silva NCF, Aquino ERB, Mello KC, Mattos JNR, Normando D. (2011). Orthodontists' and laypersons' perception of mandibular asymmetries. *Dental Press Journal Orthodontics*, 16(4):38.
- Smith SB., et al. (2014). Epistasis between polymorphisms in COMT, ESR1, and GCH1 influences COMT enzyme activity and pain. *Pain*, 155:2390-2399.
- Splitt MP, Burn J, Goodship J. (1996). Defects in the determination of left-right asymmetry. *Journal of Medical Genetics*, 33(6):498-503.

- Stefan C, Jansen S, Bollen M. (2005). NPP-type ectophosphodiesterases: unity in diversity. *Trends in Biochemical Sciences*, 30:542–550.
- Stemple DL. (2005). Structure and function of the notochord: an essential organ for chordate development. *Development*, 132(11):2503-12.
- Stolerman ES, Manning AK, McAteer JB, Dupuis J, Fox CS, Cupples LA, Meigs JB, Florez JC (2008) Haplotype structure of the ENPP1 Gene and Nominal Association of the K121Q missense single nucleotide polymorphism with glycemic traits in the Framingham Heart Study. *Diabetes*, 57:1971-1977.
- Suter E, Herzog W, Sokolosky J. (1993). Muscle fiber type distribution as estimated by Cybex testing and by muscle biopsy. *Medicine & Science in Sports & Exercise*, 25:363.
- Takeshita, N., Ishida, M., Watanabe, H., Hashimoto, T., Daimaruya, T., Hasegawa, M., et al. (2013). Improvement of asymmetric stomatognathic functions, unilateral crossbite, and facial esthetics in a patient with skeletal Class III malocclusion and mandibular asymmetry, treated with orthognathic surgery. *American Journal of Orthodontics and Dentofacial Orthopedics*, 144(3):441-454.
- Tassopoulou-Fishell M, Deeley K, Harvey EM, Sciote J, Vieira AR. (2012). Genetic variation in myosin 1H contributes to mandibular prognathism. *American Journal of Orthodontics and Dentofacial Orthopedics*, 141:51–9.
- Terkeltaub, R, Rosenbach, M, Fong, F, Goding, J. (1994). Causal link between nucleotide pyrophosphohydrolase overactivity and increased intracellular inorganic pyrophosphate generation demonstrated by transfection of cultured fibroblasts and osteoblasts with plasma cell membrane glycoprotein-1. Relevance to calcium pyrophosphate dihydrate deposition disease. *Arthritis & Rheumatism*, 37:934–941.
- Thiesen G, Kim KB. (2016). Criteria for determining facial asymmetries. *American Journal of Orthodontics and Dentofacial Orthopedics*, 150(6):910.
- Thornhill R, Gangestad SW. (1999). Facial attractiveness. *Trends in Cognitive Science*, 12:452-60.
- Ueki, K., Nakagawa, K., Takatsuka, S., Shimada, M., Marukawa, K., Takazakura, D., et al. (2000). Temporomandibular joint morphology and disc position in skeletal class III patients. *Journal of Cranio-Maxillofacial Surgery*, 28, 362-368.
- Ushiyama T, Ueyama H, Inoue K, Ohkubo I, Hukuda S. (1999). Expression of genes for estrogen receptors alpha and beta in human articular chondrocytes. *Osteoarthritis Cartilage*, 7(6):560-6.
- Undt G, Murakami KI, Clark GT, Ploder O, Dem A, Lang T, Wiesinger GF. (2006). Cross-cultural adaptation of the JPF-Questionnaire for German-speaking patients with functional temporomandibular joint disorders. *Journal of Cranio-Maxillofacial Surgery*, 34:226-233.

- Vandenberg LN, Levin M. (2009). Perspectives and open problems in the early phases of left-right patterning. *Seminars in Cell & Developmental Biology*, 20:456-463.
- Vig PS, Hewitt AB. (1975). Asymmetry of the human facial skeleton. *Angle Orthodontist*, 45(2):125.
- Wolford L, Fields R. (1999). *Surgical planning*. London: Churchill-Livingstone.
- Yamada K, Nozawa-Inoue K, Kawano Y, Kohno S, Amizuka N, Iwanaga T, Maeda T. (2003). Expression of estrogen receptor  $\alpha$  (ER $\alpha$ ) in the rat temporomandibular joint. *The Anatomical Record*, 274(2):934-941.
- Yang, N, Schindeler, A, McDonald, MM, Seto, JT, Houweling, PJ, Lek, M. (2011). Alpha-Actinin-3 deficiency is associated with reduced bone mass in human and mouse. *Bone*, 49:790–798.
- Yoshioka H, Meno C, Koshiha K, Sugihara M, Itoh H, Ishimaru Y, Inoue T, Ohuchi H, Semina EV, Murray JC, Hamada H, Noji S. (1998). *Pitx2*, a bicoid-type homeobox gene, is involved in a Lefty-Signaling Pathway in determination of left-right asymmetry. *Cell*, 94:299.
- Zebrick B, et al. (2016). ACTN3 R577X genotypes associate with Class II and depp bite malocclusions. *American Journal of Orthodontics and Dentofacial Orthopedics*, 146(5):603-611.
- Zhou Y, Cheng G, Dieter L, Hjalt TA, Andrade FH. (2009). An altered phenotype in a conditional knockout of *Pitx2* in extraocular muscle. *Investigative Ophthalmology & Visual Science*, 50(10):4531-4541.

## APPENDICES

### APPENDIX A: JAW PAIN AND FUNCTION QUESTIONNAIRE

**Jaw Pain and Function Questionnaire – English Version**

Jaw symptom and oral habit questionnaire	
First name : L	Date :
Last name : VG	19/02/2013
Identification : 004	
Instructions: Please check the appropriate answer to the following questions	Examiner : R. Nicot

A	Jaw pain questions	Doesn't hurt at all	Hurts a little	Hurts a lot	Almost unbearable	Unbearable pain without relief
1	Does it hurt when you open wide or yawn ?	X				
2	Does it hurt when you chew or use the jaws ?	X				
3	Does it hurt when you are not chewing or using the jaws ?	X				
4	Is your pain worse on waking ?	X				
5	Do you have pain in front of the ears or earaches ?	X				
6	Do you have jaw muscle (cheek) pain?	X				
7	Do you have pain in the temples ?		X			
8	Do you have pain or soreness in the teeth ?	X				
B	Jaw function questions	No	Maybe a little	Quite a lot	Almost all the time	All the time without stopping
9	Do your jaw joints make noise so that it bothers you or others?	X				
10	Do you find it difficult to open your mouth wide ?	X				
11	Does your jaw ever lock closed so you cannot open it?		X			
12	Does your jaw ever lock open so you cannot close it?	X				
13	Do you have a problem with your bite being uncomfortable?	X				

## APPENDIX B: SUMMARY OF SUBJECTS

No	Sex	Age	Sagittal	Vertical	Asymmetry Classification	JPF Score
1	W	16	Class II	Open		0
2	M	17	Class II	Normal	Asym B	0
3	W	17	Class II	Open	Asym B	2
4	W	41	Class II	Open	Asym D	2
5	W	53	Class III	Open	Asym D	0
6	W	18	Class III	Normal		0
7	M	23	Class III	Normal	Asym B	3
8	M	45	Class II	Open	Sym	0
9	M	29	Class III	Normal	Asym B	0
10	W	24	<b>Class I</b>	Deep	Asym C	0
11	W	47	Class II	Deep	Sym	9
12	M	17	Class II	Normal	Asym A	5
13	W	24	Class II	Open		5
14	W	17	Class II	Open	Sym	4
15	W	35	Class II	Open	Asym A	5
16	W	17	Class II	Normal	Sym	3
17	M	17	Class II	Open	Sym	1
18	W	14	Class III	Open	Sym	2
19	W	34	Class II	Normal		4
20	W	40	Class II	Open	Asym B	3
21	W	30	Class II	Open	Asym A	3
22	M	26	Class II	Open		0
23	W	45	Class II	Normal		1
24	W	20	Class II	Open	Sym	2
25	M	18	Class III	Open	Sym	1
26	W	38	Class III	Open	Sym	2
27	W	31	Class II	Deep	Sym	17
28	W	15	Class II	Deep	Sym	0
29	W	16	Class II	Normal	Sym	0
30	M	36	Class II	Deep	Sym	3
31	W	24	Class II	Open	Asym B	6
32	M	20	Class III	Open	Asym C	1
33	M	15	Class II	Normal		0
34	W	20	Class II	Open	Asym C	14
35	W	15	Class II	Open	Asym B	5
36	W	16	Class III	Open		2
37	W	16	Class III	Normal		4
38	W	41	Class II	Open	Asym C	14
39	W	16	Class II	Normal		1
40	W	15	Class II	Open	Asym C	6
41	W	28	Class II	Open	Asym D	3
42	W	16	Class III	Normal	Asym C	7
43	W	15	Class II	Deep	Sym	1
44	M	21	Class II	Deep	Asym C	13
45	W	34	Class III	Normal	Sym	1
46	M	19	Class III	Normal	Sym	2
47	W	16	Class II	Deep	Sym	0
48	M	16	Class III	Normal	Asym B	5
49	W	18	Class II	Open	Sym	9
50	W	34	Class II	Open	Asym B	18
51	M	16	Class II	Normal	Asym D	1
52	W	15	Class II	Normal	Sym	0
53	M	17	Class III	Normal		0
54	W	23	Class III	Normal	Asym B	9
55	M	16	Class II	Deep	Sym	0

## APPENDIX B (continued): SUMMARY OF SUBJECTS

No	Sex	Age	Sagittal	Vertical	Asymmetry Classification	JPFscore
56	M	17	Class II	Open	Asym B	13
57	M	17	Class III	Open	Asym D	4
58	W	18	Class II	Normal	Asym B	2
59	W	18	Class II	Deep	Sym	0
60	M	16	Class II	Deep		0
61	W	17	Class III	Normal	Asym B	10
62	W	18	Class II	Open	Asym B	10
63	W	17	Class III	Normal	Sym	2
64	W	16	Class III	Open	Asym B	14
65	W	18	Class II	Normal	Asym B	2
66	W	21	Class II	Normal	Sym	6
67	M	18	Class II	Deep	Sym	0
68	W	20	Class II	Normal	Asym B	13
69	W	30	Class II	Deep	Sym	2
70	M	20	Class II	Normal	Sym	0
71	M	21	Class III	Normal	Sym	0
72	W	21	Class II	Open		1
73	W	19	Class III	Normal		2
74	M	19	Class II	Normal		1
75	W	44	Class II	Open	Asym B	19
76	M	19	Class II	Normal		1
77	M	21	Class III	Deep		3
78	W	30	Class II	Deep		6
79	W	49	Class II	Open		5
80	W	57	Class I	Open		3
81	W	14	Class II	Open		3
82	W	37	Class III	Open	Asym B	13
83	M	30	Class III	Open	Asym D	0
84	M	18	Class III	Open	Asym C	6
85	M	18	Class II	Deep		2
86	M	24	Class III	Open	Asym D	3
87	W	40	Class II	Normal	Sym	6
88	W	32	Class II	Deep		4
89	W	17	Class II	Normal	Asym B	12
90	W	58	Class II	Open	Asym C	5
91	W	26	Class III	Open	Asym C	15
92	W	44	Class II	Open	Asym C	16
93	W	38	Class II	Open	Asym B	14
94	W	17	Class II	Open		0
95	W	16	Class II	Deep		2
96	W	18	Class II	Open		7
97	W	16	Class II	Deep		3
98	M	41	Class II	Normal		0
99	W	37	Class II	Open		1
100	W	23	Class II	Normal		5
101	W	34	Class II	Normal	Asym C	5
102	W	39	Class II	Normal	Asym B	9
103	W	29	Class II	Normal		3
104	M	31	Class II	Open	Asym C	7
105	W	21	Class II	Normal		7
106	M	39	Class II	Open	Asym D	7
107	W	18	Class III	Open		0
108	M	18	Class III	Open		1
109	W	14	Class II	Deep		0
110	M	26	Class II	Open	Asym A	0

## APPENDIX B (continued): SUMMARY OF SUBJECTS

No	Sex	Age	Sagittal	Vertical	Asymmetry Classification	JPF Score
111	W	27	Class III	Normal	Asym C	8
112	W	15	Class II	Normal	Asym A	0
113	M	?	Class III	Open	Asym C	12
114	M	37	Class III	Open	Asym B	0
115	M	45	Class III	Open		0
116	M	42	Class III	Open		1
117	W	68	Class II	Deep		0
118	W	20	Class III	Open		0
119	W	34	Class II	Deep		1
120	M	19	Class III	Open	Asym B	3
121	M	25	Class II	Deep	Asym c	0
122	W	23	Class III	Normal	Asym C	6
123	W	19	Class II	Normal	Asym C	11
124	W	29	Class III	Open	Asym A	4
125	W	16	Class II	Normal		0
126	W	15	Class II	Normal		0
127	W	?	Class II	Deep		0
128	W	19	Class II	Normal	Asym C	12
129	w	15	Class II	Open		0
130	W	41	Class II	Deep	Asym B	9
131	W	19	Class III	Open		1
132	M	36	Class II	Normal		1
133	W	26	Class II	Deep		5
134	W	27	Class III	Open		9
135	M	27	Class III	Open		3
136	W	?	Class II	Open	Asym B	10
137	W	31	Class II	Normal		6
138	M	48	Class II	Open		0
139	W	17	Class III	Open	Asym C	6
140	W	16	Class II	Deep		0
141	W	18	Class III	Open		1
142	W	18	Class III	Open		2
143	W	38	Class II	Deep		0
144	W	40	Class II	Open	Asym D	11
145	W	30	Class III	Deep	Asym C	10
146	M	18	Class II	Open		1
147	W	14	Class II	Open		1
148	W	34	Class II	Open		5
149	W	34	Class II	Deep	Asym C	21
150	W	37	Class II	Deep		2
151	M	24	Class II	Deep	Asym A	6
152	M	47	Class III	Open	Asym B	2
153	M	32	Class III	Open		6
154	W	35	Class III	Open	Asym D	6
155	M	18	Class III	Deep		1
156	M	19	Class II	Open		1
157	M	31	Class II	Open		3
158	W	16	Class III	Open		0
159	M	18	Class III	Open		5
160			Class III	Open	Asym C	11

## APPENDIX B (continued): SUMMARY OF SUBJECTS

No	Sex	Age	Sagittal	Vertical	Asymmetry Classification	JPF Score
161			Class III	Open		1
162			Class II	Normal		5
163			Class III	Open		3
164			Class II	Deep		0
165			Class III	Open	Asym D	8
166			Class III	Open		4
167			Class II	Open	Asym D	
168			Class III	Open		3
169			Class II	Open		0
170			Class II	Open		0
171			Class III	Open		3
172			Class II	Open		1
173			Class II	Open	Asym C	0
174			Class II	Open		2
175			Class II	Open		1
176			Class II	Deep		0
177			Class II	Open	Asym B	5
178			Class II	Deep	Asym C	19
179			Class II	Deep		0
180			Class II	Deep		1
183					Asym A	
184					Asym C	
187					Asym B	
188					Asym B	
189					Asym A	
190					Asym B	
195					Asym B	
197					Asym B	
199					Asym D	
201					Asym B	

## APPENDIX C: *PITX2* SUMMARY OF RAW DATA

No	<i>PITX2</i> Right	<i>PITX2</i> Left	RL Δ	<i>PITX2</i> Avg	% Δn
2	0.469560146	1.417733312	0.948173165	0.943646729	66.87951518
3	1.666749477	1.63652575	0.030223727	1.651637614	1.813333536
4	0.567460179	1.051808119	0.484347939	0.809634149	46.04907785
5	0.472546518	0.537007213	0.064460695	0.504776865	12.00369255
6	0.686666906	0.74926281	0.062595904	0.717964858	8.354332159
7	1.84622705	1.734817505	0.111409545	1.790522277	6.034444407
8	1.31562829	1.582725883	0.267097592	1.449177086	16.87579607
9	1.125239491	1.290887356	0.165647864	1.208063424	12.83209287
10	1.723951221	1.24443841	0.479512811	1.484194815	27.81475514
11	2.11318922	2.035928011	0.077261209	2.074558616	3.656142514
12	1.123712301	1.101561904	0.022150397	1.112637103	1.971180459
13	0.953164399	0.942605674	0.010558724	0.947885036	1.107754803
14	0.996311188	0.984338403	0.011972785	0.990324795	1.201711387
15	1.023075938	No RNA	—	1.023075938	—
16	1.350512147	1.562352538	0.211840391	1.456432343	13.55906468
17	0.257021606	0.185823351	0.071198255	0.221422479	27.70127226
18	0.526254117	0.88549906	0.359244943	0.705876589	40.5697712
20	—	—	—	1.317011237	—
21	—	—	—	1.235628009	—
24	—	—	—	1.159403443	—
25	—	—	—	0.487090528	—
26	0.897733867	0.747426867	0.150307	0.822580367	16.7429352
27	0.752363443	0.612727106	0.139636338	0.682545274	18.55969199
28	—	—	—	1.021167874	—
29	—	—	—	0.998387039	—
30	—	—	—	1.364126801	—
31	1.355945587	1.122576833	0.233368754	1.23926121	17.21077576
32	0.636268556	0.942906439	0.306637883	0.789587498	32.52049943
33	—	—	—	1.201643467	—
34	0.52408582	1.116524816	0.592438996	0.820305318	53.06097881
35	1.224665165	1.515997171	0.291332006	1.370331168	19.21718668
36	—	—	—	1.024111152	—
38	0.684915781	0.904577971	0.219662189	0.794746876	24.28338923
40	—	—	—	1.6761204	—
42	—	—	—	1.463641405	—
43	1.102769136	0.977776706	0.12499243	1.040272921	11.33441498
44	1.236429214	—	—	1.236429214	—
45	0.894928932	0.660475254	0.234453678	0.777702093	26.19802195
46	1.496068001	1.152435899	0.343632102	1.32425195	22.96901624
47	1.425672054	2.172773361	0.747101307	1.799222708	34.38468642
48	1.292551517	—	—	1.292551517	—
49	—	2.131541729	—	2.131541729	—
50	0.711053908	0.720397651	0.009343743	0.71572578	1.29702579
51	0.757666886	1.384172916	0.626506031	1.070919901	45.26212174
52	1.252447605	1.533099413	0.280651808	1.392773509	18.3061715
54	2.096672535	1.313942552	0.782729983	1.705307543	37.33200919
55	2.267292976	1.129305959	1.137987018	1.698299468	50.19144105
56	1.6855762	1.814348578	0.128772378	1.749962389	7.097444201
57	2.369578719	2.230484843	0.139093876	2.300031781	5.869983333
58	1.270820022	1.193852067	0.076967955	1.232336044	6.056558232
59	1.258222342	0.606717825	0.651504517	0.932470083	51.77976063
61	1.362723112	1.442207694	0.079484582	1.402465403	5.511313126
62	0.300530493	1.762356162	1.461825669	1.031443328	82.94723282
63	1.142306566	1.269967675	0.127661109	1.206137121	10.05231168
65	1.447973967	1.381206155	0.066767812	1.414590061	4.611119628
66	1.616145372	1.367664933	0.248480439	1.491905153	15.37488171
67	2.225854874	1.445864677	0.779990196	1.835859776	35.04227546
68	1.523206234	1.818311095	0.295104861	1.670758665	16.22961341
82	0.967900574	0.931192279	0.036708295	0.949546427	3.792568816
84	2.056251526	1.899281621	0.156969905	1.977766573	7.633789102

## APPENDIX C (continued): *PITX2* SUMMARY OF RAW DATA

No	<i>PITX2</i> Right	<i>PITX2</i> Left	RL $\Delta$	<i>PITX2</i> Ave	% $\Delta$ n
87	0.830782115	0.709386826	0.12139529	0.770084471	14.61216938
89	1.433485985	2.124278545	0.690792561	1.778882265	32.51892564
90	1.122300744	1.656756759	0.534456015	1.389528751	32.25917213
91	1.672610998	1.653632164	0.018978834	1.663121581	1.13468309
92	1.871061802	1.652550697	0.218511105	1.76180625	11.67845468
93	1.441700339	1.764053226	0.322352886	1.602876782	18.27342177
101	0.727387309	0.641330123	0.086057186	0.684358716	11.83099912
102	0.908345401	1.029768229	0.121422827	0.969056815	11.79127729
104	1.180546045	1.095209718	0.085336328	1.137877882	7.228547153
106	1.590412021	1.507702589	0.082709432	1.549057305	5.200503428
110	2.167900681	2.480275512	0.31237483	2.324088097	12.59436013
111	1.349002481	1.465292573	0.116290092	1.407147527	7.936305323
112	1.335325599	1.018832207	0.316493392	1.177078903	23.70158951
113	1.654233575	0.082626082	1.571607493	0.868429828	95.0051744
114	1.511787057	1.834632993	0.322845936	1.673210025	17.5973035

## APPENDIX D: ENPPI SUMMARY OF RAW DATA

No	ESRI Right	ESRI Left	RL Δ	ESRI Avg	% Δn
2	—	3.32714653	—	3.32714653	—
3	2.422890663	3.103078127	0.680187464	2.762984395	21.91976599
4	1.652535796	1.399316907	0.253218889	1.525926352	15.32305018
5	3.116826057	1.318363428	1.798462629	2.217594743	57.70173234
7	2.024480104	2.364845514	0.34036541	2.194662809	14.39271224
8	1.388063908	1.533091307	0.145027399	1.460577607	9.459801802
9	2.3915658	2.151755095	0.239810705	2.271660447	10.02735134
10	1.662681937	1.627364635	0.035317302	1.645023286	2.124116523
11	1.943976521	2.645811558	0.701835036	2.29489404	26.52626693
12	2.825106621	2.379981756	0.445124865	2.602544188	15.75603771
14	2.249439001	1.990258098	0.259180903	2.119848549	11.52202408
15	2.775729656	—	—	2.775729656	—
16	1.965503573	1.997534513	0.03203094	1.981519043	1.603523736
17	1.686884403	1.897170663	0.21028626	1.792027533	11.08420364
18	—	1.567543507	—	1.567543507	—
20	—	—	—	2.346753359	—
21	—	—	—	3.281085014	—
24	—	—	—	1.914039254	—
25	—	—	—	3.146585941	—
26	1.984714746	2.078794718	0.094079971	2.031754732	4.525698017
27	2.029065132	2.615054131	0.585988998	2.322059631	22.40829326
28	—	—	—	2.486615181	—
29	—	—	—	2.262802601	—
30	—	—	—	2.246805668	—
31	1.473934174	1.705370665	0.231436491	1.589652419	13.57103742
32	—	1.512289166	—	1.512289166	—
33	—	—	—	2.426113129	—
34	2.254400969	2.961883068	0.7074821	2.608142018	23.88622654
35	2.024467945	2.228667498	0.204199553	2.126567721	9.162405462
38	1.104848385	1.551189065	0.44634068	1.328018725	28.77409919
40	—	—	—	2.355615377	—
42	—	—	—	2.659295559	—
43	2.26376009	2.270870447	0.007110357	2.267315269	0.313111534
44	1.55866158	—	—	1.55866158	—
45	1.730016112	2.347677469	0.617661357	2.038846791	26.30946393
46	2.161184788	2.182104349	0.020919561	2.171644568	0.958687489
47	1.572829485	1.903581977	0.330752492	1.738205731	17.37526915
48	2.353082657	—	—	2.353082657	—
49	—	3.371748924	—	3.371748924	—
50	2.462048769	2.456174135	0.005874634	2.459111452	0.238607531
51	0.99220103	1.926361322	0.934160292	1.459281176	48.49351372
52	2.761680126	1.497722507	1.26395762	2.129701316	45.76770523
54	—	2.255498409	—	2.255498409	—
55	2.493126869	3.22045207	0.727325201	2.85678947	22.58456841
56	3.274442673	3.949545383	0.675102711	3.611994028	17.09317517
57	2.174113274	2.669656277	0.495543003	2.421884775	18.56205263
58	1.43498075	1.577301383	0.142320633	1.506141067	9.023046227
59	1.585669875	2.347679138	0.762009263	1.966674507	32.45798161
61	1.802310824	1.587054491	0.215256333	1.694682658	11.94335241
62	3.186699152	2.408551693	0.778147459	2.797625422	24.41860439
63	1.872774839	2.122019768	0.249244928	1.997397304	11.74564592
65	2.568332911	2.224609852	0.343723059	2.396471381	13.38311935
66	2.054756165	2.744390965	0.6896348	2.399573565	25.1288832
67	3.639180183	3.398260117	0.240920067	3.51872015	6.620174179
68	2.736200333	2.932161808	0.195961475	2.83418107	6.683173993
82	1.93240118	1.874517083	0.057884097	1.903459132	2.995449273
84	2.387665272	2.046589136	0.341076136	2.217127204	14.28492258

## APPENDIX D (continued): *ENPPI* SUMMARY OF RAW DATA

No	<i>ESRI</i> Right	<i>ESRI</i> Left	RL $\Delta$	<i>ESRI</i> Avg	% $\Delta$ n
87	1.331317902	1.128159046	0.203158855	1.229738474	15.25998074
89	1.591112971	2.102025032	0.510912061	1.846569002	24.30570773
90	1.573557496	3.56986022	1.996302724	2.571708858	55.92103334
91	2.169722319	1.993546844	0.176175475	2.081634581	8.11972452
92	2.317350626	2.455090284	0.137739658	2.386220455	5.61037039
93	2.042427063	2.694727182	0.652300119	2.368577123	24.20653652
101	3.086849689	2.233258724	0.853590965	2.660054207	27.6524953
102	1.67332983	1.740377545	0.067047715	1.706853688	3.852481053
104	2.024554491	1.82777226	0.196782231	1.926163375	9.719779448
106	2.065804958	3.022268772	0.956463814	2.544036865	31.64721227
110	1.304222584	1.425577581	0.121354997	1.364900082	8.512689788
111	2.078580856	1.86038053	0.218200326	1.969480693	10.49756257
112	1.467467785	1.693954825	0.226487041	1.580711305	13.37031172
113	1.71914649	5.83334589	4.1141994	3.77624619	70.52898075
114	1.427981257	1.583632112	0.155650854	1.505806684	9.828725559

## APPENDIX E: *ESRI* SUMMARY OF RAW DATA

No	<i>ESRI</i> Right	<i>ESRI</i> Left	RL $\Delta$	<i>ESRI</i> Avg	% $\Delta$ n
2	—	7.115438461	—	7.115438461	
3	5.671875477	6.414645195	0.742769718	6.043260336	11.57927984
4	—	2.19476879	—	2.19476879	
5	3.61675481	1.978558694	1.638196116	2.797656752	45.29464125
7	6.32922554	7.175850391	0.846624851	6.752537966	11.79825115
8	4.406065941	4.037169456	0.368896484	4.221617699	8.372468531
9	5.3199296	4.829425335	0.490504265	5.074677467	9.220126989
10	3.535526752	3.195547581	0.339979172	3.365537167	9.616082569
11	3.789212942	4.396661758	0.607448816	4.09293735	13.8161371
12	4.754128154	7.133303751	2.379175597	5.943715953	33.35306724
14	1.639828444	2.400545359	0.760716915	2.020186901	31.68933727
15	3.519980907	—	—	3.519980907	
16	6.27150774	6.375575542	0.104067802	6.323541641	1.632288752
17	2.927415133	3.167266369	0.239851236	3.047340751	7.572815432
18	3.606866837	5.059929848	1.453063011	4.333398342	28.71705844
20	—	—	—	3.73805666	
21	—	—	—	8.765578388	
24	—	—	—	4.463469505	
25	—	—	—	1.566149116	
26	4.88044405	4.681746006	0.198698044	4.781095028	4.071310762
27	3.192794323	4.81358099	1.620786667	4.003187656	33.67112074
28	—	—	—	5.404626369	
29	—	—	—	4.511520863	
30	—	—	—	2.594201565	
31	3.921612501	4.123820305	0.202207804	4.022716403	4.903409673
32	11.48923683	6.477699757	5.011537075	8.983468294	43.61940787
34	4.756914616	7.152124882	2.395210266	5.954519749	33.48949166
35	6.9273386	7.876732349	0.949393749	7.402035475	12.05314218
38	2.503948927	3.954774857	1.45082593	3.229361892	36.68542413
40	—	—	—	3.777178049	
42	—	—	—	4.727915764	
43	8.229634285	6.954034805	1.27559948	7.591834545	15.50007492
44	3.699961662	—	—	3.699961662	
45	2.860955954	3.424944878	0.563988924	3.142950416	16.46709492
46	6.932655334	4.895175457	2.037479877	5.913915396	29.38960296
47	3.199685812	5.01101923	1.811333418	4.105352521	36.14700592
48	5.24871397	—	—	5.24871397	
49	—	6.71628952	—	6.71628952	
50	3.2445364	3.247506142	0.002969742	3.246021271	0.091446842
51	3.76538642	9.476765763	5.711379344	6.621076091	60.26717855
52	3.638230801	3.466866255	0.171364546	3.552548528	4.710106511
54	—	8.62093544	—	8.62093544	
55	5.829278946	9.150765419	3.321486473	7.490022182	36.29736225
56	5.402524948	6.539548397	1.137023449	5.971036673	17.38688025
57	4.076622217	5.515520968	1.438898751	4.796071592	26.0881748
58	2.80963397	3.15134716	0.34171319	2.980490565	10.84340038
59	4.104793549	6.072704315	1.967910767	5.088748932	32.40583872
61	6.443107128	5.869466305	0.573640823	6.156286716	8.903170659
62	4.954944134	4.892796516	0.062147617	4.923870325	1.254254653
63	6.518145084	6.973641872	0.455496788	6.745893478	6.531691709
65	7.525489807	6.398909092	1.126580715	6.96219945	14.97019787
66	7.552458763	6.472965717	1.079493046	7.01271224	14.29326633
67	6.130060673	4.204377174	1.925683498	5.167218924	31.41377551
68	8.568557739	8.226184845	0.342372894	8.397371292	3.995688711
69	5.29694891	6.028334141	0.731385231	5.662641525	12.13246005
70	6.495662212	5.672925472	0.82273674	6.084293842	12.66594095
71	4.531644344	4.988158226	0.456513882	4.759901285	9.151952705
82	3.86375761	4.498792648	0.635035038	4.181275129	14.11567697
84	5.020188808	5.531350136	0.511161327	5.275769472	9.241167433

**APPENDIX E (continued): *ESRI* SUMMARY OF RAW DATA**

<b>No</b>	<b><i>ESRI</i> Right</b>	<b><i>ESRI</i> Left</b>	<b>RL Δ</b>	<b><i>ESRI</i> Avg</b>	<b>% Δn</b>
87	3.581685066	2.982611179	0.599073887	3.282148123	16.7260347
89	5.476831436	5.746591091	0.269759655	5.611711264	4.694255268
90	5.047247887	13.17215824	8.124910355	9.109703064	61.68245329
91	3.991320848	3.730688095	0.260632753	3.861004472	6.529987522
92	5.110383034	4.678470612	0.431912422	4.894426823	8.451664373
93	5.817372799	5.933145523	0.115772724	5.875259161	1.951287453
101	4.642710686	3.073057413	1.569653273	3.857884049	33.80898313
102	3.936125278	3.727371693	0.208753586	3.831748486	5.303530021
104	5.436355114	5.427440643	0.008914471	5.431897879	0.163978815
106	6.188838662	7.075394794	0.886556131	6.632116728	12.53012952
110	3.91064676	5.53176207	1.62111531	4.721204415	29.30558635
111	3.385901213	3.484135389	0.098234177	3.435018301	2.819470705
112	2.127134085	3.257772923	1.130638838	2.692453504	34.70588235
113	2.207299232	2.787095308	0.579796076	2.49719727	20.8028794
114	1.643623114	2.09117198	0.447548866	1.867397547	21.40182016

## APPENDIX F: FIBER TYPE AREA SUMMARY OF RAW DATA

No	Asymmetry Classification	Ramus	Type I		Type I/II hybrid		Type II		Neo-atrial	
			R	L	R	L	R	L	R	L
2	Asym B	long = left	2029.0	2766.0	1306.0	1484.0	1775.0	1835.0	2500.0	1062.0
3	Asym B	long = left	1205.0	1242.0	1306.0	1382.0	688.0	683.0	0.0	0.0
4	Asym D	long = left	4272.0	2129.0	2188.0	2059.0	451.0	1369.0	813.0	914.0
5	Asym D	long = right	1162.0	1187.0	919.0	733.0	328.0	730.0	0.0	0.0
8	Sym	right = left	4575.998	4757.3215	4063.6	3889.1	550.2	550.5	0.0	0.0
9	Asym B	long = right	2095.0	2195.0	1653.0	1692.0	1388.0	1497.0	1285.0	1041.0
10	Asym C	long = right	1271.0	940.0	812.0	1439.0	608.0	657.0	0.0	0.0
11	Sym	right = left	819.3	825.2	502.3	497.7	402.3	399.5	0.0	0.0
12	Asym A	right = left	2163.6	1717.3	1638.0	1529.0	309.0	151.0	0.0	0.0
14	Sym	right = left	1401.3	1570.6	1408.2	1402.6	2296.9	2020.8	839.8	858.6
15	Asym A	right = left	2669.0	2710.4	1628.0	1853.0	1673.0	1471.0	1596.0	1702.0
16	Sym	right = left	744.5	717.8	503.2	524.0	411.7	423.9	1063.6	1107.7
17	Sym	right = left	347.8	357.2	512.6	624.8	1154.5	1144.4	1096.5	1088.2
18	Sym	right = left	691.3	764.4	729.8	771.1	205.3	318.8	545.6	0.0
24	Sym	right = left	1521.0	1320.0	877.5	1037.0	454.0	387.9	709.1	442.5
25	Sym	right = left	3319.0	3748.0	1949.0	2462.0	1052.0	260.1	2217.0	1542.0
26	Sym	right = left	961.2	1134.3	535.7	933.6	229.7	367.7	0	0
27	Sym	right = left	2105.8	2218.0	2824	2892.5	2286.1	2363.2	0	0
31	Asym B	long = left	1504.0	1973	2787.0	2174.0	1464.0	937.0	0.0	0.0
32	Asym C	long = right	1296.0	3272.0	1372.0	1693.0	1731.0	1964.0	1174.0	717.0
34	Asym C	long = left	1329.0	1847.0	774.0	1493.0	802.0	463.0	0.0	0.0
35	Asym B	long = left	1454.0	1658.0	1544.0	1276.0	1276.0	1097.0	328.0	539.0
38	Asym C	long = right	714.0	1245.0	1109.0	691.0	522.0	839.0	0.0	0.0
39	Sym	right = left	714.3	1245.2	1109.9	690.7	522.9	839.1	0.0	0.0
40	Asym C	long = right	877.0	1555.0	0.0	0.0	1640.0	2291.0	0.0	0.0
41	Asym D	long = right	2987.0	2377.0	1399.0	1928.0	988.0	325.0	0.0	0.0
42	Asym C	long = left	2106.0	1371.0	1929.0	1072.0	326.0	522.0	0.0	0.0
43	Sym	right = left	1658.8	3198.4	1018.7	2342	1517.7	1724.4	1854.8	1974.3
44	Asym C	long = left	1187.0	2773.0	0.0	0.0	2259.0	1757.0	0.0	0.0
45	Sym	right = left	1187.2	2772.8	0	0	2259.1	1757.5	0	0
50	Asym B	long = right	1225.0	738.0	1172.0	1566.0	100.0	619.0	874.0	691.0
51	Asym D	long = right	1225.0	2104.0	2244.0	1633.0	154.0	134.0	0.0	0.0
54	Asym B	long = right	2203.0	1243.0	1098.0	2386.0	845.0	2185.0	436.0	956.0
56	Asym B	long = left	1809.0	2409.0	1295.0	983.0	1138.0	824.0	0.0	0.0
57	Asym D	long = right	1000.0	1487.0	1099.0	1785.0	1140.0	2341.0	0.0	0.0
58	Asym B	long = right	1137.0	1008.0	447.0	458.0	232.0	194.0	0.0	0.0
61	Asym B	long = right	62.0	47.0	33.0	27.0	4.0	25.0	0.0	0.0
62	Asym B	long = right	2575.0	1595.0	2129.0	1364.0	218.0	638.0	0.0	0.0
65	Asym B	long = left	2987.0	2983.0	2189.0	2104.0	2187.0	2254.0	0.0	0.0
68	Asym B	long = right	1209.0	2683.0	946.0	1846.0	786.0	2153.0	0.0	0.0
82	Asym B	long = right	2149.0	1148.0	1183.0	1784.0	786.0	1165.0	0.0	0.0
84	Asym C	long = right	2153.0	2265.0	1879.0	1153.0	1354.0	437.0	0.0	0.0
89	Asym B	long = left	1256.0	1855.0	1975.0	1267.0	2468.0	846.0	0.0	0.0
90	Asym C	long = left	2143.0	2154.0	1463.0	1394.0	745.0	736.0	0.0	0.0
91	Asym C	long = left	1785.0	2241.0	2472.0	1644.0	1135.0	846.0	0.0	0.0
92	Asym C	long = left	1235.0	2086.0	1268.0	684.0	1175.0	485.0	0.0	0.0
93	Asym B	long = right	1983.0	2467.0	1468.0	1155.0	363.0	1473.0	0.0	0.0
102	Asym B	long = right	1485.0	1353.0	1148.0	1158.0	629.0	927.0	0.0	0.0
106	Asym D	long = right	2154.0	1130.0	1856.0	629.0	1584.0	666.0	0.0	0.0
110	Asym A	right = left	1061.0	841.0	648.0	658.0	584.0	645.0	713.0	632.0
112	Asym A	right = left	1078.0	1049.0	579.0	574.0	540.0	453.0	436.0	673.0

## APPENDIX G: FIBER TYPE OCCUPANCY SUMMARY OF RAW DATA

No	Asymmetry Classification	Ramus	Type I		Type I/II hybrid		Type II		Neo-atrial	
			R	L	R	L	R	L	R	L
2	Asym B	long = left	41.0	38.0	24.0	5.0	44.0	22.0	9.0	2.0
3	Asym B	long = left	38.0	40.0	14.0	13.0	22.0	24.0	0.0	0.0
4	Asym D	long = left	46.0	33.0	17.0	17.0	18.0	43.0	5.0	5.0
5	Asym D	long = right	60.0	62.0	3.0	5.0	33.0	30.0	0.0	0.0
8	Sym	left = right	49.4	57.8	33.8	32.3	15.0	16.0	0.0	0.0
9	Asym B	long = left	54.0	25.0	34.0	7.0	8.0	51.0	3.0	9.0
10	Asym C	long = right	28.0	27.0	20.0	27.0	51.0	45.0	0.0	0.0
11	Sym	left = right	51.5	53.9	14.8	15.7	342.8	23.8	0.0	0.0
12	Asym A	left = right	36.0	32.0	55.0	63.0	9.0	5.0	0.0	0.0
14	Sym	left = right	54.6	58.9	2.6	2.6	37.7	34.1	5.1	4.3
15	Asym A	left = right	35.0	35.0	37.0	42.0	20.0	15.0	7.0	7.0
16	Sym	left = right	18.0	26.3	3.0	3.7	64.0	58.0	14.0	11.6
17	Sym	left = right	3.6	3.6	7.9	12.5	75.0	73.0	13.2	9.8
18	Sym	left = right	26.7	47.9	61.1	44.8	7.9	7.3	4.2	0.0
21	Asym A	left = right	43.0	49.0	36.0	11.0	20.0	21.0	0.0	0.0
24	Sym	left = right	64.6	51.5	11.3	22.2	23.5	24.7	0.7	1.6
25	Sym	left = right	61.2	73.5	4.1	13.5	2.4	0.7	32.4	12.3
26	Sym	left = right	83.5	89.0	12.0	5.9	0.2	1.6	4.3	3.5
27	Sym	left = right	46.1	44.7	14.6	14.8	39.1	40.4	0.0	0.0
31	Asym B	long=left	15.0	34.0	43.0	37.0	47.0	4.0	0.0	0.0
32	Asym C	long = right	32.0	61.0	24.0	22.0	31.0	12.0	2.0	5.0
34	Asym C	long = left	45.0	52.0	29.0	44.0	26.0	4.0	0.0	0.0
35	Asym B	long = right	26.0	24.0	48.0	51.0	24.0	18.0	2.0	6.0
38	Asym C	long = right	24.0	34.0	49.0	41.0	13.0	27.0	0.0	0.0
39	Sym	left = right	23.6	34	49	41.2	27.2	24.6	0.0	0.0
40	Asym C	long = right	14.0	28.0	0.0	0.0	86.0	71.0	0.0	0.0
41	Asym D	long = right	52.0	51.0	43.0	49.0	1.0	6.0	0.0	0.0
42	Asym C	long = left	50.0	63.0	49.0	30.0	1.0	6.0	0.0	0.0
43	Sym	left = right	37.8	38.1	14.9	18.6	33.5	26.1	13.6	17.2
44	Asym C	long = left	46.0	43.0	0.0	0.0	53.0	57.0	0.0	0.0
45	Sym	left = right	46.2	43.1	0	0	53.7	56.9	0.0	0.0
50	Asym B	long = right	15.0	34.0	28.0	34.0	0.2	15.0	56.0	16.0
51	Asym D	long = right	12.0	49.0	83.0	49.0	4.0	1.0	0.0	0.0
54	Asym B	long = right	49.0	18.0	25.0	37.0	18.0	36.0	7.0	9.0
56	Asym B	long = left	36.0	54.0	33.0	22.0	31.0	24.0	0.0	0.0
57	Asym D	long = right	31.0	59.0	17.0	7.0	42.0	33.0	0.0	0.0
58	Asym B	long = right	65.0	61.0	18.0	19.0	17.0	20.0	0.0	0.0
61	Asym B	long = right	62.0	47.0	33.0	27.0	4.0	25.0	0.0	0.0
62	Asym B	long = right	82.0	26.0	8.0	24.0	10.0	56.0	0.0	0.0
65	Asym B	long = left	47.0	37.0	18.0	20.0	37.0	34.0	0.0	0.0
68	Asym B	long = right	57.0	38.0	10.0	9.0	32.0	52.0	0.0	0.0
82	Asym B	long = right	65.0	35.0	22.0	36.0	13.0	29.0	0.0	0.0
84	Asym C	long = right	57.0	39.0	25.0	11.0	18.0	49.0	0.0	0.0
89	Asym B	long = left	30.0	53.0	41.0	37.0	27.0	10.0	0.0	0.0
90	Asym C	long = left	62.0	58.0	25.0	26.0	10.0	13.0	0.0	0.0
91	Asym C	long = left	32.0	49.0	26.0	44.0	23.0	14.0	0.0	0.0
92	Asym C	long = left	6.0	62.0	45.0	20.0	49.0	17.0	0.0	0.0
93	Asym B	long = right	36.0	41.0	58.0	38.0	6.0	21.0	0.0	0.0
102	Asym B	long = right	58.0	65.0	29.0	18.0	17.0	30.0	0.0	0.0
106	Asym D	long = right	31.0	42.0	25.0	18.0	44.0	40.0	0.0	0.0
110	Asym A	left = right	27.0	26.0	24.0	22.0	15.0	17.0	6.0	4.0
112	Asym A	left = right	41.0	38.0	22.0	25.0	12.0	12.0	1.0	5.0

## APPENDIX H: DC-TMD SUMMARY OF RAW DATA

No	Age	No			PITX2		ENPPI		ESRI		
		TMD	DDR	Myalgia	Arthralgia	Avg RQ	% Δn RQ	Avg RQ	% Δn RQ	Avg RQ	% Δn RQ
2	17	0				0.9436	66.8795	3.3271	—	7.1154	—
3	17	0				1.6516	1.8133	2.7630	21.9198	6.0433	11.5793
4	41	0				0.8096	46.0491	1.5259	15.3231	2.1948	—
5	53	0				0.5048	12.0037	2.2176	57.7017	2.7977	45.2946
6	18	0				0.7180	8.3543	—	—	—	—
7	23	0				1.7905	6.0344	2.1947	14.3927	6.7525	11.7983
8	45	0				1.4492	16.8758	1.4606	9.4598	4.2216	8.3725
9	29	0				1.2081	12.8321	2.2717	10.0274	5.0747	9.2201
10	24	0				1.4842	27.8148	1.6450	2.1241	3.3655	9.6161
11	47			1		2.0746	3.6561	2.2949	26.5263	4.0929	13.8161
12	17	0				1.1126	1.9712	2.6025	15.7560	5.9437	33.3531
13	24	0				0.9479	1.1078	—	—	—	—
14	17	0				—	—	2.1198	11.5220	2.0202	31.6893
15	35	0				1.0231	—	2.7757	—	3.5200	—
16	17	0				1.4564	13.5591	1.9815	1.6035	6.3235	1.6323
17	17	0				0.2214	27.7013	1.7920	11.0842	3.0473	7.5728
18	14	0				0.7059	40.5698	1.5675	—	4.3334	28.7171
20	40	0				1.3170	—	2.3468	—	3.7381	—
21	30	0				1.2356	—	3.2811	—	8.7656	—
24	20	0				—	—	1.9140	—	4.4635	—
25	18	0				—	—	3.1466	—	1.5661	—
26	38	0				0.8226	16.7429	2.0318	4.5257	4.7811	4.0713
27	31		1	1	1	0.6825	18.5597	2.3221	22.4083	4.0032	33.6711
28	15	0				—	—	—	—	5.4046	—
29	16	0				—	—	—	—	4.5115	—
31	24	0				1.2393	17.2108	1.5897	13.5710	4.0227	4.9034
32	20	0				0.7896	32.5205	1.5123	—	8.9835	43.6194
34	20	0				0.8203	53.0610	2.6081	23.8862	5.9545	33.4895
35	15	0				1.3703	19.2172	2.1266	9.1624	7.4020	12.0531
38	41		1	1	1	0.7947	24.2834	1.3280	28.7741	3.2294	36.6854
40	15		1			1.6761	—	2.3556	—	3.7772	—
42	16		1	1		1.4636	—	2.6593	—	4.7279	—
43	15	0				1.0403	11.3344	—	—	7.5918	15.5001
44	21		1	1		1.2364	—	1.5587	—	3.7000	—
45	34	0				0.7777	26.1980	—	—	3.1430	16.4671
46	19	0				—	—	2.1716	0.9587	5.9139	29.3896
47	16	0				—	—	1.7382	17.3753	4.1054	36.1470
48	16	0				1.2926	—	2.3531	—	5.2487	—
49	18		1			—	—	3.3717	—	6.7163	—
50	34		1	1	1	0.7157	1.2970	2.4591	0.2386	3.2460	0.0914
51	16	0				1.0709	45.2621	1.4593	48.4935	6.6211	60.2672
52	15	0				—	—	2.1297	45.7677	3.5525	4.7101
54	23		1	1		1.7053	37.3320	2.2555	—	8.6209	—
55	16	0				—	—	—	—	7.4900	36.2974
56	17		1	1		1.7500	7.0974	3.6120	17.0932	5.9710	17.3869
57	17	0				2.3000	5.8700	2.4219	18.5621	4.7961	26.0882
58	18	0				1.2323	6.0566	1.5061	9.0230	2.9805	10.8434
59	18	0				—	—	—	—	5.0887	32.4058
61	17		1			1.4025	5.5113	1.6947	11.9434	6.1563	8.9032
62	18			1	1	1.0314	82.9472	2.7976	24.4186	4.9239	1.2543
65	18	0				1.4146	4.6111	2.3965	13.3831	6.9622	14.9702
68	20			1		1.6708	16.2296	2.8342	6.6832	8.3974	3.9957
82	37			1		0.9495	3.7926	1.9035	2.9954	4.1813	14.1157

## APPENDIX H (continued): DC-TMD SUMMARY OF RAW DATA

No	Age	No				PITX2		ENPPI		ESRI	
		TMD	DDR	Myalgia	Arthralgia	Avg RQ	% Δn RQ	Avg RQ	% Δn RQ	Avg RQ	% Δn RQ
84	18		1			1.9778	7.6338	2.2171	14.2849	5.2758	9.2412
89	17		1	1	1	1.7789	32.5189	1.8466	24.3057	5.6117	4.6943
90	58	0				1.3895	32.2592	2.5717	55.9210	9.1097	61.6825
91	26			1		1.6631	1.1347	2.0816	8.1197	3.8610	6.5300
92	44		1	1		1.7618	11.6785	2.3862	5.6104	4.8944	8.4517
93	38		1			1.6029	18.2734	2.3686	24.2065	5.8753	1.9513
101	34	0				—	—	2.6601	27.6525	3.8579	33.8090
102	39		1		1	—	—	1.7069	3.8525	3.8317	5.3035
104	31	0				—	—	1.9262	9.7198	5.4319	0.1640
106	39		1			1.5491	5.2005	2.5440	31.6472	6.6321	12.5301
110	26	0				—	—	1.3649	8.5127	4.7212	29.3056
111	27		1			2.3241	12.5944	1.9695	10.4976	3.4350	2.8195
112	15	0				1.1771	23.7016	1.5807	13.3703	2.6925	34.7059
113	n/a		1	1		—	—	3.7762	70.5290	2.4972	20.8029
114	37	0				—	—	1.5058	9.8287	1.8674	21.4018